INFORMATION TO USERS

This manuscript has been reproduced from the microfilm master. UMI films the text directly from the original or copy submitted. Thus, some thesis and dissertation copies are in typewriter face, while others may be from any type of computer printer.

The quality of this reproduction is dependent upon the quality of the copy submitted. Broken or indistinct print, colored or poor quality illustrations and photographs, print bleedthrough, substandard margins, and improper alignment can adversely affect reproduction.

In the unlikely event that the author did not send UMI a complete manuscript and there are missing pages, these will be noted. Also, if unauthorized copyright material had to be removed, a note will indicate the deletion.

Oversize materials (e.g., maps, drawings, charts) are reproduced by sectioning the original, beginning at the upper left-hand corner and continuing from left to right in equal sections with small overlaps. Each original is also photographed in one exposure and is included in reduced form at the back of the book.

Photographs included in the original manuscript have been reproduced xerographically in this copy. Higher quality 6" x 9" black and white photographic prints are available for any photographs or illustrations appearing in this copy for an additional charge. Contact UMI directly to order.

UMI

A Bell & Howell Information Company
300 North Zeeb Road, Ann Arbor MI 48106-1346 USA
313/761-4700 800/521-0600

THE MASS BALANCE AND THE FLOW OF A POLYTHERMAL GLACIER, McCALL GLACIER, BROOKS RANGE, ALASKA

A

THESIS

Presented to the Faculty

of the University of Alaska Fairbanks

in Partial Fullfillment of the Requirements

for the Degree of

DOCTOR OF PHILOSOPHY

By

Bernhard Theodor Rabus, M.S.

Fairbanks, Alaska

August 1997

THE MASS BALANCE AND THE FLOW OF A POLYTHERMAL GLACIER, McCALL GLACIER, BROOKS RANGE, ALASKA

By

Bernhard Theodor Rabus

RECOMMENDED:

Advisory Committee Chair

Department Head

APPROVED:

Dean of College of Science, Engineering and Mathematics

Dean of Graduate School

5-1-97

Date

ABSTRACT

Studies of surface motion and geometry, ice thickness, and mass balance were carried out on the arctic McCall Glacier. They revealed characteristic processes of glacier flow and mass balance that independently reflect the polythermal temperature regime of the glacier, which consists of cold ice except for a discontinuous layer of temperate ice at the base.

Analysis of the present flow of McCall Glacier showed the longitudinal stress coupling length to be significantly larger than on temperate glaciers. This is a consequence of the smaller mass balance gradients and associated lower strain rates of arctic glaciers. Furthermore, flow analysis suggests year-round basal sliding beneath a section of the lower glacier, which accounts for more than 70% of the total motion. This sliding anomaly is reflected in corresponding anomalies of the observed ice thickness and surface profiles. Changes in surface velocity, both on a decadal and on a seasonal scale, were also studied. Velocities during the short summer season increase by up to 75% above winter values as a result of enhanced basal sliding at the temperate glacier bed. The zone affected by this speed-up extends upglacier of any obvious sources of meltwater input to the bed.

The mass balance of McCall Glacier exhibits a trend towards increasingly negative values. This is shown by both annual measurements during 1969-72 and 1993-96 and by comparing long-term values for two periods, 1957-71 and 1972-93. The contribution of refreezing surface water in the cold surface layers of firn and ice (internal accumulation) to the net accumulation was found to increase from about 40% in the 1970s to more than 90% in the 1990s. Comparative studies of long-term volume changes of neighboring glaciers showed that the McCall Glacier mass balance is regionally representative. Existing good correlations of the mass balance with meteorological parameters recorded by a weather station more than 400 km to the east furthermore suggest that McCall Glacier is representative on a synoptic scale and thus is a valuable indicator of climate change in the Arctic.

TABLE OF CONTENTS

LIST OF FIGURES

LIST OF TABLES

THE MASS BALANCE AND THE FLOW OF A POLYTHERMAL GLACIER, McCALL GLACIER, BROOKS RANGE, ALASKA

Introduction

The glaciological research on valley glaciers has been focussed at the mid-latitudes where most glacier ice is at its pressure melting point. Ignoring factors like ice fabrics, these so-called temperate glaciers deform as homogenous bodies with spatially constant flow law parameters. Basal sliding for these glaciers can occur over the entire ice/ rock interface. The mass balance of temperate glaciers is essentially a surface balance as all the surface melt is lost as runoff and the storage of liquid water in these glaciers is usually negligible on an annual base.

In contrast to what is seen in mid-latitude glaciers, most valley glaciers at arctic latitudes have a polythermal temperature regime. The cold winters and short vigorous melt seasons produce a complicated distribution of temperate and cold ice in the glacier. In the accumulation area the glacier body is warmed above mean annual surface temperatures by refreezing summer melt, which causes a fairly uniform temperature/depth distribution. Maximum temperatures are usually only a few degrees below freezing point. In contrast, the ablation areas exhibit strong temperature gradients between very cold surface ice and temperate ice at the glacier bed. At the margins and in the snout region, where the ice is thin, these glaciers are usually frozen to their beds.

To investigate whether this inhomogenous temperature distribution of arctic glaciers has important effects on both their flow and mass balance characteristics is the common theme for the following three chapters. Each of the three chapters has resulted in a separate publication. The object of our study is McCall Glacier, in the NE Brooks Range of arctic Alaska. McCall Glacier is a typical example of a polythermal glacier and was initially selected for an International Geophysical Year (IGY) project in 1957/58. The Geophysical Institute of the University of Alaska, Fairbanks conducted two further

glaciological projects during 1969-72 and from 1993-96 to study mass balance, ice motion, ice temperature and climatological parameters of this arctic glacier. The current McCall Glacier project provided the opportunity to evaluate and compare changes in glacier geometry and mean mass balance for two successive time periods: 1958-72 and 1972-93. The assessment of these changes is the topic of the first publication, which was written after the first year of the current project. This introductory paper contains a brief summary of the previous McCall Glacier projects. The second paper uses measurements of ice depth, geometry and surface motion to discuss the flow regime of McCall Glacier in the context of its polythermal temperature regime. Changes of the flow, both seasonal and long-term since the 1970s are also studied. The first section of the third paper presents the annual mass balance record of McCall Glacier from the 1970s and 1990s. The influences of mass balance processes that are unique to arctic glaciers, like the internal accumulation of refrozen surface water, are discussed in detail.

A main proposed goal of the current McCall Glacier project was to find whether the McCall Glacier mass balance is a representative indicator of climate change in the Arctic. Whether natural objects can be used as such indicators is an important question because most global change scenarios predict the strongest future warming in the Arctic; but, unfortunately, relevant meteorological data are frequently sparse and unreliable. The last two sections of the third paper are therefore dedicated to investigate the regional and synoptic scale representivity of the McCall Glacier mass balance. Comparative volume change studies on other NE Brooks Range glaciers and a climatological mass balance model were used in this investigation.

The research presented was carried out by the first author (Bernhard Rabus) who also designed and drafted all three papers. The second author (Keith Echelmeyer) provided many scientific and editorial contributions. Besides much helpful advice, Dennis Trabant and Carl Benson provided a large amount of unpublished data from the 1970s. This contribution was honored in their being additional authors on the first paper.

I. Recent changes of McCall Glacier, Alaska[1]

B.T. RABUS, K.A. ECHELMEYER, D.C. TRABANT AND C.S. BENSON

Geophysical Institute, University of Alaska, 903 Koyukuk Dr., Fairbanks, Alaska 99775-7230. U.S.A

I.1. Abstract

Detailed surveys of McCall Glacier in the Alaskan Arctic reveal changes from 1972 to 1993. The ice surface dropped everywhere, by amounts ranging from about 3 m in the highest cirques to more than 42 m near the present terminus. The total volume loss was $5.5 \pm 0.2 \times 10^7$ m^3, resulting in an average mass balance of -0.33 ± 0.01 m a^{-1}. The terminus has retreated by about 285 m at a rate of 12.5 m a^{-1} . Results from photogrammetry for an earlier period, 1958-71, were 1.16×10^7 m^3 and -0.13 m a^{-1} for volume change and mass balance, respectively; the mean terminus retreat rate was then 5.7 m a^{-1}. The changes have to be seen in the context of McCall Glacier's low mass-exchange rate; annual accumulation and ablation, averaged over the years 1969-72 were only + 0.16 and -0.3 m a^{-1}. Cross-profiles in the ablation area, surveyed at intervals of a few years, show an increased drop rate since the late 1970s. The volume-change data suggest a climate warming in the early 1970s. Enhanced thinning of the lower ablation region and accelerated terminus retreat seem to lag this climate change by not more than 10 years. This indicates a reaction time of McCall Glacier that is considerably shorter than its theoretical response time of about 50-70 years.

---

[1] published in *Annals of Glaciology*, **21**, 231-239.

I.2. Introduction

Greenhouse warming of the atmosphere should affect the Arctic regions first and most strongly. The large fluctuations of annual weather make it difficult to detect an ongoing climate change from meteorological records alone. In this paper we present recent changes in surface elevation and volume of McCall Glacier in Arctic Alaska.

Kelly and others (1982) give a good summary of the changes in seasonal and annual air temperatures in the Arctic from 1881 to 1980. Warming after 1890 culminated in the 1930s with winters and summers being warmer by about 2.5° and 1.3°C, respectively, than during the 1880s. The warming started in the Barents and Kara Seas and became most pronounced in the northwest Greenland region. The Arctic cooled in the 1950s and stayed cold during the 1960s, with annual temperatures about 0.85°C less than in the 1930s. Warming began to affect the Arctic anew in the 1970s, again starting in the Barents and Kara Seas and spreading westward. In contrast with the 1930s, the warming is most pronounced in the Alaskan regions where annual temperatures rose by about 1°C (Fig. 1). The overall warming trend since the end of the 19th century is clearly exhibited by the glaciers in Arctic Alaska; they have retreated by 150-700 m from their "Little Ice Age" moraines (Hamilton, 1965; Calkin, 1988). Our goal is to identify more recent changes in climate against this background, by using high-resolution data from McCall Glacier.

To link climate changes to glacier changes two things have to be considered:

(i) Changes in climatic variables such as precipitation, solar radiation and temperature must not cancel in their combined effect on the mass balance of a glacier. On McCall Glacier, a general warming throughout the year would increase summer melt, but winter climate is too cold and dry for winter precipitation to increase significantly. This makes McCall Glacier a sensitive indicator of climate warming.

(ii) Advance/retreat or thinning/thickening of the glacier snout is greatly amplified by ice flux but lags the original mass-balance change in an intricate way (Nye, 1965; Jóhannesson and others, 1989). Measuring the total volume change of a glacier, by photogrammetry or surveying, is more difficult than observations near the terminus. The

advantage is that a mass-balance change can be readily detected by a corresponding volume change without time lag.

McCall Glacier is located at 69°18' N, 143°48' W in the northernmost chain of the Romanzof Mountains, northeastern Brooks Range, Alaska (Fig. 2 inset). The glacier occupies a north-facing valley. It is about 8 km long, has an average width of 640 m and covers an area of 7.4 km^2. The ice originates in three cirques (referred to, from east to west, as upper, middle and lower cirque) and extends from more than 2700 m on the north face of Mount Hubley to the terminus at 1350 m. The glacier surface forms a series of bulges and treads with slopes of up to 15° and as low as 3°; the average ice slope is 7.5°. Figure 3 is a view of the lower ablation area, about 1.5 km up-glacier of the terminus, looking towards the confluence of the three cirques.

I.3. Measurements prior to 1993

McCall Glacier is the only glacier in the U.S. Arctic with a glaciological record of several decades. Shorter records exist for some of the small cirque glaciers of the central Brooks Range (Calkin and others, 1985). McCall Glacier was studied during the International Geophysical Year (IGY) in 1957/58, and from 1969 to 1975 as a contribution to the International Hydrological Decade (IHD). As part of the IGY field program, a photogrammetric map of scale 1:10,000 was produced (Brandenberger, 1959). Observations of the IGY team on the equilibrium and firn-line position are also compiled in this map. Another photogrammetric mission was carried out in 1971 by Dorrer and Wendler (1976).

Keeler (1958) mapped mass balance on lower McCall Glacier during the IGY. Mass-balance maps of the whole glacier exist for the balance years 1968/69, 1969/70, 1970/71 and 1971/72 (Wendler and others, 1972; Trabant and Benson, 1986). Maximum ablation at the terminus was 2.1 m a^{-1} in 1957/58 and 1.6–2 m a^{-1} in the 1970s. (All mass-balance values are given as water equivalent unless noted.) On McCall Glacier all the ablation and about 75% of the accumulation occur during June–September. Internal accumulation accounted for up to 54%, and superimposed ice for up to 5%, of the total accumulation

(Trabant and Benson, 1986). McCall Glacier has a low-mass-exchange rate; annual accumulation and ablation, averaged from 1970 to 1972, were +0.16 and –0.3 m a^{-1}, respectively. The mean equilibrium-line altitude from 1969 to 1972 was 2050 m; mountain shadowing and preferred snow deposition on the west side of the glacier make the equilibrium line run normal to topographic contours over an elevation range of 350 m (Wendler and Ishikawa, 1974).

The extensive mass-balance network of the 1970s was surveyed each year, giving good definition of the ice surface and the surface velocity field at that time (unpublished information from Trabant, 1969–72). Maximum annual velocity was about 16 m a^{-1}. Two detailed transects of the ice surface in the lower ablation area (Fig. 2) were surveyed for several years starting in 1969 (unpublished information from Benson, 1969–75). The upper profile was resurveyed in 1987. Maps of a perennial aufeis field below McCall Glacier show the outline and elevation contours of the terminus in 1970. These data sets give accurate base lines for measuring changes in glacier volume and terminus position.

Meteorological observations were carried out in the upper cirque at about 2300 m during 1957/58 (Orvig, 1961). An automated weather station operated from 1969 to 1972 on the rock ridge between upper and middle cirque. Sparse data were obtained during the winters. Comparison with weather stations of interior Alaska and the Arctic coast revealed a distinct mountain climate dominated by the proximity of the Arctic front in the region of McCall Glacier (Wendler and others, 1974). Approximate mean annual temperatures were about –12°C at 1700 m (Trabant and others, 1975). Annual precipitation averaged over the glacier was estimated as 500 mm a^{-1}. During summer, winds are mainly from the southwest (Wendler and others, 1974).

A polythermal temperature regime is suggested for McCall Glacier. In the accumulation zone the glacier is at about –1°C throughout its thickness (Orvig and Mason, 1963), while the ablation zone is cold at the surface (–8°C at 10 m depth) but is probably underlain by a layer of temperate ice at the bed (Trabant and others, 1975).

I.4. 1993 Field Work

The data presented in this paper were gathered from 26 June to 10 August 1993 as part of a 3 year study of recent changes of McCall Glacier. Surveying the glacier surface, using optical methods and airborne and ground-based GPS methods, was the key tool for defining the glacier surface in 1993. The new data set allows comparison with past surveys in 1958 and the 1970s. Most of the control monuments used for the 1970s survey were recovered, and the more stable ones were selected for the 1993 survey. A GPS base line about 15 km long ties the glacier-control network to a survey benchmark that is fixed to the United States Coastal Geodetic Survey network of northern Alaska.

From the 1972 survey of the IHD mass-balance network 55 reliable pole coordinates were selected (Fig. 2). On the glacier a person was iteratively directed into the known horizontal position using a theodolite with an electronic distance measurer. Most horizontal coordinates were recovered to within 0.1 m radius, and the changes in vertical coordinate ΔZ since 1972 were recorded. At some positions, stakes were drilled into the ice for mass-balance and velocity measurements. The upper and lower detailed cross-glacier profiles (Fig. 2) were resurveyed in 1993 using the bedrock markers of the previous surveys.

A complete center-line profile was obtained using ground-based stop-and-go kinematic GPS from near the pass of the upper cirque down to the terminus. A detailed outline and elevation profile of the 1993 terminus up to about 150 m up-glacier were determined both optically and by kinematic GPS methods.

The most important correction to the elevation-change data came from the different dates of the surveys in 1972 and 1993. From readings of all 1993 mass-balance stakes (Fig. 2), we interpolated ice and snow ablation for the period 29 June–5August 1993 as a function of elevation (see Fig. 4a inset). Lower and upper cirque have somewhat different ablation, possibly due to nonuniform mountain screening. The maximum value of the ablation correction was –1.38 m at stake 2 about 550 m from the terminus; the average for all points was about –1.0 m. Repetitive surveys about a month apart of several 1993 mass-

balance stakes gave horizontal and vertical velocities. The vertical movement between 29 June and 5 August is smaller than +0.01 m and can be neglected.

The 1993 vertical coordinates were corrected for refraction and earth curvature. This correction increased the 1993 elevations by less than 0.2 m for most base lines (< 1.7 km). A few exceptionally long base lines had larger corrections (0.63 m for the longest base line of 2.8 km). A similar correction was also calculated for the 1972 vertical coordinates. Due to shorter base lines, however, it was smaller than the inherent error of the 1972 survey (about 0.3 m). The final error in the 1993 elevation data is ±0.05 m; similar accuracy exists in the horizontal coordinates. The error in the elevation change from August 1972 to August 1993 is dominated by the accuracy of the 1972 survey which was 0.3 m in vertical and 2 m in horizontal.

In the context of a future long-term monitoring program that includes glaciers from all over Alaska, center-line elevation profiles of McCall Glacier and two other glaciers in the northeastern Brooks Range—Esetuk and Okpilak Glaciers, about 20 km southeast and 15 km south, respectively—were obtained using a lightweight, airborne-laser ranging system. These data will be presented elsewhere.

I.5. Changes in elevation, volume and terminus position

Figures 4a–c illustrate elevation change from 1972 to 1993. The surface dropped everywhere from a minimum of 1 m at the head of middle cirque to over 42 m near the terminus. The 1 m minimum is exceptional; the average drop in the accumulation areas of the three cirques is more like 3–3.5 m. This can best be seen from Figure 4a, where the elevation change, ΔZ, for all available positions is plotted against 1972 elevation, Z, regardless of the horizontal coordinates. The scatter represents variations in ΔZ both across the glacier and between different cirques. Figure 4b shows elevation change for selected transverse profiles. Cross-glacier variation of ΔZ ranges from about 0.5 m at the transects near the confluence of the cirques (Fig. 2) to about 5 m at the lower detailed-transverse profile. This cross-glacier variation is about 10% of the mean surface drop for each profile. No clear large-scale pattern, such as the glacier's sides dropping more than

the center, is evident. Meandering surface streams which incise channels a few meters deep into the ice are a ubiquitous feature on McCall Glacier. Some of the recovered pole locations from 1972 were in or near such streams in 1993, indicating that a shift of the surface drainage network may be responsible for cross-glacier variations in elevation change.

The ice surface along the two detailed transects on the lower glacier is shown in Figure 5 for a number of years. The surface topography is almost uniformly lowered between successive dates, making transverse variation of elevation change comparatively small. The characteristic indentation in the middle of the upper profile is preserved from year to year. A second interesting detail in Figure 5 is the constant angle of the side-moraine slope as the apparent width of the glacier diminishes over time. Direct observations show that the side moraines are ice-cored. The overlying till slides down at some angle of repose when the glacier thins, protecting more glacier ice from ablation. The bedrock valley walls are much steeper than the constant angles of repose revealed by Figure 5.

Average elevation drop of the upper profile as a function of time is plotted in the inset of Figure 5a. Around 1975 the drop rate increased from about 0.3 to about 1 m a^{-1}. The elevation drop of the upper detailed transect from 1972 to 1993 provides an independent check of the elevation change obtained at the 1972 pole positions. A pole position about 20 m up-glacier from the upper detailed transect has an elevation drop of 21.1 m while the nearby part of the upper transect dropped 20.9 m.

A map of elevation change from 1972 to 1993 has been constructed by smoothing and interpolation (Fig. 4c). Total volume change was $5.5\pm0.2 \times 10^7$ m^3 of ice. The error was estimated from the interpolation statistics and the 0.3 m error in elevation change of the 1972 locations. Mean mass-balance from 1972 to 1993, i.e. volume loss divided by mean glacier area, was -0.33 ± 0.01 m a^{-1}.

I.6. Comparison of the periods 1972-93 and 1958-72

Dorrer directly compared stereo-photo pairs from 1971 and 1958 to deduce volume loss during this period (Dorrer, 1975; Dorrer and Wendler, 1976). Due to the different illumination, scales and snow coverage prevailing during the two photogrammetric missions, elevation change could be obtained for only three regions in the ablation area, around 1500, 1715 and 1900 m elevation. Mean elevation changes in these regions were 4.5±0.4, 2.9±0.6 and 2.0±0.4 m, respectively. In Figure 6, mean annual thinning rates for the periods 1958–71 and 1972–93 are compared. In both cases a suitable exponential was fitted to the data (cf. Weidick, 1968; Dorrer and Wendler, 1976). Two features are immediately obvious: (i) in the earlier period the accumulation area is only very slightly affected while in the later period it is characterized by a noticeable surface drop; and (ii) the difference in mean annual elevation change between the two periods increases drastically down-glacier. Extrapolation of Dorrer's curve to the region close to the terminus gives rise to rather large uncertainties. According to his error bars, annual thinning of the ice there was between –0.5 and –0.85 m a^{-1} during 1958–71, while from 1972 to 1993 the terminal region thinned by almost 2.4 m a^{-1} (2.1 m a^{-1} w.e.), a value in excess of the maximum ablation at the terminus during the 1970s. Mean mass balance during 1958–71 was –0.13 m a^{-1} as compared to –0.33 m a^{-1} for the period 1972–93.

Elevation change between 1958 and 1972 can also be calculated by locating the 1972 pole positions on the 1958 IGY map. The result is shown in Figure 6: surface drop from 1958 to 1972 based on the IGY map differs greatly from Dorrer's estimate. Mean annual balance would be –0.45 m a^{-1}, which is more than three times Dorrer's value. Strong thinning would occur not only close to the terminus but also about 1.5 km up-glacier. This irregular pattern of elevation change and two further arguments make us believe that there are systematic errors in the 1958 map considerably exceeding the expected error of ±2.5 m.

The first argument is based on the time history of elevation along the upper detailed traverse (Fig. 5a inset). Elevation can be extrapolated for 1958 using the IGY map, and

the thinning rate there from 1958 to 1972 is then about 1 m a^{-1}, just as from 1975 to 1993. This implies the research period in the 1970s was characterized by exceptionally low ablation (thinning rate 0.3 m a^{-1}). In contrast, mass balance calculated by Dorrer and Wendler (1976) from weather records of Barter Island, 110 km north at the Arctic coast, indicates that during the period 1969–75 the glacier thinned at a higher annual rate than the mean rate during the 1960s. A thinning rate of 0.3 m a^{-1}, on the other hand, would give a surface drop of 3.9 m for the 13 year period 1958–71. This is very close to what Dorrer's curve shows for an elevation of 1600 m, the 1972 elevation of the upper detailed traverse. Secondly, Trabant and Benson (1986) mention several IGY mass-balance stakes that reappeared in 1969 and 1972 after they had apparently crossed the mean equilibrium line. The mean equilibrium line reconstructed in this way coincided best with the 1972 equilibrium line, making the 1972 balance of –0.19 m a^{-1} a crude estimate of the mean balance in the period 1958–72. Dorrer's value of –0.13 m a^{-1} for the mean balance is within the error range of this estimate while the value of –0.45 m a^{-1} deduced from the IGY map is not.

I.6.1 Terminus retreat

Figure 7 shows reconstructions of the 1958, 1970 and 1993 termini together with the youngest end moraine that outlines the maximum extent of the glacier around 1890 (lichen date). Terminus altitudes were 1354 m in 1993, 1327 m in 1970 and about 1320 m in 1958. Changes of retreat rate and surface elevation at the terminus were derived from direct observation and geometric considerations, treating the terminus up to the lower detailed profile as a wedge with constant surface and bed slope (see Table 1) . Implications are: (i) Terminus-retreat rate more than doubled between the time periods 1958–70 and 1970–93. (ii) Thinning from 1958 to 1970 is faster than Dorrer's curve suggests for the terminus (Fig. 6) but still within the expected error range. (iii) The thinning rate from 1970 to 1993 is less than the 2.4 m a^{-1} interpolated from Figure 6; it is almost constant down-glacier of the lower detailed transverse, suggesting a stagnant, passively melting terminus for most of that period. (iv) Surveys from 1970 to 1972 of the

lowermost mass-balance stake (about 40 m from the 1970 terminus) imply that thinning of the terminus accelerated more gradually compared to the step-like increase in thinning rate around 1975 documented at the upper detailed-transverse profile.

I.7. Interpretation - evidence for recent climate change?

A significant climate change within the total observation period 1958–93 is strongly implied by the available data. Mean mass balance calculated from volume change became more negative by a factor of about two between the periods 1958–71 and 1972–93. If Dorrer's estimate of –0.13 m a^{-1} for the 1958–71 mean mass balance is accurate, this factor would be 2.5; a value of –0.2 m a^{-1}, which is considered a minimum, would reduce the factor to about 1.7. The difference in mean mass balance between these two periods corresponds to the stepwise change in temperature in the 1970s (Fig. 1).

The terminus has doubled its retreat rate from 1970–93 as compared to 1958–70. Data from the early 1970s (last column of Table 1) favor a steadier increase in retreat rate beginning around 1970 rather than a step change. The similar relative increases of terminus-retreat rate, thinning rate of the lower ablation area and mean mass balance imply that all three are indicative of the same climate change.

I.7.1 Reaction and response times of McCall Glacier

Jóhannesson and others (1989) describe the delayed adjustment of a glacier's terminus to a change in mass balance by a response time $\tau_v \approx (h)/(-b_T)$ where (h) is mean glacier thickness and b_T mass-balance rate at the terminus. For a step change in mass balance this is approximately the time it takes the glacier to change its volume by $1-1/e \approx 63\%$ of the total volume difference between the initial and final steady states. Temperate valley glaciers have a τ_v of 10–100 a (e.g. McClung and Armstrong, 1993). Application of the formula to McCall Glacier, $b_T = 2$ m a^{-1}, (h) Å 150 m, gives $\tau_v = 75$ a, much longer than the observation record of McCall Glacier. On the other hand, the characteristics of the recent changes suggest that the amplified *reaction* of the lower ablation region of McCall Glacier lags the original climate change by not more than 10 years. As reaction time we

define the time after a mass-balance change when there is a strong increase or decrease in the rates of elevation change and terminus retreat. If the glacier was in steady state before the mass balance was disturbed the reaction time corresponds to the time of maximum retreat or advance of the terminus. Jóhannesson and others (1989) describe the time evolution of the ratio f = average thickness change/thickness change at the terminus. They find a rapid decrease of f from its initial value of 1 to its long-term value of about $\Delta b/(-b_T)$ where Δb is the disturbance of the mass balance. This step-like change in f, which seems to occur at about 20–30% of τ_v (Jóhannesson and others, 1989, Fig. 6), presumably defines the above reaction time of the glacier. In accordance with our findings for McCall Glacier, Sigurdsson and Jónsson (1995) observe reaction times of Icelandic glaciers to be much shorter than their response times.

There is also a pronounced asymmetry between advance and retreat of the glacier terminus which is often overlooked. If glacier ice were perfectly plastic, i.e. ice velocity scaled with a power $n \rightarrow \infty$ of the basal shear stress $u \sim (\tau/\tau_{yield})^{n+1}$, a positive mass-balance disturbance would lead to instantaneous advance of the terminus, while the retreat caused by a negative mass-balance disturbance would never be by active movement of the ice but only by melting of the stagnant terminus in finite time. According to suggested laws o ice deformation and basal sliding, n should be in the range of about 2–3 (e.g. Paterson, 1981, p. 87, 116). Both advance and retreat rates of the terminus are then finite, but terminus retreat still depends on passive melting. Therefore, most theories of glacier response strictly apply only to positive mass-balance disturbance and terminus advance. In a steady state, ice flux at the terminus equals ablation losses there. A uniform negative mass-balance disturbance therefore causes an initial retreat rate $\Delta b/\tan(\alpha_{surface}-\beta_{bed})$. Complete stagnation of the terminus leads to a maximum retreat rate $b_T/\tan(\alpha_{surface}-\beta_{bed})$. For McCall Glacier, minimum and maximum retreat rates are about 2 and 13–14 m a^{-1}, respectively, the latter being close to the retreat rate actually observed.

I.8. Conclusions

(1) The increase in the rate of volume wastage by a factor of more than two from the earlier to the later time period indicates a severe change in mass balance, most likely near the border of the periods, i.e. in the early 1970s.

(2) The observed mass-balance change is probably mainly due to higher summer temperatures.

(3) The step-like increase in surface-drop rate of the lower ablation area between about 1975 and 1980, and the increase in terminus-retreat rate, appear to be correlated with the recent climate change. This suggests a fast reaction time of McCall Glacier of less than a decade.

(4) How representative the detected climate change is for the region cannot be decided at the moment. Limited data from other Brooks Range glaciers and an approach to modeling the mass balance of McCall Glacier from atmospheric data will be employed to answer this question in the future.

I.9. Acknowledgements

We wish to thank J. DeMallie and U. Adolphs for helping with the field work and W. Harrison for commenting on the manuscript.

I.10. References

Bowling , S.A. 1991. Problems with the use of climatological data to detect climatic change at high latitudes. *In* Weller, G., C.L. Wilson and B.A.B. Severin, *eds. International Conference on the role of the Polar Regions in Global Change: proceedings of a conference held June 11-15, 1990 at the University of Alaska. Vol. 1.* Fairbanks, AK, University of Alaska. Geophysical Institutes, 206-209.

Brandenberger, A.J. 1959. *Map of the McCall Glacier, Brooks Range, Alaska.* New York, American Geographical Society. (AGS Report 11.)

Calkin, P.E. 1988. Holocene glaciation of Alaska (and adjoining Yukon Territory, Canada). *Quat. Sci. Rev.*, 7(2), 159-184.

Calkin, P.E., J.M. Ellis, L.A. Haworth and P.E. Burns. 1985. Cirque glacier regime and neoglaciation. Brooks range, Alaska. *Z. Gletscherkd. Glazialgeol.*, **21**, 371-378.

Dorrer, E. 1975. Contribution to a general stereoscopic block analytical aerotriangulation. *Deutsche Geodätische Kommission, Reihe B* 214, 125-136.

Dorrer, E. And G. Wendler. 1976. Climatological and photogrammetric speculations on mass-balance changes of McCall Glacier, Brooks Range, Alaska. *J. Glaciol.*, **17**(77), 479-490.

Hamilton, T.D. 165. Comparative glacier photographs from northern Alaska. *J. Glaciol.*, **5**(40), 479-487.

Jóhannesson, T., C. Raymond and E. Waddington. 1989. Time-scale for adjustment of glaciers to changes in mass balance. *J. Glaciol.*, **35**(121), 355-369.

Keeler, C.M. 1958. Ablation studies: lower McCall Glacier, June 23 to September 1, 1957, 1957. *IGY Glaciol. Rep.* 1, XII-11-XII-15.

Kelly, P.M., P.D. Jones, C.B. Sears, B.S.G. Cherry and R.K. Tavakol. 1982. Variations in surface air temperatures: Part 2. Arctic regions, 1881-1980. *Mon. Weather Rev.*, **110**(2), 71-83.

McClung, D.M. and R.L. Armstrong. 1993. Temperate glacier time response from field data. *J. Glaciol.*, **39**(132), 323-326.

Nye, J.F. 1965. A numerical method of inferring the budget history of a glacier from its advance and retreat. *J. Glaciol.*, **5**(41), 589-607.

Orvig, S. 1961. *McCall Glacier, Alaska: meteorological observations, 1957-1958.* Montreal, Arctic Institute of North America. (AINA Research Paper 8.)

Orvig, S. And R.W. Mason. 1963. Ice temperatures and heat flux, McCall Glacier, Alaska. *International Association of Scientific Hydrology, Publication* 61 (General Assembly of Berkeley 1963—*Snow and Ice*), 181-188.

Paterson, W.S.B. 1981. *The physics of glaciers. Second edition.* Oxford, etc., Pergamon Press.

Sigurdsson, O. And T. Jónsson. 1995. Relation of glacier variations to climate changes in Iceland. *Ann. Glaciol.*, **21** (see paper in this volume).

Trabant, D.C. and C.S. Benson. 1986. Influence of internal accumulation and superimposed ice formation on mass balance of McCall Glacier in Alaska. *Mater. Glyatsiol. Issled.* 58, 157-165.

Trabant, D.C., W.D. Harrison and C.S. Benson. 1975. Thermal regime of McCall Glacier, Brooks Range, northern Alaska. In Weller, G. And S.A. Bowling, *eds. Climate of the Arctic.* Fairbanks, AK, University of Alaska. Geophysical Institute, 347-349.

Weidick, A. 1968. Observations on some Holocene glacier fluctuations in West Greenland. *Medd. Grønl.*, **165**(6).

Weller, G., D. Trabant and C. Benson. 1975. Physical characteristics of the McCall Glacier, Brooks Range, Alaska. *International Association of Hydrological Sciences Publication* 104 (General Assembly of Moscow 1971—*Snow and Ice*), 88-91.

Wendler, G. And N. Ishikawa. 1974. The effect of slope, exposure and mountain screening on the solar radiation of McCall Glacier, Alaska: a contribution to the International Hydrological Decade. *J. Glaciol.*, **13**(68), 213-226.

Wendler, G., C. Fahl and S. Corbin. 1972. Mass balance studies on the McCall Glacier, Brooks Range, Alaska. *Arct. Alp. Res.*, **4**(3), 211-222.

Wendler, G., N. Ishikawa and N. Streten. 1974. The climate of the McCall Glacier, Alaska, in relation to its geographical setting. *Arct. Alp. Res.*, **6**(3), 307-318.

I.11. Figures

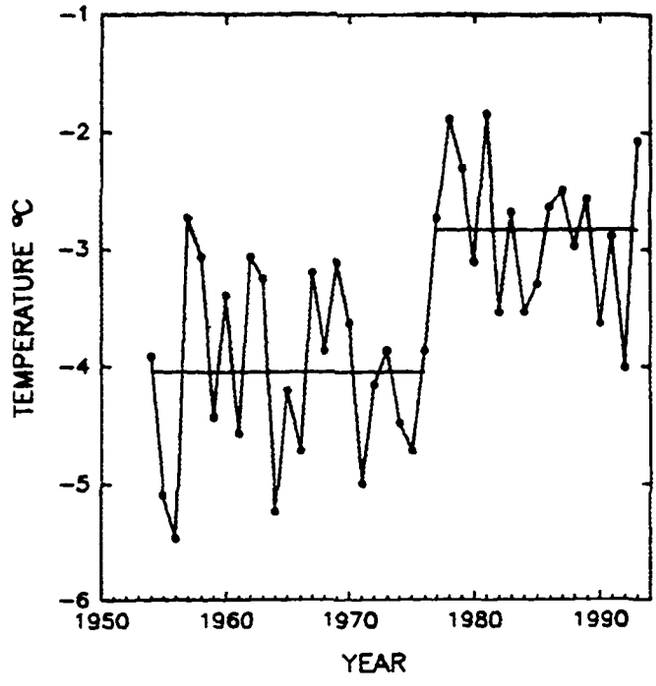

Figure I.1: Annual mean temperature, average of Anchorage, Barrow, Fairbanks and Nome (adapted from Bowling (1991)).

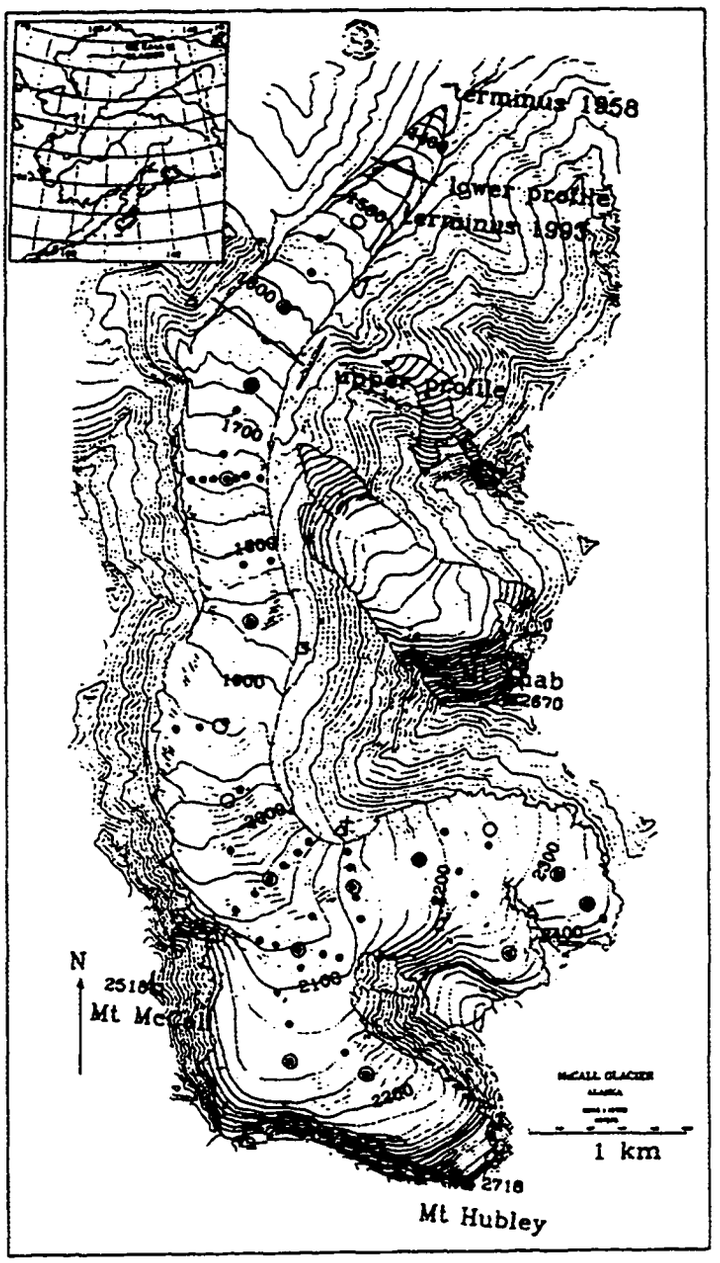

Figure I.2: Map of McCall Glacier, showing 1972 pole positions resurveyed in 1993 (black dots); control monuments (triangles); 1993 mass-balance stakes (open circles); upper and lower detailed-transverse profiles; and position of 1993 camp (cross).

Figure I.3: Looking up-glacier from the upper detailed-transverse profile. Note "Hanging" Glacier to the left and snow-capped Mount McCall in the right background.

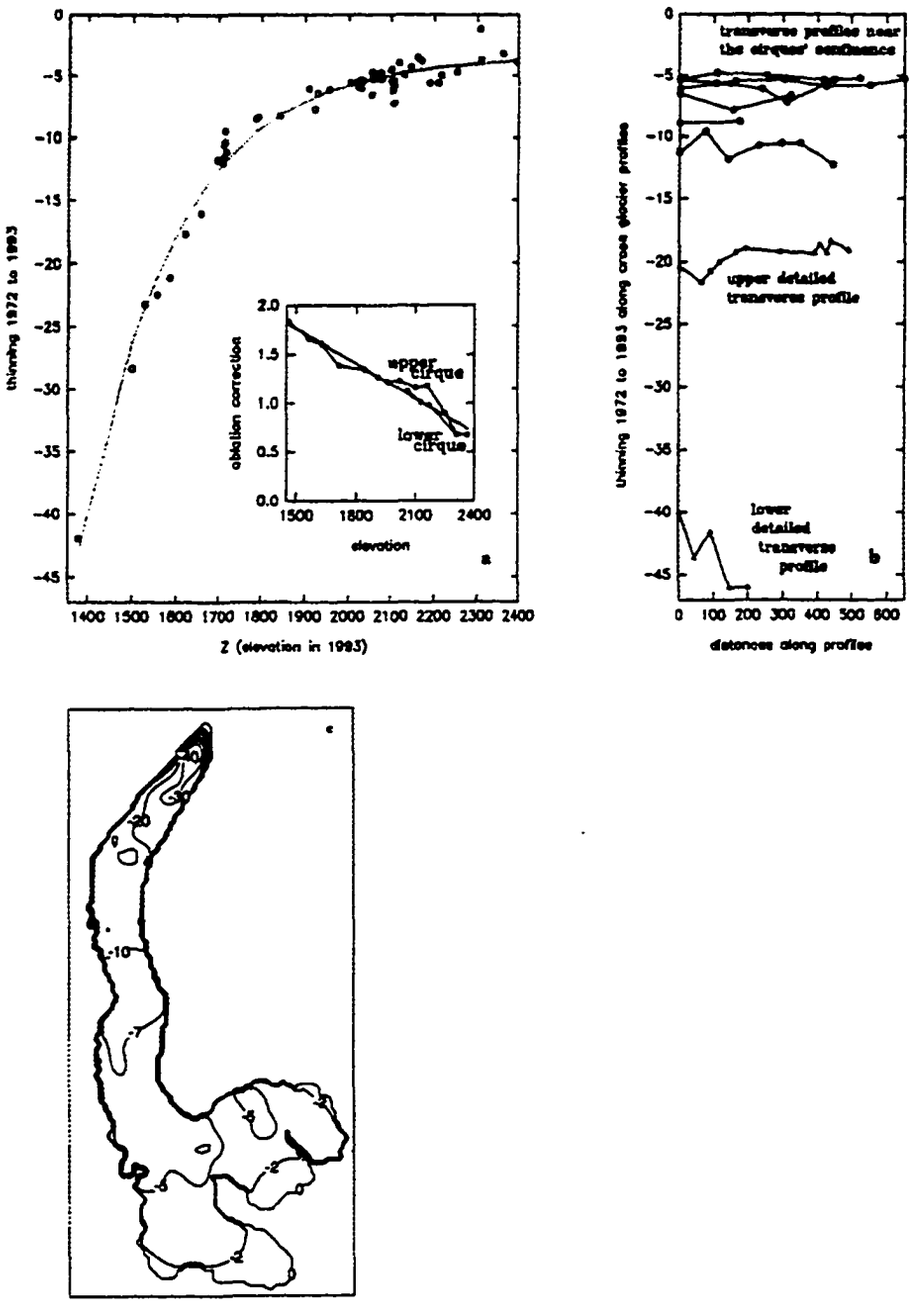

Figure I.4: Elevation change, 1972–93: a. vs elevation, b. cross-glacier variation, c. contour map.

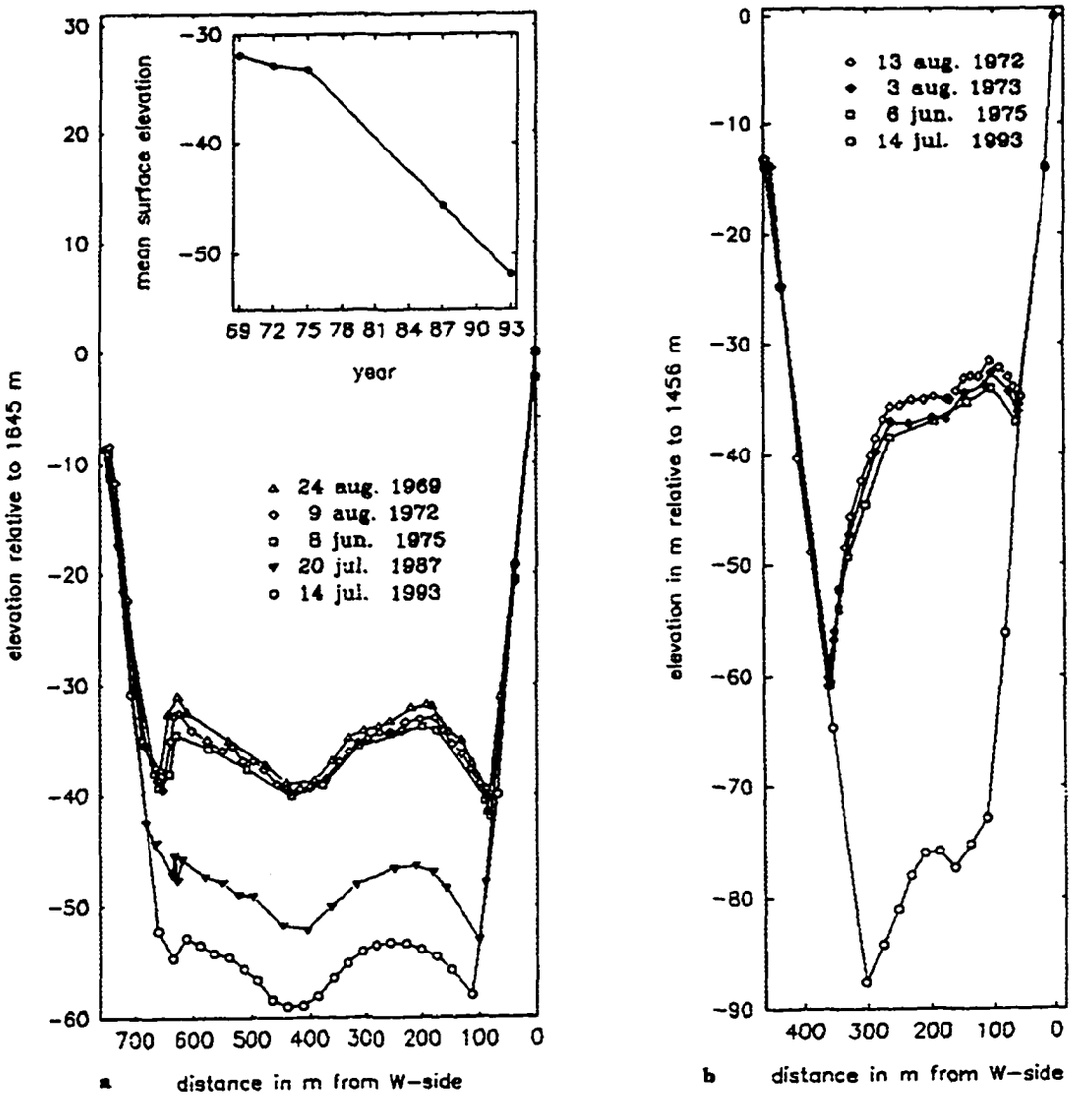

Figure I.5: Time evolution of ice surface along a) upper and b) lower detailed-transverse profile

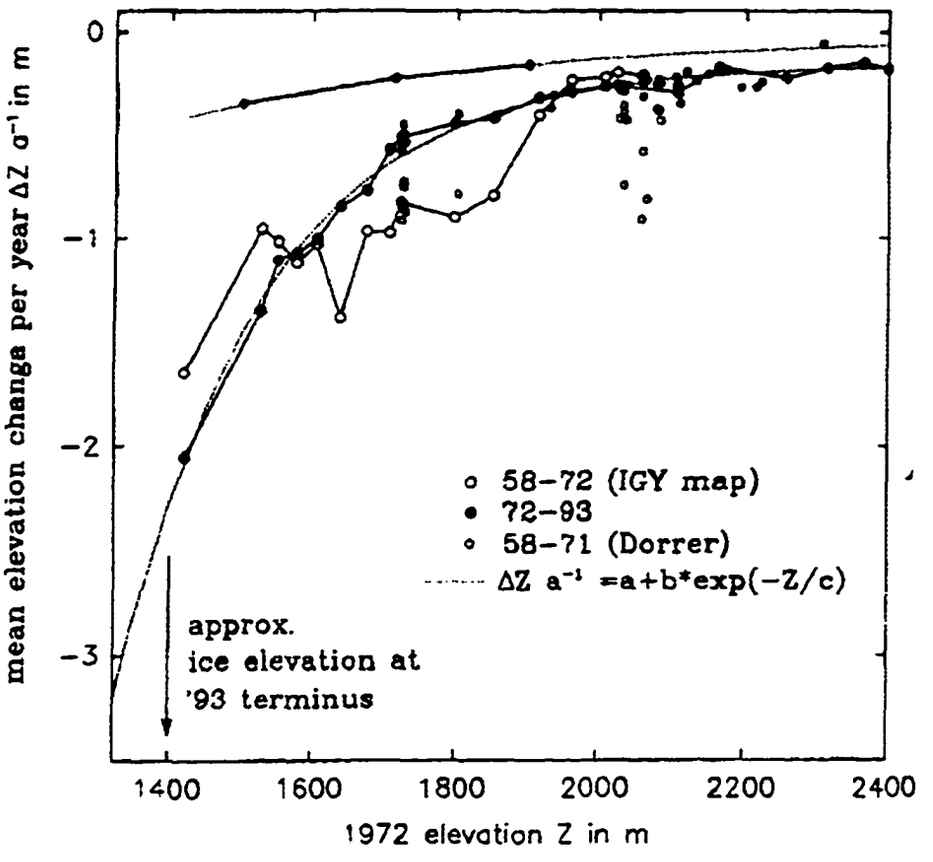

Figure I.6: Mean annual thinning vs elevation: 1972–93 (this paper), 1958–72 based on the IGY map, and 1958–71 from Dorrer and Wendler (1976). Positions along the center line of the glacier are connected by lines.

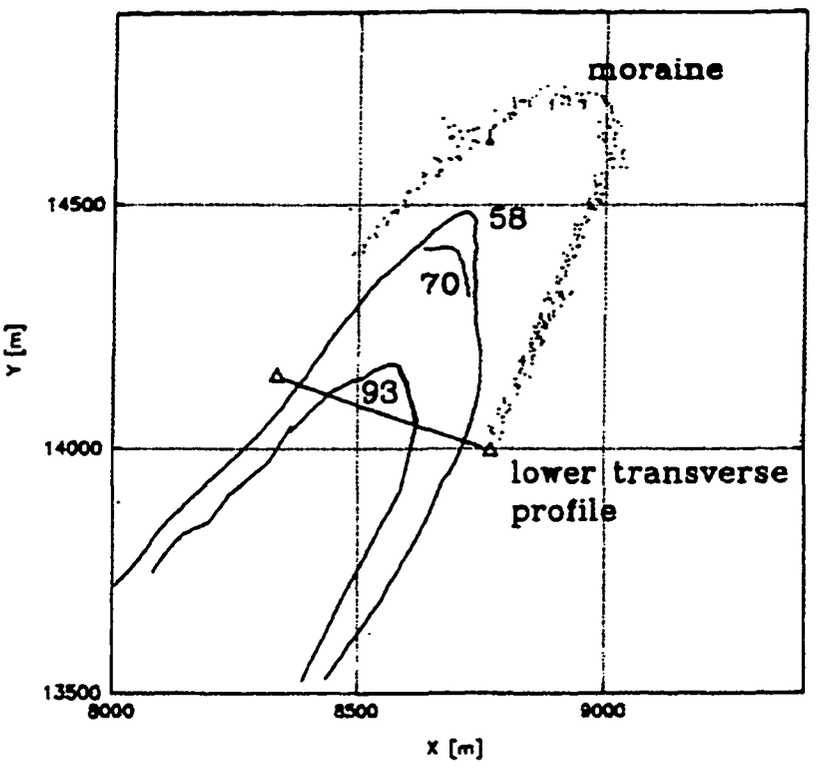

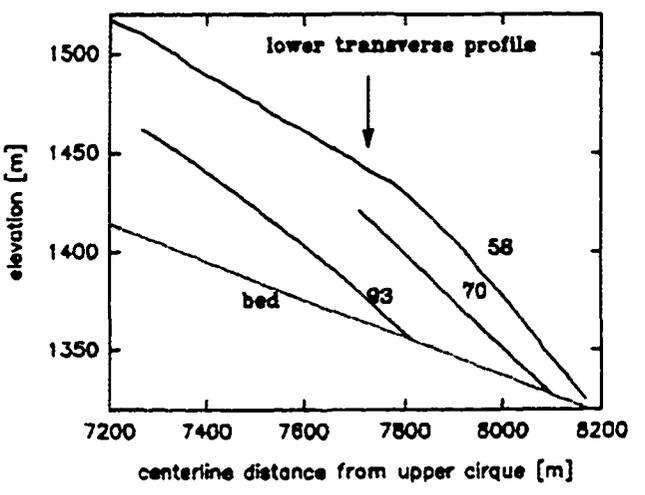

Figure I.7: The terminus of McCall Glacier for the years 1993, 1970 and 1958, and before the retreat from its "Little Ice Age" maximum (presumably around 1890).

I.12. Tables

Table I.1: Retreat rate of the terminus for different time periods; thinning rate at terminus position corresponds to the end of each time period

time period	surface slope (°)	bed slope (°)	Terminus retreat m	Retreat rate m a^{-1}	Thinning at terminus m	Thinning rate m a^{-1}
1890[r]–1958	–	–	300	4.4	–	–
1958–70	14.4[ld]	6[d]	68[d]	5.7	10	0.8
1970–71	12.8[td]	0–6	6–12	6–12	1.3[d]	1.3
1971-72	–	–	–	–	1.4[d]	1.4
1970–93	14.0[ld]	5.3[d]	285[d]	12.5	41	2.0

[d] Direct observations from surveys or photogrammetry.

[l] Average surface slope measured from terminus to lower transverse profile.

[t] Average surface slope measured from terminus to about 50 m up-glacier.

[r] Lichen date.

II. The flow of a polythermal glacier: McCall Glacier, Alaska[2]

B.T. RABUS AND K.A. ECHELMEYER

Geophysical Institute, University of Alaska, 903 Koyukuk Dr., Fairbanks, Alaska 99775-7230. U.S.A

II.1. Abstract

We have analyzed the flow of polythermal McCall Glacier in Arctic Alaska. Using measurements of surface velocity from the 1970s and 1990s, together with measurements of ice thickness and surface slope, we have investigated both the present flow, and seasonal and long-term flow variations. Our analysis of the present flow reveals that (i) longitudinal stress coupling is important along the entire length of the glacier, and (ii) there is significant basal sliding beneath a 2-km long section of the lower glacier. This sliding exists year-round, and it accounts for more than 70% of the total motion there. We have developed a numerical model which shows that such a sliding anomaly causes an asymmetric decrease in ice thickness. Accompanying this decrease in ice thickness is a decrease in surface slope at the center of the anomaly and an increase in slope upglacier of it. Both effects are reflected in the observed surface profile of McCall Glacier. The longitudinal stress coupling length of McCall Glacier is 3.5 times the ice thickness, almost twice that typical of temperate glaciers. This is a direct effect of lower strain rates, which themselves are associated with the smaller mass balance gradients of arctic glaciers. Long-term variations in surface velocity between the 1970s and 1990s are explained solely by the effects of changes in glacier geometry on the deformational flow contribution. This means that long-term variations in the spatial patterns of longitudinal stresses and basal sliding must have been small. Seasonally, velocities reach their annual minimum in spring

---

[2] submitted to *Journal of Glaciology*

and increase during the short summer melt season by up to 75% above mean winter values. However, the extra motion associated with the period of elevated velocities is only about 5% of the total annual motion. The speed-up is due to an increase in basal sliding. This implies that most of the glacier bed is at the melting point. The zone affected by the melt season speed-up extends well upglacier of any moulins or other obvious sources for meltwater at the bed.

II.2. Introduction

In contrast to temperate and cold glaciers, which have a uniform temperature regime, polythermal glaciers consist of regions of both temperate and cold ice. A unifying feature of polythermal glaciers at arctic latitudes is a strong vertical temperature gradient in the ablation area. Around the centerline, a thick armor of cold ice covers a finite layer of temperate basal ice, while the thin ice at the margins and in the snout region is mostly frozen to the underlying bedrock. A significant contribution to the flow of most temperate glaciers comes from sliding during the melt season; cold glaciers on the other hand show little sliding and no seasonal variations of flow. An important question, therefore, is whether the distribution of temperate and cold ice within polythermal glaciers, together with the concentrated melt water input during their short ablation seasons, leads to a distinct flow regime with unique spatial and seasonal characteristics.

In this paper we describe the flow of polythermal McCall Glacier in arctic Alaska. We find a significant year-round sliding contribution to the flow along one section of the lower glacier. There is also a pronounced summer increase in flow over the entire ablation area that to some extent persists after the end of the melt season. Similar seasonal fluctuations have been observed on other polythermal glaciers, such as Kitdlerssuaq Glacier in western Greenland (Andreason, 1985) and White, Crusoe and Thompson Glaciers in the Canadian Arctic (Iken 1974), but not on Jakobshavns Isbrae in Greenland (Echelmeyer and Harrison, 1990). The spatial and temporal evolution of velocity fluctuations on some of these polythermal glaciers seems to indicate differences in

subglacial drainage and basal conditions with respect to temperate glaciers. Andreason (1985) speculates that melt-water is trapped by the marginal zone of thin ice that is frozen to the bed. Some of the melt-water is forced upglacier, thereby causing high water pressures and sliding above the lowest points of surface water input. Surges of some polythermal glaciers on Spitsbergen might also be influenced by similar effects.

II.2.1 McCall Glacier

McCall Glacier is located at 69°17'N, 143 °50'W in the Romanzof Mountains of the northeastern Brooks Range, Alaska. It is situated on the northern front of the mountain range, about 100 km south of the Arctic Ocean across the coastal plain (Figure II.1, inset). The glacier is about 8 km long and has an area of 7.4 km^2. Ice originates in three cirques referred to, from east to west, as upper (UC), middle (MC) and lower cirque (LC), and it flows from an elevation of more than 2700 m to the terminus at 1350 m (Figure II.1). The surface is relatively steep, with a mean slope of 8°; there is a series of bulges along its length with slopes up to 15° separated by treads of 3 to 5°. Seasonal mass exchange is quite small: winter balance is around 0.2 m a^{-1} and summer balance is around -0.6 m a^{-1}. Because of mountain shading and wind deposition patterns, the concept of an equilibrium line altitude (ELA) is ill-defined on this glacier: the equilibrium line spans an elevation range of 350 m on average (Trabant and Benson, 1986, Rabus and others, 1995). The mean annual air temperature is about -12 °C at 1700 m elevation.

Ice temperatures in the accumulation area are between -1 and -1.5 °C both near the surface and at the base (Orvig, 1963). In the ablation area, surface ice temperature is less than -10 °C but the basal ice is temperate at least in the vicinity of the centerline. By extrapolation of a deep temperature profile at cross section T6 (Figure II.2), Trabant and others (1975) predicted the 0° isotherm to be at 120 m. The present ice depth at T6, corrected for the known thinning of the glacier since 1972, suggests a basal layer of temperate ice that is about 30 m thick at this location (Rabus and others, 1995). Surface temperatures indicate that this temperate layer exists beneath much of the ablation area, at

least near the centerline. Such an extensive temperate layer has been measured in the ablation area of polythermal White Glacier by Blatter(1987).

The drainage system in the upper two-thirds of the glacier is almost entirely supraglacial. Meltwater drains by means of two major surface streams, one located near the centerline of the glacier and the other on the east side of the glacier. Both streams originate at about 2200 m elevation in the lower and upper cirque, respectively. Below the confluence of the cirques the central stream becomes strongly meandering and deeply incised (>10 m); it becomes englacial at about 1950 m elevation, or about 3.5 km from the snout. The drainage pattern observed in the 1990s is similar to the one described by Sater (1959). Crevasses in the upper ablation area, mainly formed during the cold season, fill with meltwater during summer. While this process might contribute to accumulation within the glacier, the dimensions of the crevasses (mostly < 0.5 m) seem too small to facilitate meltwater input to the bed.

Previous studies of the surface velocity field of McCall Glacier, along with those of the surface geometry and mass and energy balance, were made during the International Geophysical Year (IGY) in 1957/58 (e.g. Sater 1959) and during the period 1969 to 1975 (e.g. Wendler and others, 1972 and 1974). Our continuing investigations began in 1993 (Rabus and others, 1995), with measurements of surface and bed geometry, mass balance, meteorological variables, ice temperature, and ice velocity.

II.3. Geometry of the glacier

II.3.1 Ice thickness

The thickness of McCall Glacier was determined in June 1993 by radio echo sounding along two longitudinal and eight transverse profiles. A portable monopulse radar system operating at 10 MHz provided unambiguous identification of the ice/bedrock interface. Transmitter and receiver were placed 50 m apart at each of the surveyed measurement sites shown in Figure II.1. For a given bedrock echo, the locus of possible reflectors was taken to be a semi-ellipse, with transmitter and receiver at the focal points (Echelmeyer,

unpublished). In this method the bed along a given profile is found as the envelope of these intersecting ellipses. This method naturally smoothes the actual bottom topography at a scale related to the spacing of the measurements, which in our case was 100 to 200 m. Accuracy of the ice thickness measurements was conservatively estimated to ±10 m; this error is mainly a result of timing errors. The speed of electromagnetic waves in ice depends only weakly on ice temperature and fabric; we use a constant value of 168 m μs^{-1} (Paterson, 1981).

Cross sections and longitudinal profiles of the glacier obtained from the radio echo sounding are shown in Figure II.2. The contour map of bed geometry in Figure II.1 was constructed by kriging the combined data set of the radio echo sounding results and the mapped topography of the unglacierized valley (U.S. Geological Survey 1:63,360 map). The maximum ice thickness is 250 m in the pronounced overdeepening of the lower cirque. The average ice thickness along the centerline is about 140 m. There are marked asymmetries in the valley shape near the confluence of the shallow eastern cirques with the deeper lower cirque (cross section T10); these are reflected in the velocity profiles described later. The deep trough situated on the west side of the glacier above the confluence gradually shifts towards the center below the confluence.

In a later section we describe changes in annual ice velocity over time. As part of the interpretation of these changes, we need to know the changes in ice thickness since the 1970s. These changes were determined at about 55 locations on the glacier by comparing the surface elevation as surveyed in the 1970s by D. Trabant and C. Benson (unpublished) with that surveyed in the 1990s at the same horizontal position in space (Rabus and others, 1995). These elevation changes, and, therefore changes in ice thickness (assuming erosion of the bed to be small), are known to an accuracy of about ± 0.3 m. The observed thinning of the glacier increases almost exponentially with decreasing elevation, from about 4 m on the upper glacier to 42 m at the terminus (Rabus and others, 1995).

II.3.2 Surface slope

Knowledge of present and past surface slopes, in addition to ice thickness, is a prerequisite for an interpretation of the velocity field and its temporal changes. The present surface slopes were determined from two elevation profiles of McCall Glacier acquired in 1993 using an airborne laser profiling system (Echelmeyer and others, 1997). These profiles approximately follow the centerline, one descending through the upper cirque to the terminus and the second through the lower cirque. Surface elevation along these profiles is accurate to about 0.3 m, and measurements are spaced at approximately 1.5 m intervals along the flight path. Accurate surface slope can thus be derived on scales of 10 to several 100 meters. For application to the flow modeling described later, we have calculated the centerline surface slope over an averaging length of 150 m, corresponding to approximately one ice thickness. This averaging scale also corresponds approximately to the horizontal resolution of the depth measurements presented previously.

No continuous elevation profiles or topographic maps of this glacier were made in the 1970s, and the density of surveyed markers on the surface was insufficient to determine the surface slope everywhere over an averaging length of 150 m. However, a 1:10,000 topographic map with a 5-m contour interval was constructed from aerial photographs taken in 1958 (Brandenberger, 1959). The overall vertical accuracy of this map is probably on the order of ±10 m (Rabus and others,1995). For most areas of the glacier this error is a spatially slowly varying "offset" that should have little influence on the calculation of surface slopes over a distance of 150 m. Rabus and others (1995) have shown that more than 80% of the elevation change between 1958 and 1993 occurred between 1972 to 1993. Therefore, except in the terminal region, the 1958 surface slope should be a reasonable approximation to the surface slope in 1972. To check this approximation, we compared the surface slope between markers spaced 300 to 500 m apart, which were surveyed in 1972, with the surface slope measured on the 1958 map at about the same locations. Except for the lowermost 1.5 km of the glacier, differences are random and generally smaller than ±0.5°. For areas where the preceding statement about

vertical map accuracy is met, the random error of the map contours (±2.5 m) translates into a error of ±1° for the 1972 slope. For the 1993 slopes the error is ±0.3°.

The centerline surface slopes for the two time periods are shown in (Figure II.3). In this figure and throughout the paper, *s* is a curvilinear coordinate that follows the centerline of the glacier, extending from the upper or lower cirque to the terminus, as indicated in Figure II.1. Like many other valley glaciers in the region, McCall Glacier shows an interesting periodic succession of maxima and minima of surface slope. These bulges are accompanied by an almost linear increase in average slope towards the snout. There is a similar, but proportionally smaller, variation in ice thickness along the glacier. The wavelength of these oscillations is about 1500 m, or approximately 11 ice thicknesses. While some of the steeper and thinner reaches of the glacier may be caused by resistant bedrock ridges along the valley walls (Figure II.1), there is not a one-to-one correspondence between the waves of the glacier and these ridges.

According to Hooke (1991), waves in glacier beds initially stem from bedrock inhomogeneities, but the series of ridges and overdeepenings then tends to be enhanced by a positive feedback of erosion with subglacial water pressure. At the headwall of overdeepenings, abrupt variations in water pressure cause erosion by quarrying. On the downglacier side of an overdeepening the reversed bed slope causes a constant, high water pressure that inhibits the formation of subglacial channels, thus minimizing erosion there. This process then causes amplification and broadening of the overdeepenings.

An alternative theory that explains regular oscillations in valley glacier geometry, without the help of existing bedrock inhomogeneities, is the one proposed by Mazo (1989). He studied the coupled system between the flow of a glacier and the erosion of its bed. Bed geometry determines glacier geometry, which in turn controls the erosion of the bed through the distribution of basal shear stress. For a glacier with an initially uniform thickness h and a constant bed slope θ, a small sinusoidal perturbation in θ produces a corresponding oscillation in h. The oscillation in ice thickness then translates into a variation of basal erosion at the same wavelength but generally out of phase with respect

to the initial disturbance. As a result, the disturbance in the bed migrates upglacier with a speed that depends on its wavelength, and the amplitude of the disturbance generally remains small. However, there is one wavelength, $\lambda = 2h/\tan\theta$, that is stationary and whose amplitude grows by "constructive erosion". For McCall Glacier the mean bed slope is $\langle\theta\rangle = \langle\alpha\rangle \approx 7.6°$ and the mean thickness $\langle h\rangle$ is 140 m. Here α is the surface slope. This leads to $\lambda \approx 15h$, or about 2100 m. Considering the approximate nature of Mazo's (1989) theory, this is reasonably close to the observed wavelength of the topographic wave.

Transversely-averaged surface slopes in 1993 are also shown in Figure II.3. Transverse variations in surface slope lead to transverse shear stress gradients, and, consequently, a transverse average of surface slope should enter into one-dimensional longitudinal flow analyses, such as that presented later. These slopes were obtained by averaging the longitudinal surface slope across a 500 m-wide swath about the centerline. We assumed that the ratio of the transversely averaged slope to the centerline slope did not change since 1958. The transversely averaged slope is not significantly different from the centerline value except at two local maxima located at centerline positions of 2500 and 5200 m, where the two measures of slope differ by about 0.5 to 1°.

As seen in Figure II.3, there was a general steepening of up to 2° along the lower glacier from 1972 to 1993. This is a product of the observed thinning (Rabus and others, 1995). Such steepening should, to some extent, counterbalance the effects of the observed decrease in thickness on the ice velocity in this region of the glacier. The 1993 terminus (s= 7000 m, Figure II.1) was considerably less steep than the terminus shown on the 1958 map (at s = 7370 m). The terminus slope in 1972 is clearly not well represented on the 1958 map because of the ca. 8 m thinning and 70 m horizontal retreat from 1958 to 1972. On the upper glacier (above 1700 m centerline distance), the large differences between 1972 and 1993 slopes are artifacts of known errors in the 1958 topographic map (Rabus and others, 1995).

II.3.3 Thrust faults

Conspicuous features in the mid to lower ablation area of McCall Glacier are discontinuities in the ice that extend over much of the glacier's width (Wakahama and Tusima, 1981; Shapiro, pers. comm.). These discontinuities form downglacier arcs and are marked by dirt-laden ice bands. They dip upglacier at shallow angles of about 30°. Topographic steps at these bands sometimes occur, with the upglacier sides being up to 30 cm higher than the downglacier sides. Also observed are dirt-laden lateral discontinuities, some ten meters from the ice edge, that parallel the eastern margin of the glacier over several km. Both types of discontinuities resemble the surface expressions of the spoon-shaped thrust faults observed by McCall (1952) on cirque glaciers. Several alternative explanations have been proposed for these features: 1) movement across a thrust fault in the ice, perhaps facilitated by differing rheological properties of the dirt-laden ice (e.g. Nye, 1951); 2) differential ablation caused by albedo differences of dirty and clean ice, and the accumulation of heat-absorbing dust on the downglacier side of the discontinuity; and 3) former crevasses that have been closed and are deformed by viscous flow. The latter explanation can be ruled out on McCall Glacier as there are no large crevasses which could be the predecessors of the observed surface features.

About 20-30 of these features are found in a region of the glacier (s = 4000 to 6000 m) where modeling suggests a high, non-plastic contribution to the flow. This contribution is likely due to year-round basal sliding, but alternatively might be caused by displacement across such faults. To investigate the latter idea, we made measurements on three such "faults" in this region in order to determine whether significant differential motion exists across them. Pairs of wooden poles were drilled vertically into the ice, about 1 m apart, above and below the faults. Each fault had a well-developed vertical offset. Relative motion between the pairs of poles was carefully determined over a one-year period. At two of the sites there was no differential motion, and at the third there was a convergence of 0.03 ± 0.01 m. Total surface displacement at each of these sites during the same time period was on the order of 10-15 m a^{-1} . The average longitudinal strain rate in this region

was about 0.005 a^{-1}, corresponding to a net convergence of 10 m a^{-1} over a 2 km stretch. These measurements thus show that, if there were 30 such faults, a maximum of 30 × 0.03 m a^{-1} = 0.9 m a^{-1}, or less than 1% of the net convergence in this region, is due to strain on the "thrust faults". This lack of significant strain agrees with measurements made on similar features found on Barnes Ice Cap (Baker, 1986). Either such features are entirely passive, or they form by shear displacement over a relatively short time interval and then become inactive. In support of the latter mechanism, a new fault was observed to form on Hubley Glacier (3 km SE of McCall Glacier) over a four week period in an area that was previously undisturbed (Figure II.4a and b). The fault showed an offset of about 0.4 m and it extended laterally over several hundred meters in clean ice. It had an upglacier dip of about 20 to 30°. Along this particular fault there appeared to be little or no dirty ice concentrated on the actual fault surface. No obvious dirt band had been observed before the offset formed, and thus differential ablation could not have caused it.

II.4. Ice Velocity

II.4.1 Velocity measurements

Ice velocity was first measured on McCall Glacier by Sater (1958). An unfortunate choice of survey geometry caused substantial errors in his data, and the 1957 reference frame is not given, so that these results could not be compared with later measurements. From 1969 to 1972 an extensive mass balance network was maintained on McCall Glacier (Wendler and others, 1972; Trabant and Benson 1986). The marker poles in this network were frequently surveyed by theodolite triangulation (Trabant, unpublished). We used this raw survey data to calculate mean annual surface velocities between 1970 and 1972. In some cases we also were able to calculate seasonal velocities for the two month period from mid-June to mid-August, 1971. Our analysis of the 1970s surveying data leads to an estimate of about ±0.3 m a^{-1} for the accuracy of the 1970s annual velocities.

In 1993, a number of poles were emplaced in the ice at a subset of the 1970 locations. These were carefully surveyed two to five times a year during early June to mid

August until 1995, and both annual and seasonal velocities were derived. The surveys were carried out using a 1-second theodolite and electronic distance meter. Based on an error of 5 mm in distance and 2 arcseconds in angle, we found typical errors of ±0.02 m a^{-1} for annual velocity, and 0.45 m a^{-1} for velocities determined over a ten-day period. Corresponding azimuthal accuracies are 1° and 10° for the annual and short-term velocity vectors, respectively. We used the same network control as in the 1970s; this was resurveyed with Global Positioning System (GPS) methods in 1993. This allowed justification of the 1970s and 1990s surveys in an absolute coordinate frame, consisting of UTM Northing and Easting and height above the WGS84 ellipsoid.

II.4.2 Horizontal velocities: general characteristics

Figure II.5 shows velocity vectors, averaged over the entire period of measurement 1993-95 (heavy arrows) and over a period of high melt, from 3 to 24 July 1993 (light arrows). In Figure II.6, mean annual velocities from 1993 to 1995 along the centerline are shown together with those of 1970-72. Annual velocity along the centerline reaches a maximum of 16-18 m a^{-1} at $s = 4000$ m, just downglacier of a pronounced narrowing and shallowing of the channel (Figure II.1). A second local maximum of about 14 m a^{-1} occurs over another bedrock threshold at $s = 2300$ m, while a shallow velocity minimum at $s = 3000$ m corresponds to thicker ice. The local velocity maximum at $s = 2300$ m seems to be associated with the "steady state" equilibrium line, approximated by the boundary of the ablation zone in 1970 (stippled area in Figure II.5), when McCall Glacier had a mass balance close to zero (Trabant and Benson, 1986). Centerline velocities in the 1970s show the same pattern as in the 1990s, but there was an additional local maximum around $s = 5200$ m. In a later section we calculate the change in velocity from the 1970s to the 1990s using changes in ice thickness and surface slope. Our calculations predict that the maximum at s=5200 m would disappear in the 1990s and that there would be no upglacier migration of the other two velocity maxima (open symbols on the 1990s velocity curve in Figure II.6).

Transverse profiles of mean annual velocity are presented in Figure II.7. Solid and dotted lines represent the annual averages 1993-95 and 1970-72, respectively. Both the actual velocity vectors, as well as their decomposition in components parallel and perpendicular to the central flow line, are shown. Note that velocity was not measured at the glacier margins, but was set arbitrarily to zero there. All velocity profiles, except T6, are parabolic in shape. This suggests that flow occurs primarily by ice deformation. The T6 velocity profile is somewhat more plug-shaped, hinting at significant sliding there. Transverse velocities are small at T3, T6 and T11. At T20, where the combined flow of upper and middle cirques spreads into the confluence area, the transverse velocities show divergence. In contrast, there is pronounced convergence at T10, where the ice of the confluence is focused into the main trunk of the glacier. The small velocity changes between the 1970s and 1990s at T10, T11 and T20 will be discussed later.

In Figure II.8, we compare mean annual and seasonally averaged velocities from 1993 to 1995. A detailed discussion of seasonal velocity fluctuations will follow in a later section; here we make some general remarks. Annual velocities and those measured during winter and spring are all similar (filled symbols in Figure II.8), while velocities observed during the melt season (small, unfilled symbols) are considerably higher. It is interesting that these elevated seasonal velocities tend to peak near s = 2300 m rather than at s = 4000 m, where the annual velocity has its maximum. Short-term velocities during periods of intense melt (large, unfilled symbols) also show this tendency of an overall upglacier shift of the region of maximum velocities. The highest measured velocity was 28 m a^{-1} at s = 2880 m, averaged over a period of seven days during summer 1995.

II.4.3 Longitudinal strain rate and climatic regime

The velocity field of McCall Glacier is characterized by small longitudinal strain rates ($\dot{\varepsilon}_{xx} \leq 0.004$ a^{-1}); these are about an order of magnitude less than those typically found on temperate glaciers. Here we show that these small strain rates reflect the arctic climate regime of the glacier, as characterized by a small mass balance gradient with elevation, $\partial \dot{b} / \partial z$.

The mass balance rate at a longitudinal position s on a glacier of constant width w and bed slope β is given by $\dot{b}(s) = (\partial\dot{b}/\partial z)w\beta(s_{EL}-s)$, where s_{EL} is the position of the equilibrium line relative to the glacier head (s = 0). Here we have neglected the small contribution to elevation difference that arises from changes in ice thickness along the glacier. In this approximation the steady state length is $L = 2s_{EL}$, and the flux at the equilibrium line is

$$q_{EL} = \frac{wL^2}{8}\beta(\partial\dot{b}/\partial z).$$

The mean longitudinal strain rate (absolute value) along the glacier is given by $\langle|\dot{\varepsilon}_{xx}|\rangle = 2u_{EL}/L \approx 2\frac{n+2}{n+1}q_{EL}/(wh_{EL}L)$, where u_{EL} and h_{EL} are the surface velocity and ice depth at the equilibrium line, respectively and we have assumed a power law rheology. For $n = 3$ we find

(1) $$\langle|\dot{\varepsilon}_{xx}|\rangle \approx \frac{5L\beta(\partial\dot{b}/\partial z)}{16h_{EL}}$$

This shows that the average longitudinal strain rate is proportional to the mass balance gradient. (A similar result for the local value of longitudinal strain rate was obtained by Nye, 1957). Arctic glaciers therefore show smaller longitudinal strain rates than temperate glaciers with similar geometry.

A complication in Equation (1) is that h_{EL} itself depends on L, β and $\partial\dot{b}/\partial z$, and the flow law parameter A. We may take this into account by noting that, for slopes steeper than about 5° , β is approximately equal to the surface slope at the equilibrium line, α_{EL} . Then, assuming deformational flow only, $h_{EL} \propto (q_{EL}/\beta^n)^{\frac{1}{n+2}}$ and, using Equation (1), we find

(2) $$\langle|\dot{\varepsilon}_{xx}|\rangle \propto L^{3/5}\beta^{7/5}(\partial\dot{b}/\partial z)^{4/5}A^{1/5}$$

Lower ice temperatures of arctic glaciers lead to smaller values of A, and this will add to the effects of smaller balance gradients in decreasing the mean strain rate.

As a comparative example, we calculate longitudinal strain rates using Equation (1) for two glaciers: McCall, with $\partial \dot{b}/\partial z$ = 1.9 m a^{-1} km^{-1}, $\beta = 7.6°$, h_{EL} = 220 m, and L = 7.8 km; and subarctic Storglaciaren, a glacier in northern Sweden which has a significantly larger mass balance gradient ($\partial \dot{b}/\partial z$ = 10.0 ma^{-1} km^{-1} ,evaluated from Haeberli and others, 1993) and somewhat different geometry: $\beta = 6.3°$, h_{EL} = 165 m, L = 3.8 km (evaluated from Hooke, 1989). For McCall Glacier, $\langle|\dot{\varepsilon}_{xx}|\rangle$ = 0.0028 , while for Storglaciaren $\langle|\dot{\varepsilon}_{xx}|\rangle$ = 0.0079. These calculated values agree reasonably well with those observed (0.0036 and 0.0111, respectively, as determined from $2u_{EL}/L$, and u_{EL} = 14 m a^{-1} on McCall and u_{EL} = 21 m a^{-1} on Storglaciaren (Hooke, 1989)). The larger strain rates on Storglaciaren are a direct effect of a larger mass balance gradient (i.e. a warmer climate) there. The smaller bed slope and length of Storglaciaren will decrease the mean strain rate somewhat relative to that on McCall Glacier, but the climatic effect dominates.

II.4.4 Emergence velocities

Emergence velocity, defined as the vertical rise or subsidence of the ice at a given horizontal position, can be calculated as

$$v_E = v - u_H \tan\alpha_l \quad , \tag{3}$$

where u_H and v are horizontal and vertical velocity components of a marker pole, and α_l is the local surface slope in the flow direction. Measurements of emergence velocity can be used to evaluate effects of vertical advection on the ice temperature distribution of a glacier or to determine the longitudinal ice flux $q(s)$ by using the continuity equation. Relative errors in v_E are generally larger than errors in u_H, due to the fact that emergence velocities are at least an order of magnitude smaller than u_H and because of additional uncertainties in v and α_l. Emergence velocities, calculated from Equation (3) for a number of poles along the centerline, are shown as open circles in Figure II.9. Local surface slopes over distances of 25-40 m were obtained from a kinematic GPS profile along the glacier

that passed through the poles. Maximum errors in the emergence velocity are 0.15 m a^{-1}, as indicated.

Average emergence over the width of the glacier can also be obtained indirectly from the difference between annual elevation change and the mass balance rate, each averaged over *w*:

$$\langle v_E \rangle_w = \langle \partial h / \partial t \rangle_w - \langle \dot{b} \rangle_w \quad (4)$$

The broken line in Figure II.9 shows emergence velocities, calculated from Equation (4), using mean elevation change and mass balance during 1993-95. Both methods suggest that vE has a maximum of about 0.5 m a-1 at around s = 4000 m. Emergence at the centerline is consistently higher than the width-averaged value. This is to be expected because the equilibrium line of McCall Glacier is not perpendicular to the center line (Figure II.5). This leads to (negative) accumulation area contributions in the width average of emergence velocity upglacier of s = 3000 m, while the centerline itself is in the ablation area till about s = 500 m. In particular, the negative emergence velocity between TU and T20 calculated from Equation (4) is caused by including the entire accumulation bowl of the middle cirque in the width average. Furthermore, an upglacier shift of the equilibrium line leads to emergence velocities that are temporarily higher at the centerline than at the margins because the glacier needs to build a crown in the new ablation area. For McCall Glacier this effect might partly account for centerline emergence being higher than width-averaged emergence between cross sections T9 and T6.

II.4.5 Analysis of surface velocity

It is generally assumed that there is little or no basal sliding beneath cold-based glaciers (e.g. Echelmeyer and Zhongxiang, 1987). However, for a polythermal glacier whose base is at least locally at the melting point, basal sliding could be significant. In order to investigate this, we analyze the deformational speed, u_d, of McCall Glacier in terms of ice geometry.

Following Nye (1965), the centerline surface speed of a glacier flowing without sliding in a channel of parabolic cross section is given by

$$u_d = \frac{2A}{n+1}(\rho g f \sin\alpha)^n h^{n+1} \tag{5}$$

where ρ is the density of ice, g the acceleration of gravity, n = 3 the flow law exponent, A the flow law parameter, h the local centerline ice thickness, α the local surface slope, and f is a shape factor that depends on the width to depth ratio of the channel. If ice temperature varies with depth, $T=T(z)$, an effective depth-weighted flow parameter

$$A_{eff} = \frac{(n+1)}{h^{n+1}} \int_0^h A(T(z)) z^n dz \tag{6}$$

that produces the correct surface value of u_d in Equation (5) can be used. Because we do not know how the temperature-depth profile varies along the channel, we use $T(z)$, as was determined at cross section T6 by Trabant and others (1975). Using this temperature profile and $A(T)$ as given by Paterson (1981), we obtain A_{eff} = 0.179 a^{-1} bar^{-3}, which corresponds to an effective ice temperature of -0.5 °C. In reality, A may vary along the glacier, especially as the thickness of the temperate layer at the bed varies, but it should be between 0.145 (for an ice column at -1 °C) and 0.194 (for a 50 m temperate layer beneath ice at -5 °C).

Surface speed along the glacier was calculated from Equation (5) using local ice thickness and surface slope as evaluated along the centerline at 150 m intervals (Figures II.2 and II.3, respectively). The parameters are shown together with the channel shape factor in Figure II.10a. The shape factor was interpolated as a function of s by assuming a best-fit parabola at each cross section in Figure II.2. The fit between Equation (5) and the observed speed is poor (Figure II.10b). It is unlikely that the quality of the fit can be improved by reasonable variations in A, and, as the deviation between the calculated and observed speed is highly variable, it is equally unlikely that the fit can be improved by including fluctuations in basal sliding at this stage.

The large variations in surface slope and ice thickness give rise to longitudinal stress gradients, which require modification of Equation (5). Following the analysis of Kamb and

Echelmeyer (1986), the deformational velocity of a glacier with small perturbations in slope and thickness is given by an exponentially-weighted average of these perturbations along the glacier length L:

$$(7) \qquad u_d = u_d^{(0)} + \frac{u_d^{(0)}}{2l} \int_0^L \Delta \ln(\alpha^n f^n h^{n+1}) \exp(-|s'-s| / l) ds' \quad .$$

Here $u_d^{(0)}$ is the velocity defined for some average parallel-sided datum state and Δ specifies deviations from this datum state (e.g. $\Delta \ln h^n = \ln h^n - \ln h_0^n$ for ice thickness $h(s)$ and the datum thickness h_0). The range of the stress coupling is governed by the characteristic length, l, of the exponential averaging kernel. For temperate glaciers with typical longitudinal strain rates of 0.01 to 0.05 a^{-1}, l is about 1.5 to 2.5 times the ice thickness. The strain rates on McCall Glacier are smaller (0.003 - 0.005 a^{-1}), being an indirect effect of the small mass balance gradient of the glacier, as discussed above. The low strain rates lead to a longer averaging length for McCall Glacier of 3.0 to 3.5 times the mean ice thickness.

In applying Equation (7) to McCall Glacier we recast it in a computationally more efficient form [Kamb and Echelmeyer (1986), Eqn. (35)], in which the datum state is defined by the average thickness, surface slope and shape factor at one representative location where the surface velocity u_0 is known. The velocity at any other location along the glacier may then be determined by integration from this datum state. This procedure was applied to the local parameters given in Figure II.10c for $l = 3.0h$ (results for a typical "temperate" coupling length, $l = 1.8h$, are shown as a dashed line for comparison). The fit to the observed speed is much improved over that resulting from Equation (5). However, in the middle reaches of the glacier, between s = 4000 and 5000 m, the fit is not good, as the modeled speed is less than two-thirds the observed speed. Unlike other parts of the glacier, where decreasing depth is largely counterbalanced by increasing surface slope, here depth and slope decrease almost simultaneously from s=3800 to 4800 m (Figure II.10a). This leads to a low predicted deformational speed in this region.

Use of the transverse-average surface slope, as defined in the preceding paragraph, gives no significant improvement. The same is true if longitudinal variations of the flow law parameter A are introduced. An upglacier increase of A, which accounts for possible warming in the accumulation area caused by refreezing of meltwater, makes the fit worse. Using A for T= 0 °C between s = 4000 and s = 5000 m, and A at T= -2 °C elsewhere (admitting that the observed layer of temperate basal ice could be a local phenomenon), yields modeled velocities which are still about 25% too low. Finally, any observed motion on the thrust faults in this region is insufficient to explain the anomalous speed there.

The most likely explanation for the high velocities is a significant contribution of sliding at the temperate bed underlying the mid-glacier region. Introduction of such sliding *a priori* into the longitudinal averaging of Equation (7), following the procedures outlined by Kamb and Echelmeyer (1986), produces excellent agreement between modeled and measured velocities along the entire glacier (Figure II.10d). While the details of the sliding distribution are not unique, the main features of u_B are well constrained: u_B must be concentrated at the center of the velocity anomaly, and it must account for the major part of ice motion there. As was mentioned before, the transverse velocity profile at cross section T6 (Figure II.7) shows more of a "plug" shape, which independently suggests significant sliding in this region. Thus, we infer that significant sliding occurs over this one region of the glacier, but little sliding need occur elsewhere.

II.4.6 Surface expression of a sliding anomaly

How is localized basal sliding reflected in the surface profile of a glacier? To investigate this question we develop a relation between $h(s)$ and $\alpha(s)$ and the measured ice flux, $q(s)$, prescribed bed geometry, $z_b(s)$, and an estimated sliding velocity, $u_B(s)$. We then apply this relation to an idealized glacier with constant bed slope and flux gradient to illustrate the general topographic features associated with a sliding anomaly. This is followed with an application to the actual geometry and flux of McCall Glacier. The approach is complementary to the one in the previous section, in which measured h and α were given as inputs into Equation (7) to determine u_s.

The flux q through cross section $S(s)$ is not calculated from velocity measurements, which we only have at the ice surface. Rather, it is obtained from measured annual elevation change $\partial h/\partial t$ and mass balance $\dot{b}$ at a given time via mass continuity:

$$\frac{\partial q}{\partial s} = \int \left(\partial h / \partial t - \dot{b} \right) dw \quad . \tag{8}$$

The left hand side of Equation (8) equals the emergence velocity $\langle v_E \rangle_w$, averaged over the width of the glacier, w (Equation 4 and Figure II.9). $\langle v_E \rangle_w$ is insensitive to the particular time period that is used to determine $\partial h/\partial t$ and $\dot{b}$ because inter-annual variations of these data sets are synchronous and tend to cancel out. We use an average of 1994 and 1995 values. The flux, integrated from Equation (8), can be separated into contributions from cross-sectionally averaged ice deformation and sliding according to

$$q = \left(\langle u_d \rangle_S + u_B \right) S \quad . \tag{9}$$

For a parabolic cross section we have $S=(2/3)hw$, and for the simple deformational flow given in Equation (5) we have $\langle u_d \rangle_S = f_1 u_d$ with a second shape factor f_1 from Nye (1965). While f and f_1 depend weakly on the dimensions of the cross section, they are here approximated by their mean values for the cross sections in Figure II.2. For small surface slopes, $\alpha \approx \partial(z_b + h) / \partial s$, and from Equations (5), (8) and (9) we obtain

$$\frac{\partial h}{\partial s} = \frac{1}{f \rho g} \left(\frac{n+1}{2 A f_1} \right)^{1/n} \left(\frac{3}{2w} \int_0^s w \left[\left\langle \frac{\partial h}{\partial t} \right\rangle_w - \langle \dot{b} \rangle_w \right] ds' - u_B \, h \right)^{1/n} h^{-1-2/n} - \frac{\partial z_b}{\partial s} \quad . \tag{10}$$

Equation (10) can be used to solve for the surface geometry, $z_s = z_b + h$, given $\partial h/\partial t$ and $\dot{b}$. This surface geometry will depend on the prescribed distribution of sliding velocity. In a different approach, Balise and Raymond (1985) calculated how the sudden temporal onset of a basal sliding anomaly changes the patterns of horizontal and emergence velocity for a linearly viscous parallel slab. Contrary to our method, they used glacier geometry as input to calculate emergence velocity. Their emergence velocity was no longer consistent with the given glacier geometry after initiation of sliding.

The ordinary differential Equation (10) was numerically integrated upglacier from $s=L$ using a constant effective flow parameter A_{eff} (Eqn. 6) and $n=3$. The glacier snout

was treated as a rigid wedge with constant velocity to avoid the singularity at $s=L$, where h goes to zero.

As a first example of the influence of localized sliding on ice thickness and surface topography, we consider a constant bed slope of 6.3°, equal to the mean bed slope of the modeled section of McCall Glacier, and a constant emergence velocity $< v_E >_w = +0.75$ m a^{-1}. Changes in ice thickness and surface slope relative to the no-sliding case are denoted by Δh and $\Delta\alpha$, respectively; as the bed z_b is fixed ($\Delta z_b = 0$), we have $\Delta\alpha = \partial(\Delta h)/\partial x$. The effect of gaussian-shaped sliding anomalies of different widths is illustrated in Figure II.11a. There is a decrease in ice thickness within a limited region around the sliding anomaly relative to the no-sliding case (labeled as curve "0"). The maximum of $|\Delta h|$ is located upglacier of the maximum sliding speed and $|\Delta h|$ is non-zero well upglacier of the sliding anomaly but not downglacier of it. For the narrow anomaly there is an abrupt decrease in surface slope. The wider anomaly shows a corresponding decrease in slope at its center, but an increase upstream of center. The rectangular sliding anomaly shown in Figure II.11b consists of two opposite step changes in u_B. These steps asymptotically cause constant upglacier offsets in ice thickness (of opposite sign). In terms of their effect on deformational velocity, the observed changes in h and α restore the (prescribed) total mass flux within and around the region that transports mass by sliding. Smaller ice thickness upglacier and outside the sliding anomaly requires a higher overall ice velocity; this is achieved by an increased surface slope there. Within the sliding anomaly deformational velocity must decrease, and this is accompanied by decreasing ice thickness and surface slope.

Next we solved Equation (10) for the measured bed profile and emergence velocity of McCall Glacier ($v_E = <\partial h/\partial t - \dot{b}>$ in Figure II.9). The results for no sliding anomaly are shown in Figure II.12a, together with measured ice thickness and surface slope (dashed lines). These solutions for h and α differ markedly from the measured quantities in the anomalous region $s = 4000$ m to $s = 5000$ m: h is too large there and α is too large in the lower part and too small in the upper part of the anomalous region. This resembles

qualitatively the typical "fingerprint" of a sliding anomaly found above (Figure II.11). The surface expression of a trapezoidal sliding anomaly similar to the one proposed in the previous section is shown in Figure II.12b. There is excellent quantitative agreement between calculated and measured ice thicknesses and surface slopes.

The effect of longitudinal stresses and sliding was equally important when flow was modeled directly from measured h and α in Equation (7). However, longitudinal stresses have a far less profound effect on the solutions h and α from Equation (10) than sliding does. The reason for this asymmetry is that flow depends sensitively on measured ice thickness and surface slope, $q \propto h^{n+2} \alpha^n$,while the change in ice thickness depends only weakly on flux, $\partial h/\partial s \propto q^{1/n}$. Solutions of Equation (10) are therefore relatively insensitive to small variations in q. The flux itself is an integral of the measured emergence velocity, which introduces further smoothing in Equation (10).

An important result of this section and the previous one is that there exists localized sliding at the base of this polythermal glacier over a 2 km long region that accounts for up to 70 % of the annual ice flux there. The measured velocity increase during the short summer season (Figure II.8)[SIaP1] can account for at most 5-7% of the annual ice flux and thus the glacier must slide year-round at an almost uniform rate. Why does the glacier slide in this region but not in others? One reason could be that just upglacier of the anomalous region the largest superglacial stream on McCall Glacier disappears beneath the surface. From the analysis of Shreve (1972) the englacial channel should dip at about 11 times the surface slope, or at least 70°. Surface water could therefore reach the bed near the beginning of the anomalous region and facilitate sliding there. However, there is no water flow from September to May. Perhaps there is significant water storage and correspondingly high water pressures throughout the winter.

II.4.7 Long-term changes of annual velocity between the 1970s and 1990s

Annual velocities on the lower glacier have changed markedly since the 1970s (Figure II.6 and diamond symbols in Figure II.13). To determine whether these changes can be quantitatively understood from corresponding changes in the geometry of the glacier, we

calculate the expected variations in deformational ice velocity (Eqn. 5) that arise from small changes in surface slope, $\Delta\alpha$, and ice thickness, Δh. To first order this variation is given as

$$\frac{\Delta u}{u} = (n + 1)\frac{\Delta h}{h} + n\frac{\Delta \alpha}{\alpha} \quad . \tag{11}$$

The local values of $\Delta u/u$, calculated from Equation (11) with n=3 (heavy solid line) are compared with the observed velocity changes in Figure II.13. Measured $\Delta h/h$ and $\Delta\alpha/\alpha$, represented by solid and dotted lines, respectively, were both averaged over 300 m or about two times the ice thickness. The agreement over the entire lower ablation area is quite good. Between T9 and T10 observed $\Delta u/u$ is close to zero while the calculated value is negative because the surface slope appears to have decreased. This apparent decrease is caused by the extrapolated 1970s slope being erroneously high due to known inaccuracies of the 1958 topographic map in this region.

While effects of localized sliding and longitudinal stress coupling are important to understand the flow of McCall Glacier, *changes* in flow are apparently well represented by Equation (11), which neglects these effects. As a consequence, any change in the spatial distributions of basal sliding and longitudinal stress since the 1970s must have been small.

Velocity profiles across T10, T11 and T20 (Figure II.7) all show subtle changes from the 1970s to the 1990s. As the horizontal positions of poles in 1993 where chosen identical to those in 1972, these changes are likely real. The velocity at T11 actually increased by 5% despite the observed thinning of about 5 m since 1972 at that location. Surface slopes from the 1970s are not available in this region, so we cannot determine whether it is a change in surface slope or in the seasonal sliding rate that offsets the effects of thickness change across T11.

II.4.8 Spatial pattern of seasonal velocity fluctuations on McCall Glacier

The higher velocities which we observed during the melt season (Figure II.8) are likely due to temporal increases in the rate of sliding as a result of melt-water production from

early June to early August. To study the spatial pattern of enhanced ice motion, we calculate the differences Δu_s between seasonal velocities and average winter velocity for the years 1993-95. Seasonal velocity is evaluated from the first to the last survey in a given year. Almost the entire melt season is covered by the 1995 "summer season" (20 June to 11 August) while the 1993 "summer season" (3 to 24 July) represents a warm period with higher than average ablation and the 1994 (11 June to 5 July) data span a cold period with very little melt.

The seasonal difference Δu_s from the winter velocity is shown in Figure II.14b. In 1995, Δu_s had a maximum near cross section T10, well upglacier of the maximum in u_w. The ratio $\Delta u_s / u_w$ shows a minimum close to the position of the maximum in u_w and it reaches maxima in the lower ablation area and above the equilibrium line. While the percentage increase in velocity is relatively large, the short duration of the "summer season" leads to only a small additional displacement in the summer season. Thus, only 3% of the annual ice flux in the lower ablation area and 5% at the equilibrium line are due to the extra motion in summer.

During the warm measurement period in 1993 the spatial patterns of Δu_s and $\Delta u_s / u_w$ on the lower glacier were similar to 1995, but above T9 the short term velocity was greater than in 1995. During the cold spell in 1994 the patterns of Δu_s and $\Delta u_s / u_w$ were different than those in 1993 and 1995. A limited region between T3 and T6 showed a velocity increase, while the lowermost glacier and the confluence region had velocities that are lower than the winter average.

The pattern of Δu_s observed during the cold spell in June 1994 may possibly be typical for the early stages of the ablation season. Speed-up starts between T3 and T6, where the presence of a temperate basal layer with finite thickness prevents the glacier from freezing to the bed in winter. As the melt season progresses, the region of strongest velocity increase is shifted upglacier as indicated in the 1993 and 1995 patterns of Δu_s. We can only speculate on how this shift is accomplished. A possible mechanism could be an upglacier migration of the zone of highest melt-water input during the progressing melt

season. However, upglacier of s=3500 m there are no moulins or deep crevasses that might facilitate meltwater passage to the bed. Andreason (1985) has proposed that a velocity increase in the upper reaches of a polythermal glacier might be caused by the backing-up of melt-water along the glacier sole due to weak basal drainage on the lower glacier.

The relative summer speed-up over winter velocity, $\Delta u_s / u_w$ was also measured across profiles T6, T10, T11 and T20 during summer 1995 and for T10 in summer 1971 as well. In all cases $\Delta u_s / u_w$ showed little transverse variation. However, in 1971 $\Delta u_s / u_w$ at T10 was consistently smaller than in 1995.

II.4.9 Temporal variations in velocity and ablation for McCall and White Glacier

Short-term velocity measurements during summer 1995 allow us to investigate the relation between temporal changes in ablation and velocity on McCall Glacier. Figure II.15a shows velocity of the centerline poles at T11, T9, T6 and of a pole at the confluence of upper and middle cirque (UC/MC). For all poles, the velocity shown up to June 20 is an average from 5 July 1994, i.e. it approximately represents the mean annual velocity. Ablation at T11 is shown in the lower diagram of this figure; it was determined from a combination of direct measurements and an interpolation using air temperature. This ablation record applies qualitatively to most of the ablation area. It shows that melt-water generation ceased glacier-wide during a cold spell from 25 June to 1 July.

Velocity at T11 and UC/MC, averaged over the 8-day period containing the cold spell, is greater than mean annual velocity. Within the error of measurement, velocity maintains this elevated value when averaged over the next 7-day period when a maximum in the ablation rate occurred, and during the following 36-day period, when there were periods of high and low ablation. For the upper ablation area this suggests that there is no short-term causal direct relation between ablation and velocity.

Velocity at cross section T9, averaged over the period containing the cold spell, is smaller than mean annual velocity, while velocity during the subsequent period of high ablation shows an increase. There appears to be no time lag between ablation and velocity

in this mid-ablation area, at least at the resolution of the measurements. If velocity from 6 July to about 20 July would maintain the high value from the preceding period, velocity from 20 July to 13 August would be required to be less than the mean annual velocity, which does not seem reasonable. Therefore, at this site, sensitivity of velocity to ablation appears to *decrease* in the second half of the ablation season.

In order to bring out effects that are typical for polythermal glaciers, we compare our data with the high-time resolution record of horizontal velocity and ablation from White Glacier, Axel Heiberg Island, Canada (Iken, 1974). White and McCall Glaciers share the same arctic climate that limits significant ablation to early June through early August, with a prominent period of high melt in July. Ice surface temperatures and ice depth are similar, but White Glacier is longer (14.5 km), wider (1 km) and has a somewhat gentler slope (6°) than McCall Glacier. The measured velocities on White Glacier show maximum winter values of about 30-35 m a^{-1}. None of the observed profiles show features associated with year-round sliding. Seasonal velocity variations in the lower ablation area of White Glacier are shown in Figure II.15a. Ablation is also shown at the same scale as the velocity (heavy bars in lower part of figure). Following Iken (1974), the relation between ablation and velocity at this site can be summarized as follows: until early July, velocity lagged ablation by about 3 days. Thereafter, high ablation events and corresponding velocity peaks were synchronous. Velocity was more sensitive to high ablation events before the period of strong melt in early July than afterwards. With ceasing ablation, velocity generally dropped to a "constant" value in fall. This fall value was higher than the corresponding value in spring. Because of the limited time resolution of our data, we cannot determine if similar fine-scale correlations occur on McCall Glacier. Averaging the White Glacier data on the lower resolution of our data (heavy curve in Fig. 15b) clearly obscures the correlation between velocity and ablation.

Common features of seasonal velocity variations on McCall and White Glaciers are (i) a substantial seasonal velocity increase on both glaciers that contributes only a small fraction to the annual ice motion, (ii) at some locations, velocity may lag ablation by

several days, (iii) on the lower glacier, the sensitivity of the velocity to high ablation diminishes with the progress of the melt season, and (iv) minimum velocities are reached at the onset of the melt season and velocity in autumn is somewhat higher than this minimum.

However, there is a significant difference between the seasonal motion of the two glaciers. The magnitude of the extra motion due to seasonal sliding on White Glacier decreases monotonically upglacier from about 7% in the lower ablation area to about 1.4% at the equilibrium line, while on McCall Glacier the highest contributions of 5% were found near the equilibrium line.

II.4.10 Speculations on the velocity fluctuations of polythermal glaciers

Temperate glaciers reach their maximum velocity in early summer, while minimum velocities coincide with the end of the melt season. This is probably a consequence of the seasonal evolution of the englacial drainage network (Roethlisberger, 1972). In autumn, the englacial drainage channels (Roethlisberger- or R-channels) have their maximum diameters and melt-water input is small; this leads to low water pressure and minimum sliding velocities. In the course of winter, R-channel closure by creep causes a gradual increase in water pressure and consequent sliding velocity.

Polythermal glaciers (this paper; Iken, 1974; Andreason, 1985; Willis, 1995) seem to behave somewhat differently: (i) highest velocities occur during highest melt, (ii) velocities in the late melt season are higher than those at the beginning of the melt season when they actually seem to be at a minimum and (iii) at some locations in the upper ablation area there is evidence for a time lag of several days between ablation and velocity events. All three observations may be related to prolonged water storage in polythermal glaciers. This could, in turn, indicate that a mature R-channel network is absent during mid- to late summer. The short arctic ablation season, with surface melt rates comparable to those on temperate glaciers, may cause high basal melt-water input but insufficient time for any R-channels to enlarge. Secondly, the cold ice along the margins and at the terminus may lead

to poor subglacial drainage in the lower ablation area. This would prolong water storage. Such storage could extend upglacier and may explain why the observed summer speed-up affects regions that are far upglacier of the uppermost moulins, where water can potentially reach the bed. Some water is gradually released from storage during winter, as is evidenced by the growth of a large aufeis field in front of McCall Glacier in winter.

II.5. Conclusions

We conclude that the flow regime of polythermal glaciers in the Arctic is in many ways distinct from that of temperate and cold glaciers. These differences root in peculiarities of the Arctic climate that include a small mass balance gradient, strong seasonality of melt-water input and low temperatures that cause formation of a thick layer of cold ice overlaying a thin, discontinuous layer of temperate basal ice.

The small mass balance gradients of arctic glaciers leads to smaller longitudinal strain rates than those of temperate glaciers with similar geometry. This, in turn, leads to longer coupling lengths for longitudinal stresses. In the case of McCall Glacier, the stress coupling length is about a factor of two greater than what would be expected for a comparable temperate glacier.

The annual surface velocity of McCall Glacier was estimated from measured ice thickness and surface slope, with the longitudinal stress gradients taken into account. A close fit with observed velocities could only be achieved by introducing a localized year-round sliding anomaly that accounts for more than 70% of the annual velocity over a 2 km stretch of the ablation area.

A numerical model was derived to study the influence of localized sliding on surface geometry. Results show that a sliding anomaly causes a local decrease in ice thickness, while the surface slope is decreased near the center of the anomaly and locally increased upglacier of it. This characteristic signature is seen in the measured profiles of surface slope and ice thickness of McCall Glacier. Our results indicate that substantial year-round sliding can occur at the base of polythermal glaciers, even though the bulk of the ice within them is cold.

In contrast to the absolute surface velocity of McCall Glacier, changes in velocity since the 1970s can be understood by observing changes in ice thickness and surface slope and neglecting sliding. This suggests that the year-round sliding anomaly on the lower glacier cannot have significantly changed from the 1970s to the 1990s.

Contrary to temperate glaciers, seasonal velocity of McCall Glacier reaches its minimum in spring, at the onset of melt. Velocity is highest during peak ablation and stays above the annual mean value even after ablation ceases. The observed behavior may be indicative of an immature drainage network that leads to prolonged water storage near the glacier bed. On polythermal White and McCall Glaciers, excess ice motion in summer provides only about 5% of the mean annual ice flux. On White Glacier this flux contribution decreases steadily upglacier, while for McCall Glacier an increase is documented at least up to the equilibrium line.

II.6. Acknowledgments:

This study was supported by grant NSF-OPP-9214954 as part of the LAII program. We wish to thank G. Adalgeirsdottir, U. Adolphs, J. DeMallie, S. Campbell, J. Sapiano, K. Swanson, D. Trabant and C. Trabant for skillful help with the fieldwork during sun, rain, hail, snow, fog and insect plagues. We also thank W. Harrison for useful comments on an earlier version of the manuscript.

II.7. References

Andreason, J.O. 1985. Seasonal surface-velocity variations on a sub-polar glacier in west Greenland. *J. Glaciol.*, 31(109), 319-323.

Baker, R.W. 1986. The role of debris-rich ice in flow near the margins of glaciers. *Ann. Glaciol.*, 8, p.201.

Balise, M.J. and C.F. Raymond. 1985. Transfer of basal sliding variations to the surface of a linearly viscous glacier. *J. Glaciol.*, 31(109), 308-318.

Blatter, H. 1987. On the thermal regime of an arctic valley glacier: A study of White Glacier, Axel Heiberg Island, N.W.T., Canada. *J. Glaciol.*, 33(114), 200-211.

Brandenberger, A.J. 1959. *Map of the McCall Glacier, Brooks Range, Alaska.* New York, etc., American Geographical Society. (AGS Report No.11.)

Echelmeyer, K.A. and W. Zhongxiang. 1987. Direct observations of basal sliding and deformation of basal drift at subfreezing temperatures. *J. Glaciol.*, 33(114) 83-98.

Echelmeyer, K.A. and W.D. Harrison, 1990. Jakobshavns Isbrae, west Greenland: Seasonal variations in velocity - or lack thereof. *J. Glaciol.*, 36(122) 82-88.

Echelmeyer, K.A., W.D. Harrison, C.F. Larsen, J. Sapiano, J.E. Mitchell, J. DeMallie, B. Rabus, G. Adalgeirsdottir and L. Sombardier. 1997. Airborne surface profiling of glaciers: a case-study in Alaska. *J. Glaciol.*, 43(141) ???-???

Haeberli, W., M. Hoelzle and H. Boesch, *comps.* 1994. Glacier Mass Balance Bulletin. Bulletin No.2 (1990-1991). IAHS Press; Nairobi, UNEP; Paris, Unesco.

Hooke R.L. 1991. Positive feedbacks associated with erosion of glacial cirques and overdeepenings. Geological Society of America Bulletin, 103, 1104-1108

Hooke R.L., P. Calla, P. Holmlund, M. Nilsson and A. Stroeven. 1989. A 3 year record of seasonal variations in surface velocity, Storglaciaren, Sweden. *J. Glaciol.*, 35(121) 235-247.

Hooke, R.L., J. Brzozowski, J. and C. Bronge. 1983. Seasonal variations in surface velocity, Storglaciaren, Sweden. *Geografiska Annaler* 65(A), 263-277.

Iken, A. 1974. Velocity fluctuations of an arctic valley glacier, a study of the White Glacier, Axel Heiberg Island, Canadian Arctic Archipelago. Axel Heiberg Island Research Reports McGill University Montreal. (Glaciology No. 5)

Kamb, B. and K.A. Echelmeyer. 1986. Stress-gradient coupling in glacier flow: longitudinal averaging of the influence of ice thickness and surface slope. *J. Glaciol.*, 32(111), 267-284.

Mazo, V.L. 1989. Waves on glacier beds. *J. Glaciol.*, 35(120) 179-182.

McCall, J.G. 1952. The internal structure of a cirque glacier. *J. Glaciol.*, 2(12), 122-130.

Meier M.F., W.B. Kamb, C.R. Allen and R.P. Sharp. 1974. Flow of Blue Glacier, Olympic Mountains, Washington, U.S.A. *J. Glaciol.*, 13(68), 187-212.

Nye, J.F. 1951. The flow of glaciers and ice-sheets as a problem in plasiticity. *Proc. R. Soc. London*, Ser. A, 207, 554-572

Nye, J.F. 1965. The flow of a glacier in a channel of rectangular, elliptic or parabolic cross-section. *J. Glaciol.*, 5(41) 661-690.

Orvig, S. and R.W. Mason. 1963. Ice temperatures and heat flux, McCall Glacier, Alaska. *In General Assembly of Berkeley*. International Association of Scientific Hydrology, I.U.G.G., 181-188. (IASH Publication No.61.)

Paterson, W.S.B. 1981. *The physics of glaciers. Second edition.* Oxford, etc., Pergamon Press.

Rabus, B.T., K.A. Echelmeyer, D.T. Trabant and C.S. Benson. 1995. Recent Changes of McCall Glacier. *Ann. Glaciol.*, 21, 231-239.

Roethlisberger, H. 1972. Water pressure in intra- and subglacial channels. *J. Glaciol.*, 11(62) 177-203.

Sater, J.L. 1959. Glacier studies of the McCall Glacier, Alaska. *Arctic*, 12(2), 82-86

Sater, J.L. 1958. Surface motion studies of the McCall Glacier, June to October, 1957. *In IGY Glaciology Report Series* No.1. New York, IGY World Data Center, Glaciology, American Geographical Society, XII-4-XII-10.

Shreve, R.L. 1972. Movement of water in glaciers. *J. Glaciol.*, 11(62) 205-214.

Trabant, D.C. and C.S. Benson. 1986. Internal accumulation and superimposed ice on McCall Glacier, Alaska: part of the IHD glacier mass balance program. *Materialy Glyatsiologicheskikh Issledovaniy*, 58, 157-165.

Trabant, D.C., W.D. Harrison and C.S. Benson. 1975. Thermal regime of McCall Glacier, Brooks Range, northern Alaska. *In* Weller, G. and S. Bowling, *eds. Climate of the Arctic*. Fairbanks, Geophysical Institute, University of Alaska, 347-349. (Proceedings of the 24th Alaska Science Conference, 15-17 August 1973.)

Wakahama, G. and Tusima, K. 1981. Observations of inner moraines near the terminus of McCall Glacier in arctic Alaska and laboratory experiments on the mechanism of picking up moraines into a glacier body. *Ann. Glaciol.*, 2, 116.

Wendler, G. and N. Ishikawa. 1974. The effect of slope, exposure and mountain screening on the solar radiation of McCall Glacier, Alaska: a contribution to the International Hydrological decade. *J. Glaciol.*, 13(68), 213-226.

Wendler, G., C. Fahl and S. Corbin. 1972. Mass balance studies on the McCall Glacier, Brook Range, Alaska. *Arct. Alp. Res.*, 4(3), 211-222.

Willis, I.C. 1995. Intra-annual variations in glacier motion: a review. *Progress in Physical Geography*. 19(1), 61-106

II.8 Figures

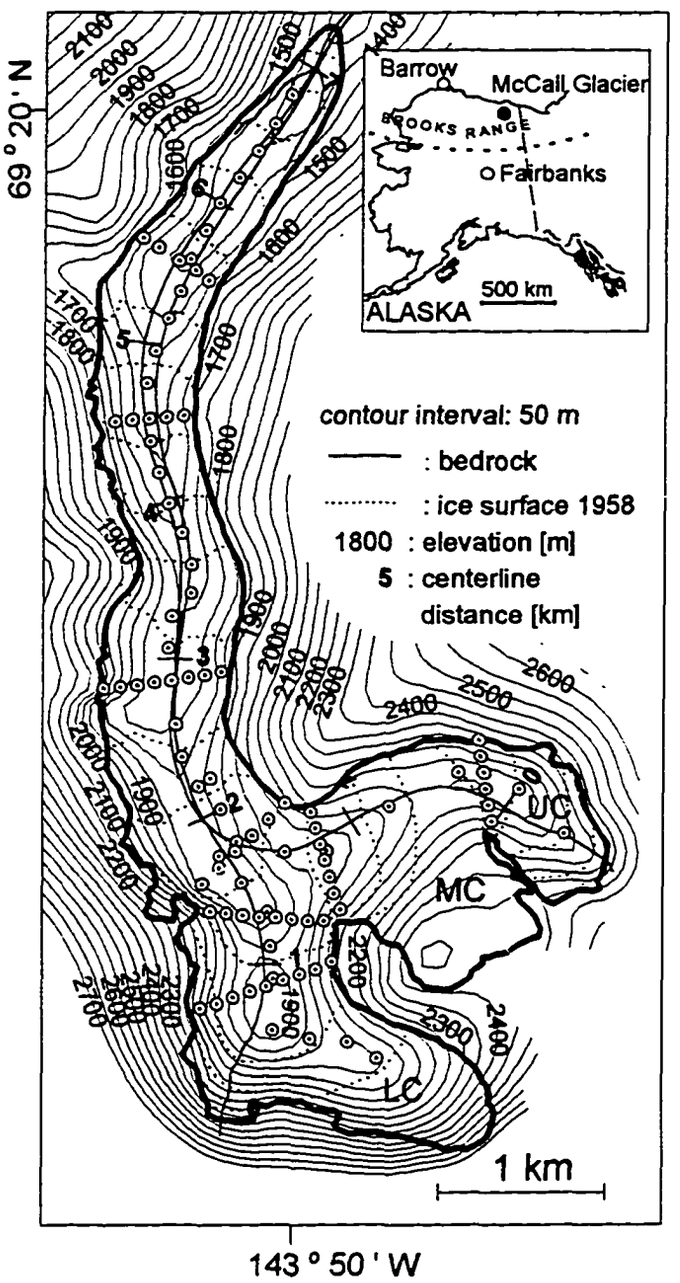

Figure II.1: Bed topography of McCall Glacier, interpolated from radio echo sounding measurements made at the dotted circles. The heavy line shows the glacier margin in 1958. Elevations are in meters above mean sea level.

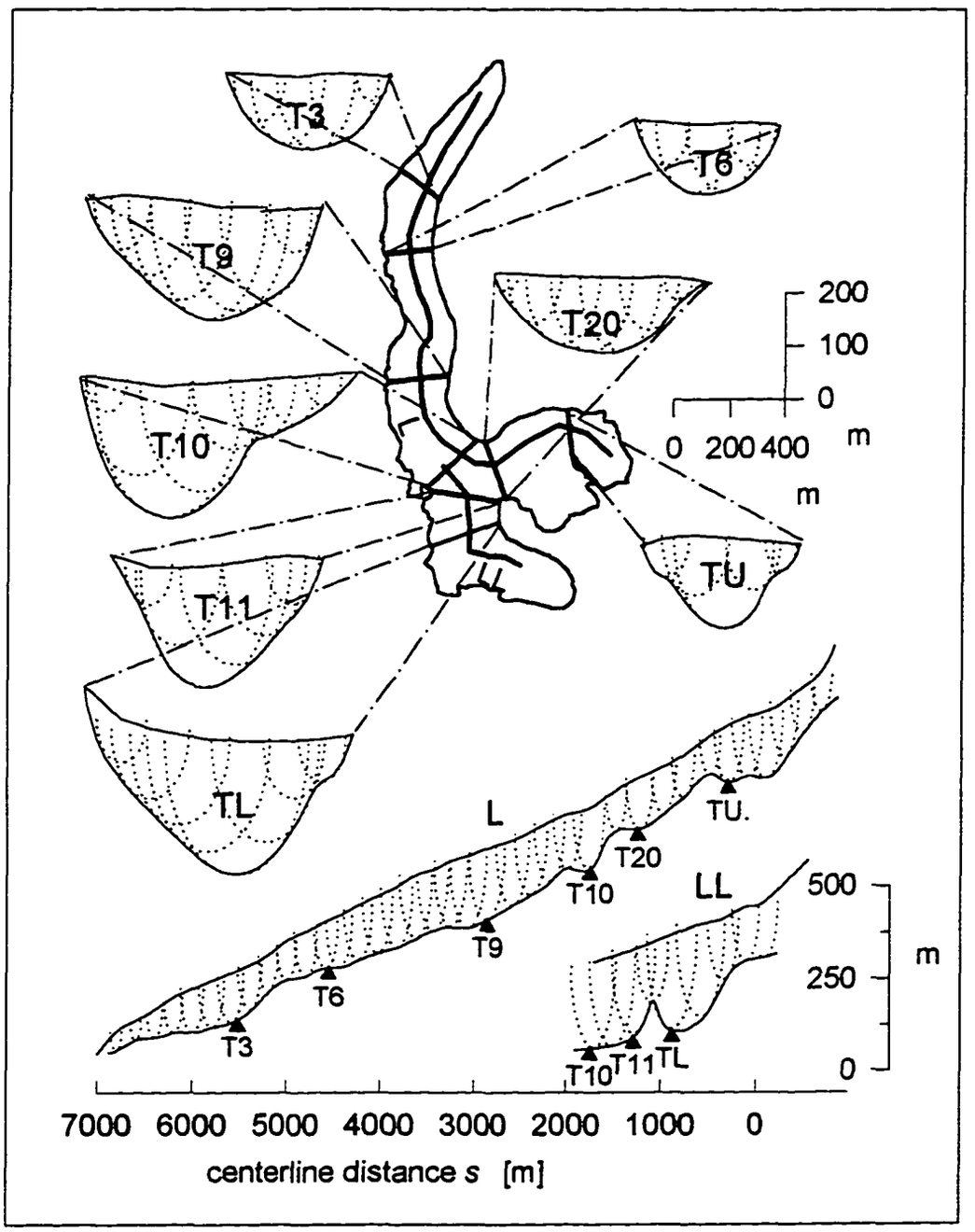

Figure II.2: Cross sections (T-) and longitudinal (L-) profiles of McCall Glacier in 1993. The loci of potential radio echo reflectors are shown as the dotted ellipses. Vertical exaggeration: cross sections 2x, longitudinal profiles 4x. All scales are in meters.

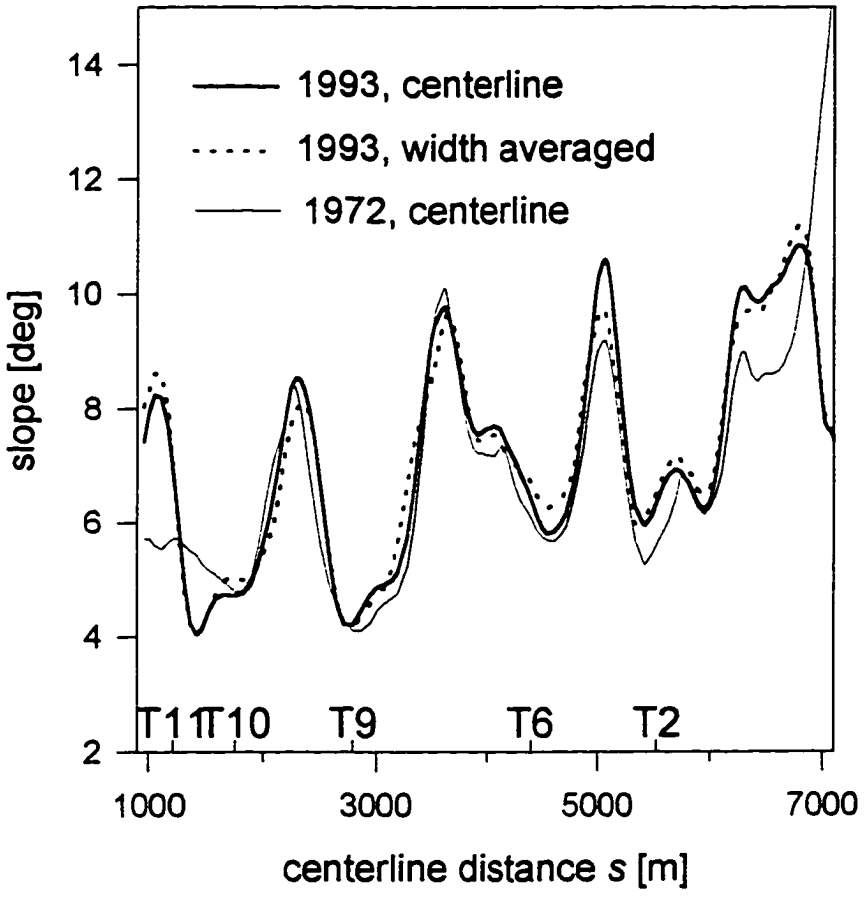

Figure II.3: Surface slopes in 1972 and 1993 along the centerline, and transversely averaged slopes in 1993.

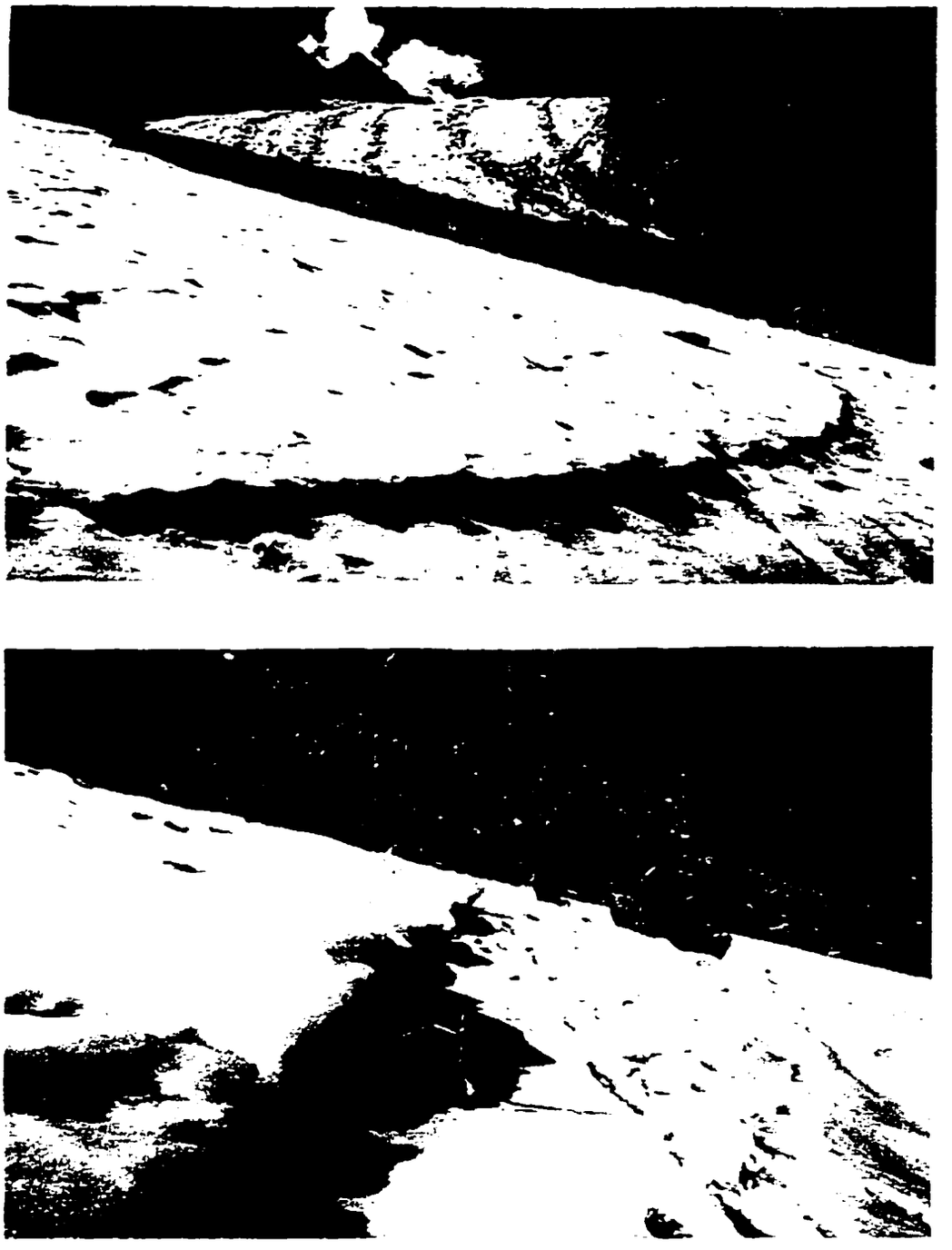

Figure II.4: a) Arcuate "thrust fault" on South Hubley Glacier, newly formed in July 1995. Snout of North Hubley Glacier in the background. b) close-up showing offset and upglacier dip of the "fault". The instrument indicating the dip is ca. 40 cm long.

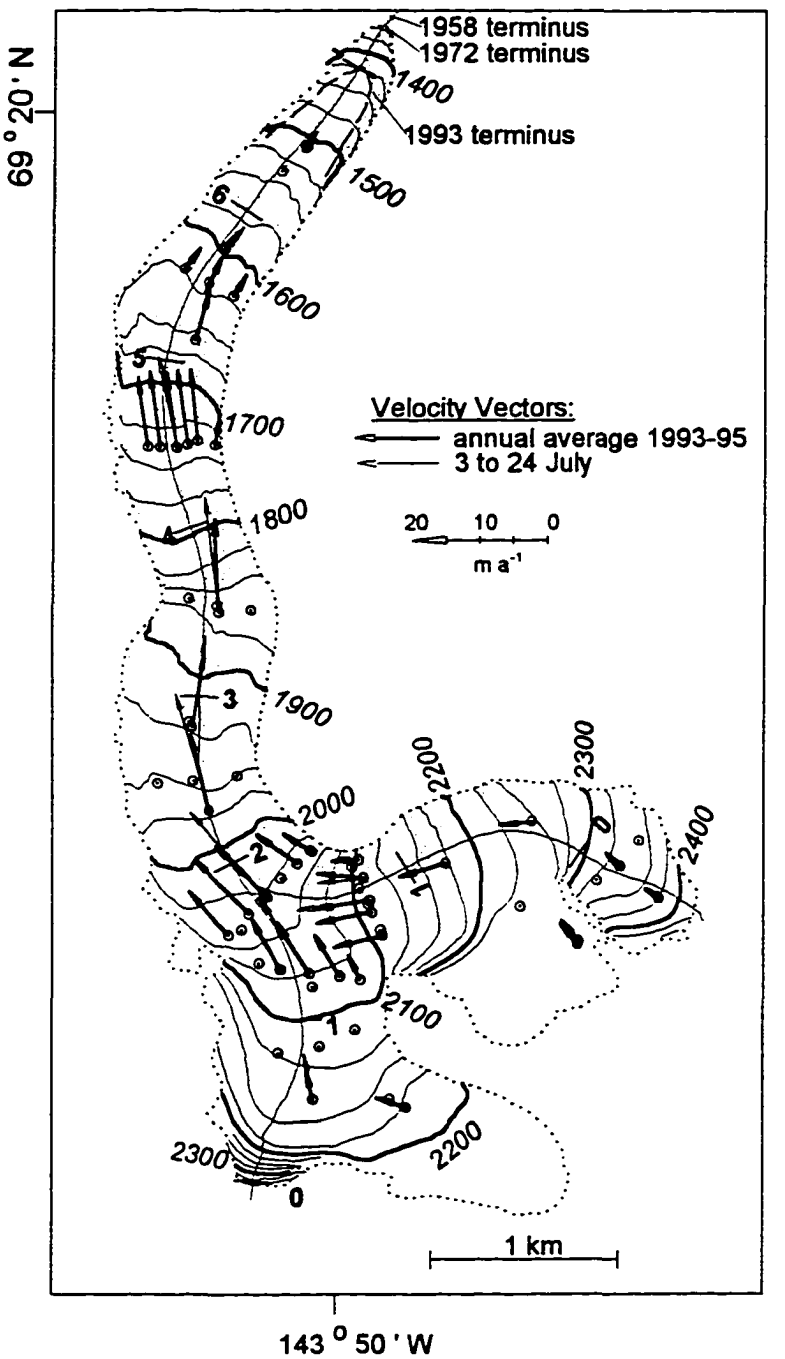

Figure II.5: Velocity vectors, mean annual value 1993-95 and during the peak melt season, 3 to 24 July 1993. Elevation contours are in meters above sea level; they refer to 1958 topography. The stippled area marks the approximate outline of the ablation zone in 1970, when the net balance was close to zero (Trabant and Benson, 1986).

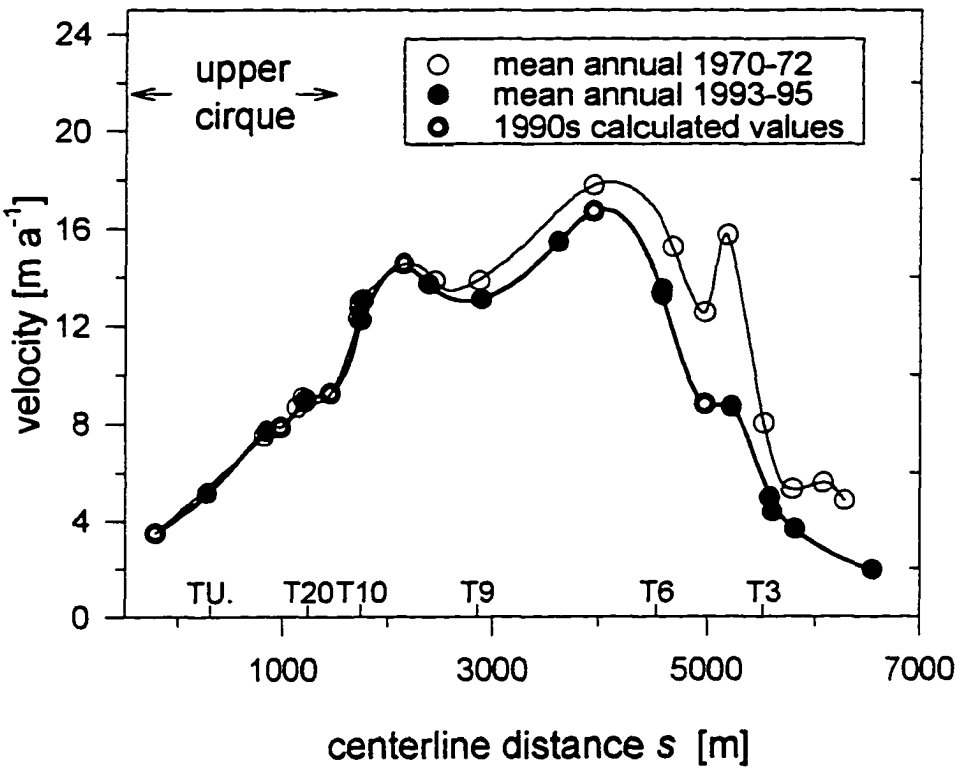

Figure II.6: Mean annual velocity along the centerline during 1970-72 and 1993-95. The open symbols represent values that were calculated from Equation (11).

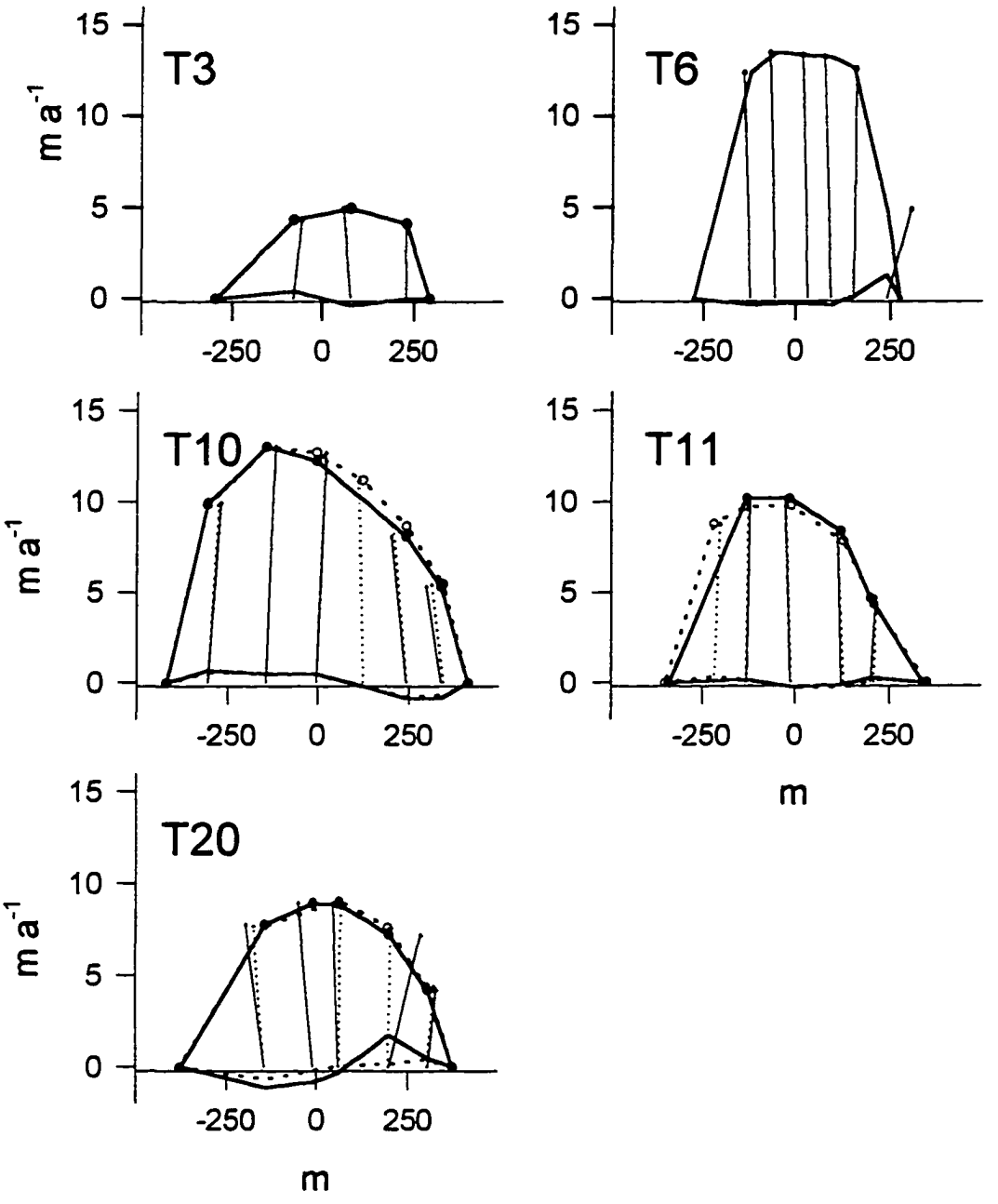

Figure II.7: Transverse profiles of mean annual velocity [m a^{-1}]: 1970-72 (dotted) and 1993-95 (solid). Shown for each profile are: annual velocity vectors, longitudinal (heavy line with symbols), and transverse component (heavy line without symbols at base of each plot). Horizontal scales are in meters.

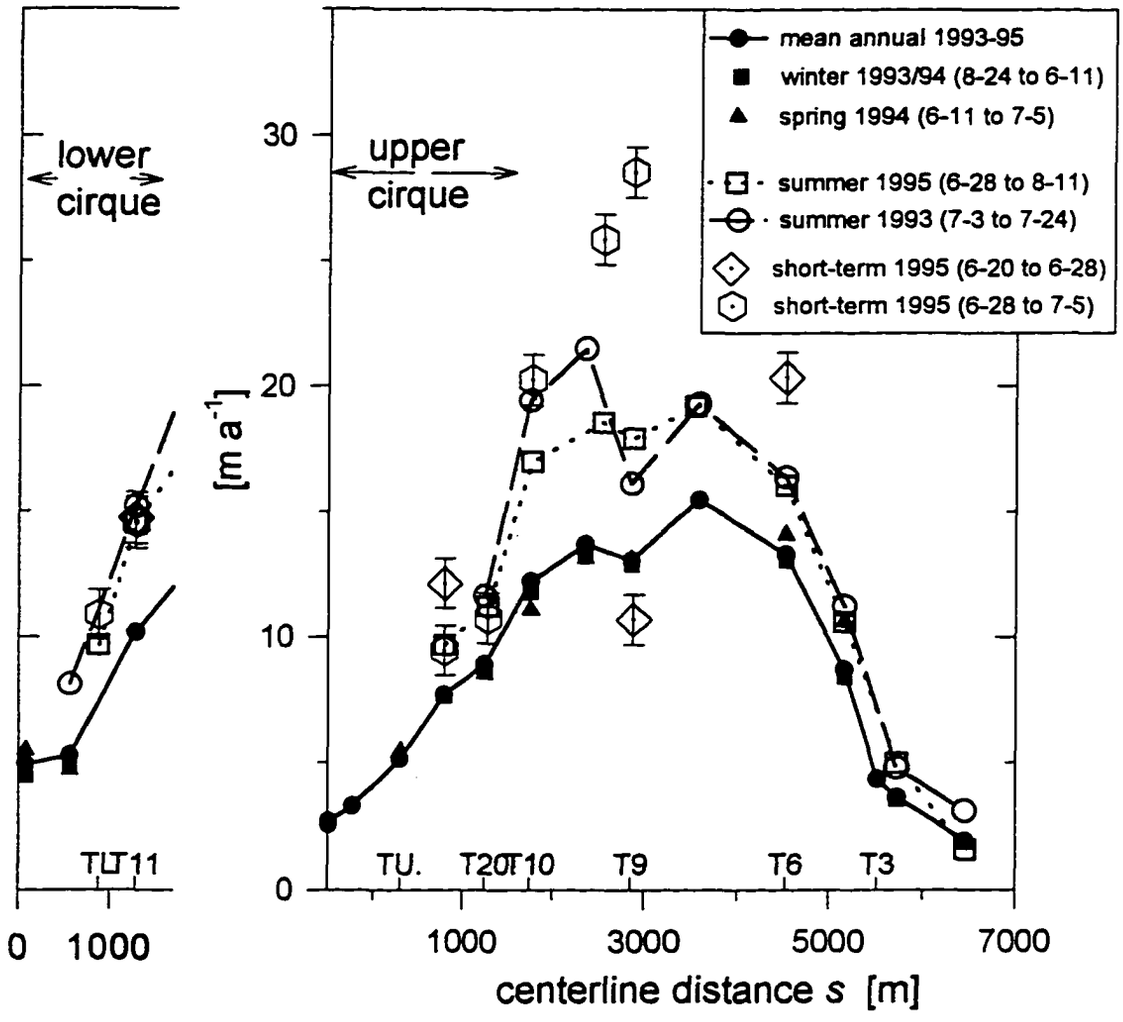

Figure II.8: Intra-annual variations of centerline velocity, 1993 to1995.

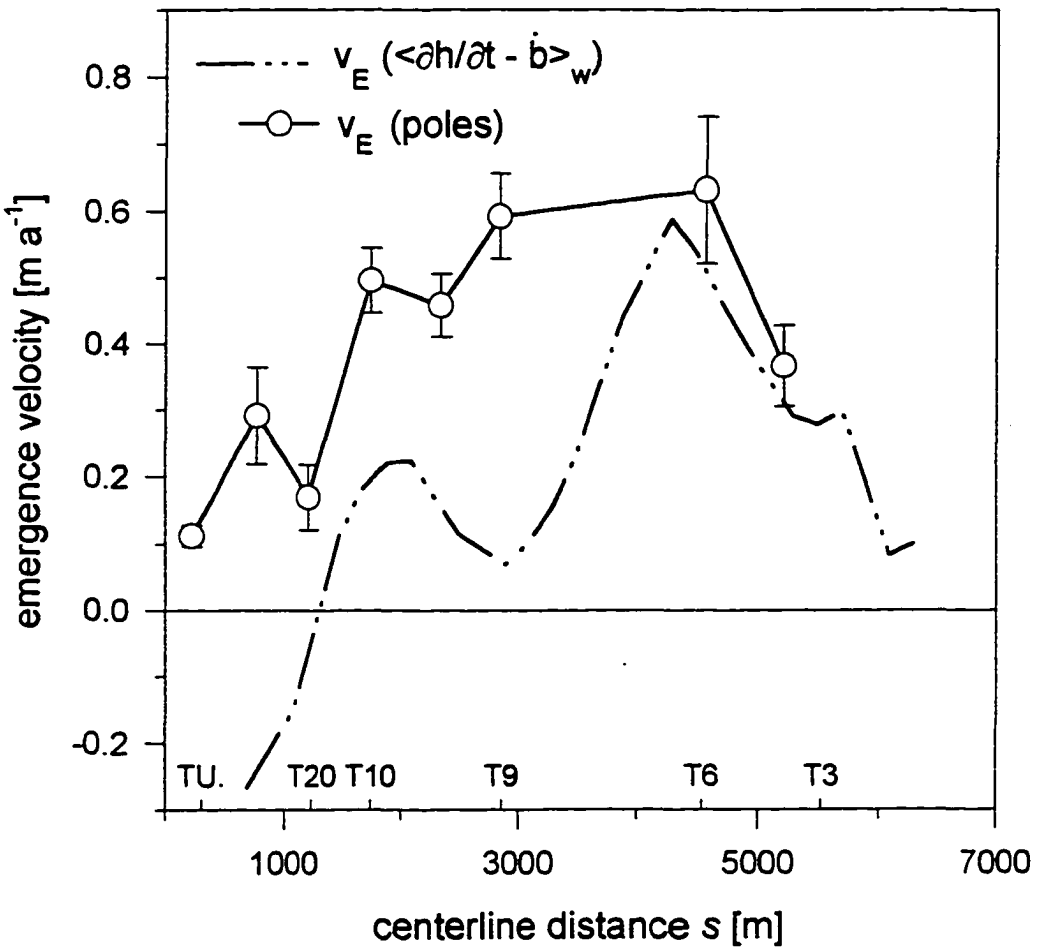

Figure II.9: Average emergence velocities 1993-95: (i) on the centerline, calculated from surveys of individual marker poles and local surface slopes in their vicinity, and (ii) width average, calculated from width-averaged local mass balance and elevation change.

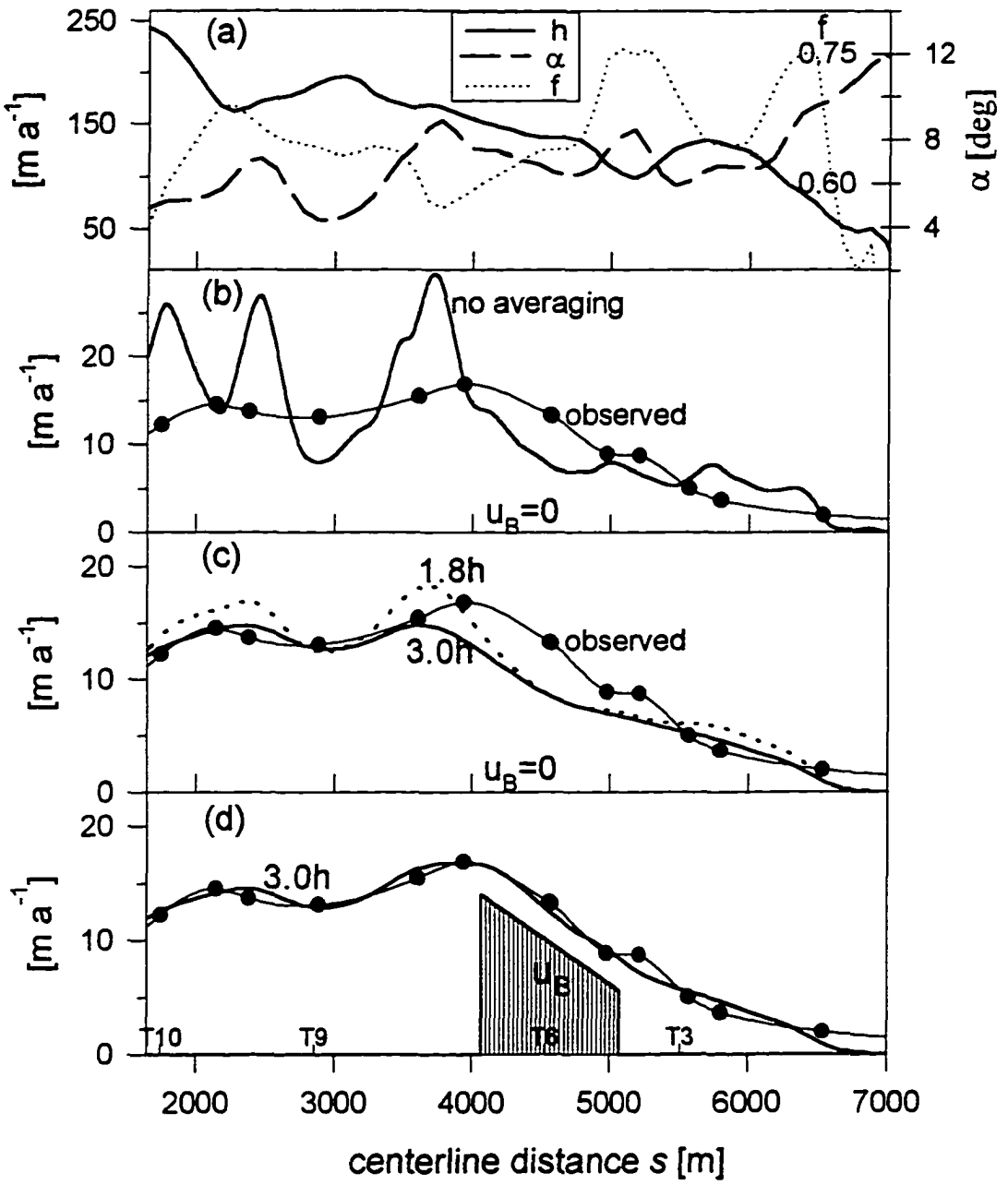

Figure II.10: Modeled velocity of McCall Glacier compared to measurements (solid symbols): a) local input parameters, b) velocity from Equation (5) using local parameters, c) longitudinal averaging following Equation (7) with best-fit coupling length l = 3.0h (solid line) and l = 1.8h (dashed line) and no sliding, and d) longitudinal averaging (l =3.0h) with a localized sliding anomaly included (u_B).

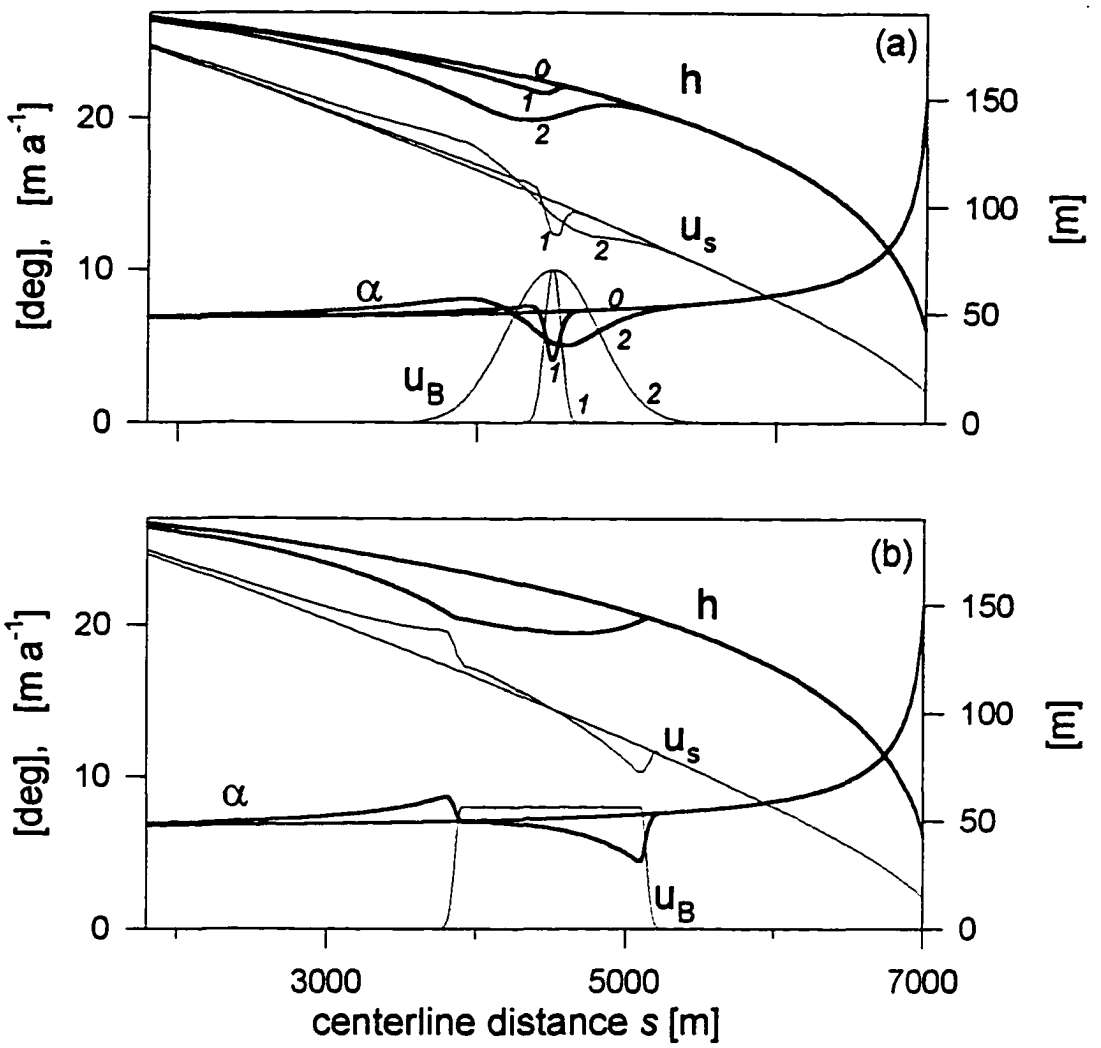

Figure II.11: Modeled profiles of ice thickness and surface slope on a linear bed. a) without sliding (0) and with narrow (1) and broad (2) gaussian-shaped sliding anomalies, and b) with a rectangular-shaped sliding anomaly.

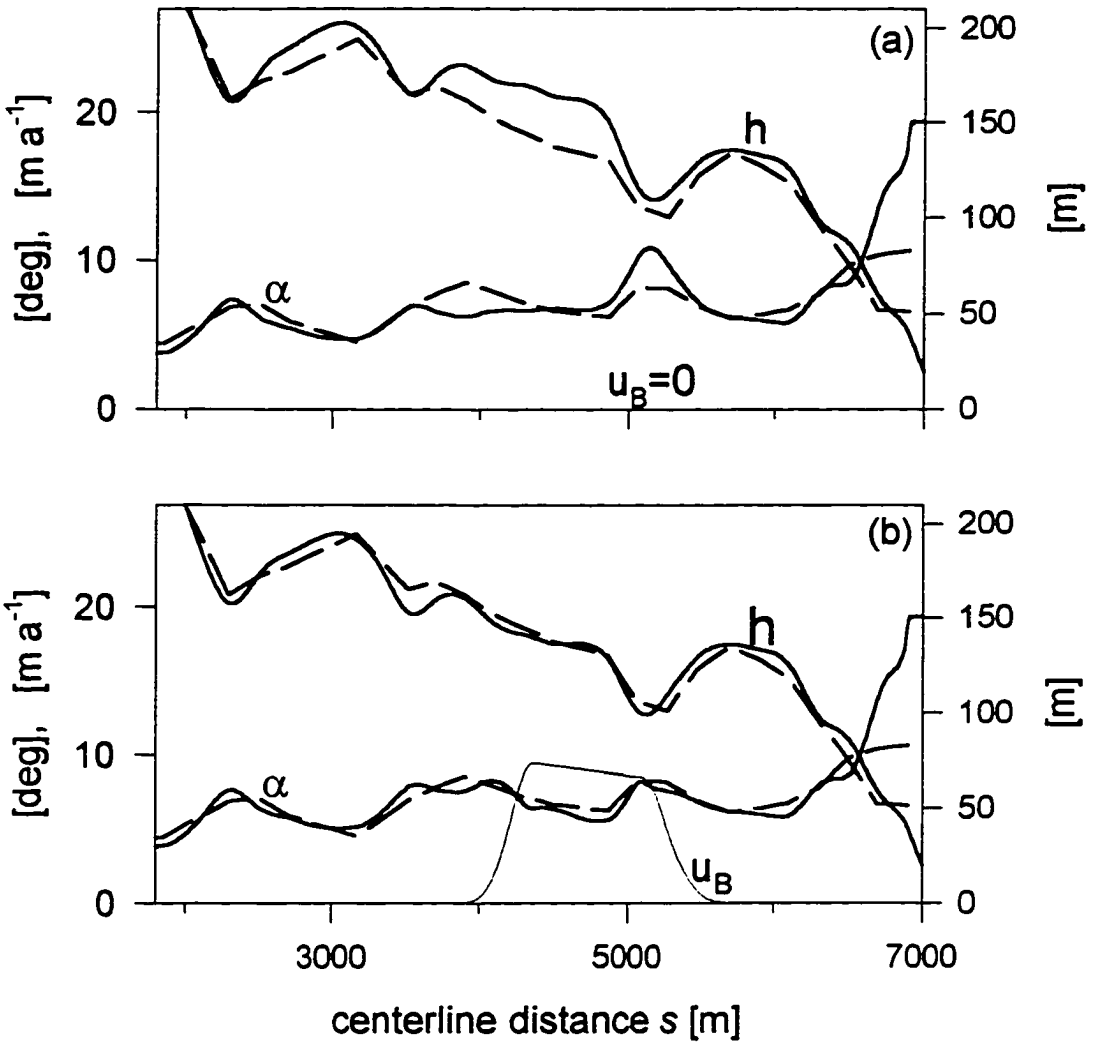

Figure II.12: Modeled profiles (dashed curves) of ice thickness and surface slope of McCall Glacier compared to measured values (solid curves) for: a) no basal sliding and b) a trapezoidal shaped sliding anomaly.

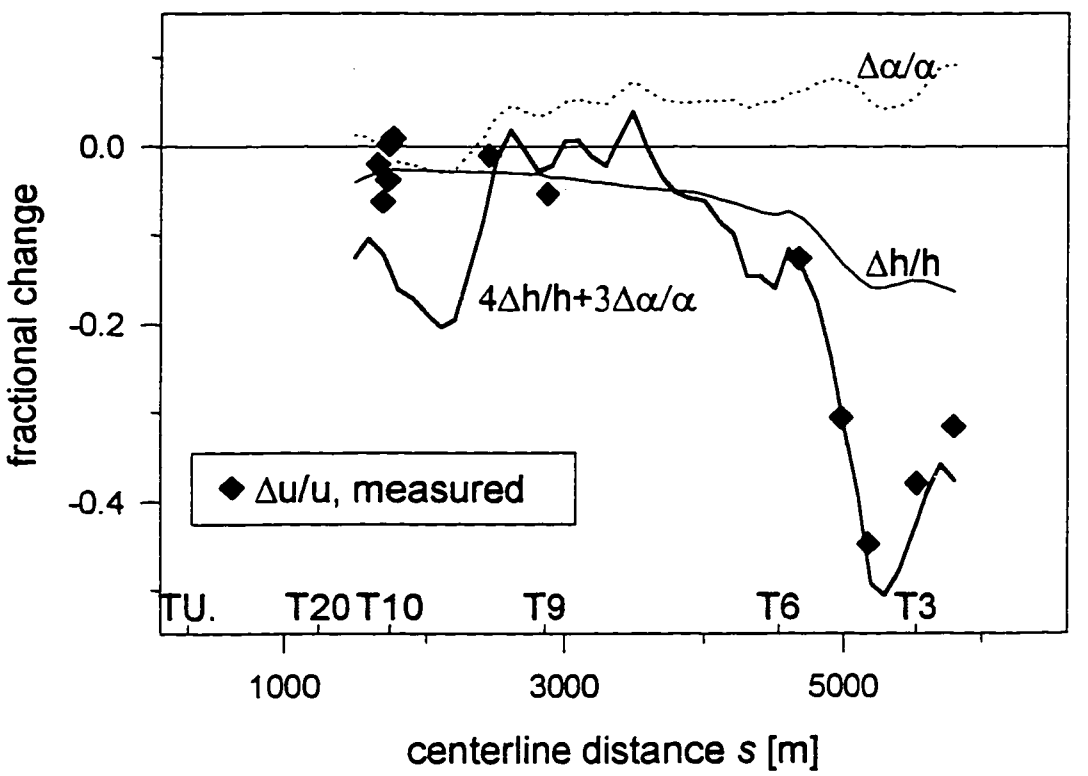

Figure II.13: Comparison of measured (symbols) and modeled (curve) relative velocity change $\Delta u/u$ since the 1970s.

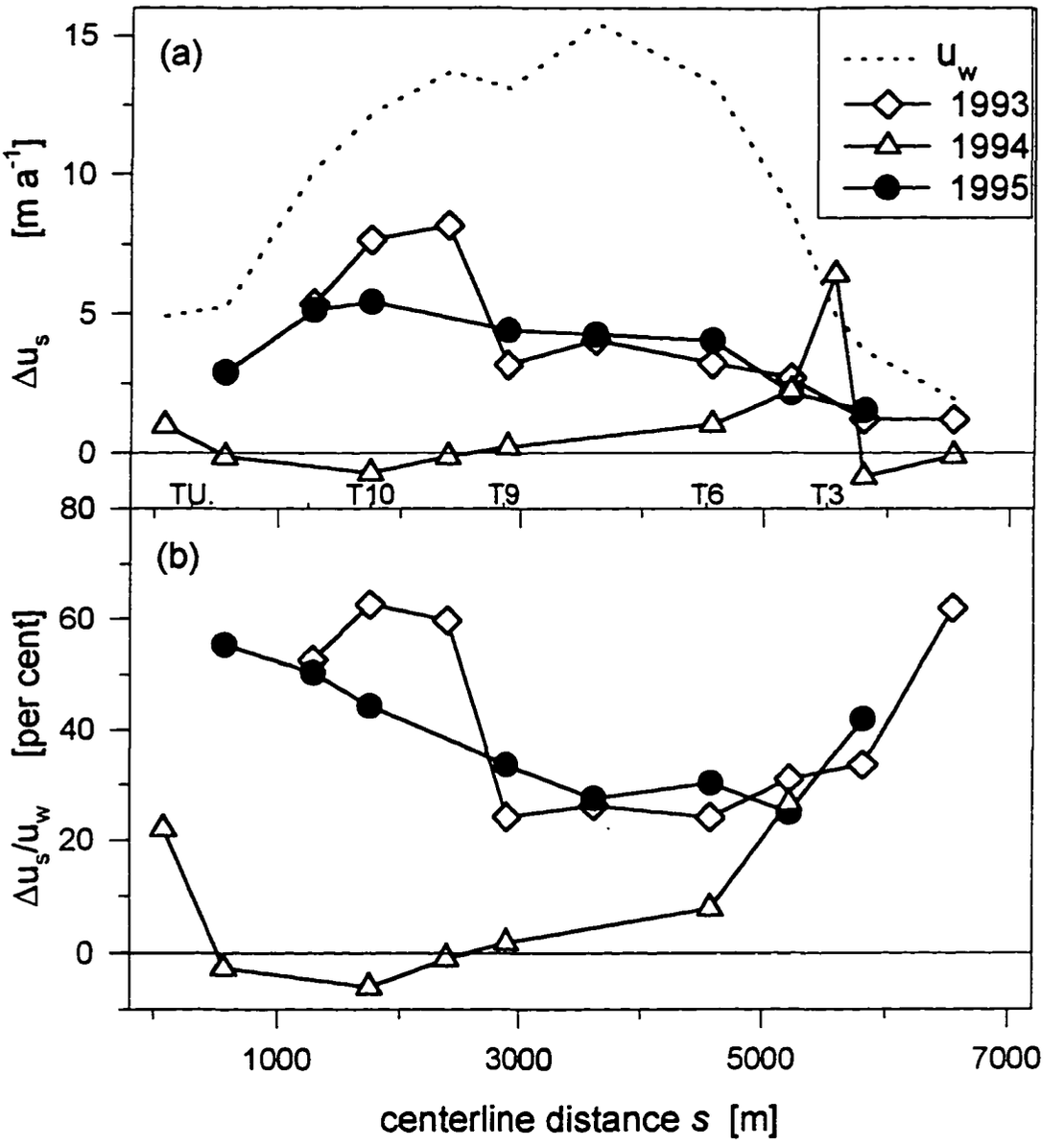

Figure II.14: a) Seasonal velocity increase $\Delta u_s = (u_s - u_w)$ for the 1993, 1994 and 1995 "summer" seasons, and b) percent increase in velocity relative to the winter velocity, $\Delta u_s/u_w$. These results are shown for the centerline markers.

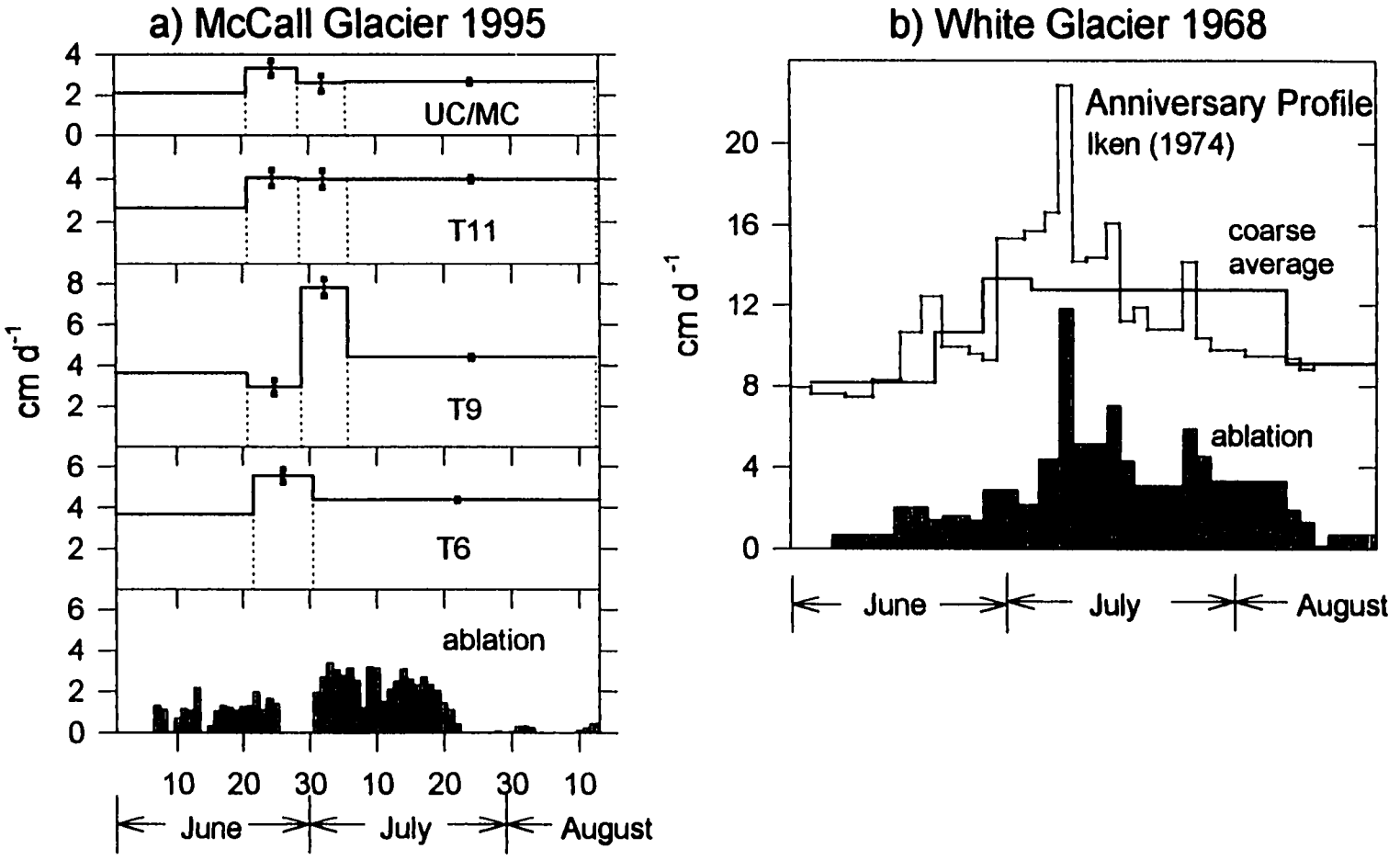

Figure II.15. Seasonal velocity variations and ablation: a) McCall Glacier, summer 1995, and b) White Glacier, summer 1968 (Anniversary profile from Iken, 1974). The heavy curve in (b) is an average at the same temporal resolution as the McCall Glacier data.

III. The mass balance of McCall Glacier, Brooks Range, Alaska; Its Regional Relevance and Implications for Climate Change in the Arctic[3]

B.T. RABUS AND K. A. ECHELMEYER

Geophysical Institute, University of Alaska, 903 Koyukuk Dr., Fairbanks, Alaska 99775-7230, U.S.A

III.1. Abstract

McCall Glacier has the only long-term mass balance record in Arctic Alaska. Mean annual balances over the periods 1958-72 and 1972-93 were -15 cm a^{-1} and -33 cm a^{-1} respectively; recent annual balances (1992-95) are around -60 cm a^{-1}. For an arctic glacier with low mass exchange rate, this marks a dramatically negative trend. We recently acquired elevation profiles using airborne and ground-based GPS methods on McCall and ten other glaciers of various sizes within a 30 km radius, and these were compared with topographic maps made in 1956 or 1973. Comparison of the elevation changes on McCall and the other glaciers shows no major differences in the common parts of their elevation ranges. Most of these glaciers had average balances between -25 and -33 cm a^{-1} (McCall Glacier's average for 1956-93 was -28 cm a^{-1}). This indicates that McCall Glacier is representative for the region. Contrary to the similar average balances, changes in terminus position for the different glaciers vary markedly. Retreat rates are dominated by effects of glacier geometry and flow dynamics near the terminus. Thus, mass balance disturbances cannot be estimated from fractional length changes in this region at time scales of a few decades.

---

[3] to be submitted to *Journal of Glaciology*

We developed a simple, two parameter, degree day/accumulation mass balance model for McCall Glacier in order to test its synoptic scale representivity.The model uses precipi- tation and radiosonde temperatures from weather stations at Inuvik, Canada or Barrow, Kaktovik or Fairbanks, Alaska as input and is calibrated with the measured annual balances of McCall Glacier. Positive degree days and accumulation calculated by the model show significantly different trends for the different weather stations. The Inuvik data reproduce all measured mass balances of McCall Glacier well, and also quantitatively reproduce the long-term trend towards more negative balances. Data from the other stations do not produce satisfactory model results. We speculate that the Arctic front, oriented East-West in this region, causes the differences in model results. The average summer position of the front separates Inuvik and McCall Glacier from Barrow and Kaktovik, and creates distinct climatic regions with different climate change scenarios.

Given our results, we conclude that McCall Glacier is representative of a synoptic scale region and its mass balance record is an important measure of ongoing climate change in the Arctic.

III.2. Introduction

The Arctic appears to have played a crucial role during changes in global climate, both recent and past. The onset of ice ages and their abrupt endings are possibly related to large-scale changes in the atmospheric and oceanic circulations of the Northern Hemisphere through their interaction with the Arctic cryosphere (e.g. Alley,1995). General circulation models indicate that increased greenhouse gas concentration in the atmosphere may lead to climate warming, and that this warming is most pronounced in the Arctic (e.g. IPCC, 1992). Close monitoring of the Arctic climate is essential to test these predictions.

There are few weather stations in the Arctic, and the climatic interpretation of their records is hampered by high inter-annual variability, short record lengths, heat island effects and unknown spatial representivity (e.g. Kelly and others, 1982; Bowling, 1991). A complementary approach to detect potential changes in the arctic climate is to study

corresponding changes of natural settings, such as on glaciers (e.g. Cogley and others, 1995 and 1996; Dowdeswell, 1995) or in permafrost (Osterkamp and Romanovsky, 1996; Lachenbruch, 1994). The remoteness of glaciers and the cumulative nature in which changes of their mass balance are displayed in their volume and length make glaciers useful and sensitive indicators of climate change. On the other hand, the climatological interpretation of short-term changes of individual glaciers can be difficult because errors in mass balance measurements can obscure existing trends and because it is not known *a priori* how representative a particular glacier is within a geographic region. Changes in glacier length are also complicated by glacier flow, and there is a poorly understood time lag between changes in mass balance and terminus response (Johannesson and others, 1989, Schwitter and Raymond, 1993; Echelmeyer and others, 1996). Furthermore, there are mechanisms, largely unrelated to climate, such as the tidewater glacier cycle, surging glaciers and volcano-glacier interactions, which can also produce major changes in glaciers (Sturm and others, 1991).

In this paper we present annual and long-term cumulative mass balance data from McCall Glacier, Alaska. This glacier is part of the northernmost glacierized region in the United States, and its mass balance provides a direct measure of climate change in this arctic region. Short-term comparative studies on neighboring glaciers indicate that McCall Glacier is regionally representative. Furthermore, the successful modeling of its mass balance record using meteorological parameters from distant weather stations implies synoptic-scale representivity of this glacier's mass balance. We use our results to estimate trends in summer temperature and winter precipitation since the 1960s for this part of the Arctic.

III.3. Background on McCall Glacier

McCall Glacier is located in the Romanzof Mountains at 69° 17' N, 143° 50' W, close to the northern front of the northeastern Brooks Range (Figure III.1). The glacier is about 8 km long and has an area of 7.4 km^2. Ice originates in three cirques, from east to west, Upper, Middle and Lower, and flows from an elevation of more than 2700 m to the

present terminus at 1350 m (Figure III.2). The surface is relatively steep, with a mean slope of 8°. Precipitation sources for the glaciers in this region are the Bering Sea, about 700 km to the west, and the Arctic Ocean, about 100 km to the north across the coastal plain. Seasonal mass exchange on McCall Glacier is quite small: the current winter and summer balances are around 20 cm a^{-1} and -60 cm a^{-1}. The total annual precipitation is about 0.5 m (Wendler and others 1974), more than half of which falls in solid form near the beginning and end of the short summer season from June to August. Trabant and Benson (1986) showed that superimposed ice formation and internal accumulation are significant on the glacier, with the latter contributing more than 40% to the annual net accumulation. Because of patterns in mountain shading and wind deposition, the equilibrium line altitude (ELA) is not well defined but spans an elevation range of 350 m for an average year (Trabant and Benson, 1986; Wendler and Ishikava, 1974). The mean annual air temperature is about -12 °C at 1700 m elevation. The near-surface and basal ice temperatures in the accumulation area are between -1 and -1.5 °C (Orvig and Mason, 1963). In the ablation area, surface ice temperatures are less than -10 °C, while the basal ice is temperate, at least near the centerline (Trabant and others, 1975).

Previous studies of the surface geometry and the mass and energy balance of McCall Glacier were made during the International Geophysical Year (IGY) in 1957/58 (e.g. Sater 1959) and during the period 1969 to 1975 (e.g. Wendler and others, 1972 and 1974). Our continuing investigations began in 1993 (Rabus and others, 1995), with measurements of surface and bed geometry, mass balance, meteorological variables, ice temperature, and ice velocity (Rabus and Echelmeyer, submitted).

III.4. Definitions

It is important to set forth several definitions of mass balance terms used in this study. They are excerpted from Ostrem and Brugman (1991).

The mass balance of a glacier can be measured using either *glaciological*, *topographical* or *hydrological* methods. The glaciological method involves measurements of local mass balance poles sunk into the ice or firn, and of snow density in pits. These

data are used to calculate the net surface balance for a given hydrological year (HY), either beginning and ending at a specified date in autumn (*fixed date system*) or from one summer surface to the next (*stratigraphic system*). The topographical method compares two surfaces, defined by surveying the glacier (by photogrammetry or other methods) at two different times. To convert the calculated volume change to mass balance, one must assume an estimated bulk density for the (unknown) proportions of ice, firn and snow which are lost or gained. In contrast to the glaciological method, in which systematic errors accumulate, the topographic method becomes more accurate when evaluated over a longer time span (Krimmel, 1989). Both glaciological and topographical methods have been used on McCall Glacier (Trabant and Benson, 1986; Rabus and others, 1995). The hydrological method determines mass balance from precipitation and evaporation measurements, and the discharge of a glacier's outlet stream. The geometry of the drainage basin and the formation of aufeis make this method unfavorable for McCall Glacier (Wendler and others, 1972).

Two sources of accumulation that complicate mass balance measurements on arctic glaciers such as McCall, which have cold surface temperatures, are *internal accumulation* and *superimposed ice* (e.g. Trabant and Mayo, 1985; Trabant and Benson, 1986; Wakahama and others, 1976). Internal accumulation occurs by the refreezing of surface water that percolates below the previous summer surface. Superimposed ice forms near the equilibrium line by refreezing of water on top of this summer surface. Both contributions to the mass balance are considered by using the topographical method over sufficiently long time periods. In contrast, the glaciological method, which usually determines the *surface balance* above the last summer surface, includes only superimposed ice. Internal accumulation must be estimated independently.

Various methods can be used to calculate the balance for the entire glacier given the local pole balances. In the *balance versus elevation method*, the local balances are plotted versus elevation, and a low order polynomial is fit to the data. Local balance at the center of successive elevation bands is obtained from the polynomial fit and net balance is then

obtained as a sum of these local balances, weighted according to the area-elevation distribution of the glacier. In a different approach, a contour map of mass balance is constructed by two-dimensional interpolation of the local balances. We call this the *balance contour map method.* Numerical integration of the balance contour map over the glacier surface gives the net balance in this case. This method can only be implemented successfully if the mass balance poles provide sufficient areal coverage.

We also distinguish between *net accumulation*, which is the net amount of annual precipitation and possibly refrozen melt that is added to the glacier, and *winter balance*, which is the maximum snow balance on top of the last summer surface in the spring. The net balance minus the net accumulation gives the *net ablation,* while the net balance minus the winter balance is the *summer balance.* The net balance determines the mass flux of a glacier, while the difference between winter and summer balance determines its climatic activity index (Meier, 1962).

All mass balances are given in water equivalent unless otherwise noted.

III.5. Mass balance record of McCall Glacier

The mass balance record on McCall Glacier is discontinuous and fragmented. A few measurements were made in the mid 1950s (Keeler, 1958), a new program was initiated in 1969 and continued until 1972 (Trabant and Benson, 1986; Wendler and others, 1972), and our ongoing program began in 1993. These monitoring programs generally involved measurements of annual balances with the glaciological method for selected periods. In addition, average balances over longer periods were determined using the topographic method, as described by Dorrer and Wendler (1976) and Rabus and others (1995). In this section we present the results of these programs in an internally consistent framework. Because the measurement techniques and methods used to calculate annual balance were different under the various programs, we first describe the methods by which the basic data was obtained, and then describe a reevaluation of the earlier data within our present framework, along with an analysis of the errors. We are then able to discuss changes in

mass balance, focusing on the differences between those measured in the 1970s and those in the 1990s.

No annual mass balance measurements are available from the IGY (1957). Keeler (1958) describes ablation measurements made from late June to early September on the lower glacier. He notes that there was 2.1 m of ice melted near the terminus (at about 1350 m elevation) during that period.

III.5.1 Glaciological mass balance methods: 1970s

In 1969, Trabant and Benson (1986) established a network of about 70 mass balance poles on McCall Glacier. The heights of the poles were measured monthly from May to September, and snow pit measurements were made in spring and fall. A fixed hydrological year, beginning 1 October, was used. Glacier-wide net balance was determined, along with the individual components of ice, superimposed ice, internal accumulation, and snow. However, the exact computational method used in calculating glacier-wide balances from local balances is not known. Most likely the balance contour map method was used. They estimated the error in the net balance to be ±5 cm for the 1970, 1971 and 1972 balances and ±8 cm for the 1969 balance because the initial (1968) snow balance had to be estimated for that year.

In situ measurements of internal accumulation were carried out by Trabant and Benson. They monitored the growth of individual ice layers in the firn at specific locations. However, the spatial pattern of internal accumulation was irregular, and it was felt that extrapolation to unmeasured areas would be inaccurate. Instead, an indirect method was used. Potential internal accumulation was restricted to where the glacier surface was judged to be permeable to water - both melt water and rainfall. For each pole in this permeable area a maximum capacity for internal accumulation was calculated using shallow firn and ice temperatures. The average capacity was about 45 cm per unit area (water equivalent), with only small spatial and year to year variations. The available surface water was calculated from measured summer precipitation plus the difference between the spring snow balance and the autumn firn balance. Internal accumulation was

then taken to be the smaller of the available water and the maximum capacity. An important result of this analysis was that the capacity for internal accumulation was usually much larger than the available water (Trabant and Benson, 1986). Therefore, internal accumulation on arctic glaciers is probably "liquid-limited" versus "thermally-limited". It was also found that up to 40% of the total annual accumulation on the glacier was in the form of internal accumulation, making it a very significant contribution to the mass balance of an arctic glacier.

III.5.2 Glaciological mass balance methods: 1990s

Our mass balance measurements cover the period 1993 to 1996. A network of 16 poles along the centerline of the glacier and in the three cirques was established in mid June 1993. It was extended to 34 poles in 1995 in an effort to establish an areal coverage similar to that in the 1970s. For each of the four years the pole heights were measured early in the spring (May to mid June) and near the end of the ablation season (July to early September). Additional ablation measurements were made during some summers. Density profiles of the snowpack were measured in spring and autumn at one to three locations. No autumn density measurements were made in 1994 or 1996.

Contrary to the 1970s, we have used the stratigraphic system to define the hydrological year in the 1990s. Late summer surfaces at each pole were determined by probing through the winter snow each spring. With the exception of an area in the upper cirque in 1994, identification of the summer surface was usually unambiguous. Snow balance was measured at each pole and at some additional surveyed sites. In total, snow depths at 24 to 54 locations were measured each year in late May or June and winter balance was calculated from them.

For the years 1995 and 1996 we established correlations between the local balance measured at the poles within the limited network originally set up in 1993 (with 16 poles) and the additional poles of the extended network. We then used these correlations to extend the limited measurements in 1993 and 1994 to a greater areal coverage in those years. Balance contour maps were constructed from each year's data, using this

extrapolated coverage as needed. All net balances for 1993 through 1996 were calculated using this method, sampling the map on a 100×100 m grid.

A sonic ranger was installed at the confluence of the three cirques, somewhat below the mean 1970's equilibrium line. This instrument recorded local accumulation and ablation at a few hours time resolution. Continuous records exist for June 1993 to June 1994, and for May to September 1996. The record for 1996 is shown in Figure III.3. It shows that the ablation season began on about 5 June and ended in mid August, thus being less than two and a half months in duration. The maximum snow depth was about 60 cm; this snow and about 25 cm of additional ice were melted during the short ablation season. Most of the snowfall occurred in early autumn (late August and September) and late spring (May); there is little winter precipitation. 1996 was anomalously cold and cloudy during the summer, so the magnitude of the total ablation was lower than normal. However, the dates for the start and end of the ablation season are typical also of other years, as are the timing of snowfall and the maximum depth of snow at this location.

Internal accumulation was estimated following a procedure similar to that used in the 1970s. The total available water percolating into the permeable zone was approximated by the spring snow balance minus the autumn firn balance, plus summer precipitation. Rainfall was measured at a precipitation gauge located on the eastern moraine at an elevation of 2100 m. The extent of the permeable zone was delineated from field observations. This provided a relatively crude, but consistent, estimate of internal accumulation. We further discuss this important contribution when the results are presented below.

How do we obtain an error estimate for the balance contour map approach? Lliboutry (1974) models the mass balance of an individual pole as the sum of three terms: a spatial term, a temporal term, and a random error. Lliboutry estimated a magnitude of ±20 cm for the error. This error incorporates (i) the individual reading error, typically largest in the accumulation area, (ii) the local unrepresentivity of the individual pole and (iii) the glacier-wide unrepresentivity of the entire network. Cogley and others (1996) claim that the error of the glacier-wide net balance equals Lliboutry's value for an

individual pole. We take a different view point: If the network has sufficient areal coverage, then the error is dominated by the second component, (ii) above. As this local unrepresentivity should be randomly distributed among the poles, the average glacier-wide error should be reduced according to $1/\sqrt{n}$, where n is the number of poles in the network. For example, with 30 poles we obtain a value of ±4 cm a^{-1} for an estimate of the random error in annual balance. Insufficient areal representation of the mass balance network and systematic measurement errors in the extrapolation of snow and firn density will increase this value somewhat. Given these and other sources of error, we arrive at ±8 cm a^{-1} as a conservative error estimate for the annual balances. It applies only to the surface balance, without internal accumulation. Errors in the internal accumulation cannot be analyzed rigorously with the measurements in hand. When we present the results of the mass balance measurements they are discussed in terms of minimum and maximum scenarios for internal accumulation.

III.5.3 Reevaluation of the 1970s balance data

In order to ascertain the specific methods utilized with the earlier data set, and to place all the mass balance calculations into a consistent framework, we have reevaluated the glaciological mass balance data from the 1970s (D. Trabant, unpublished) under the protocol just described for our 1990s data. First we calculated the balances using a fixed date system in order to check our values with those published by Trabant and Benson (1986). These calculations were carried out on the entire data set of about 70 poles and on a subset of the network which is equivalent to the 34 poles measured in 1995-96. We re-evaluated the net balance on these two networks using two approaches (Table III.1): balance contour maps (b_{map}) and the balance versus elevation method (b_{elev}) with a third-order polynomial fit to the balance curve and an area-elevation curve derived from the 1956 USGS 1:63,360 map. Net accumulation, a_{map}, and the accumulation area ratio (AAR), both derived from the balance contour maps, are also given in the table. In the last

section of Table III.1 are listed the published values of these parameters from Trabant and Benson (1986), along with their value of total internal accumulation, $a_{(i)}$. (The surface accumulation is the difference between the net and internal accumulations.)

There are several points to notice from this table. First, the values which we calculated using only data from the 1995-96 subset agree with those from the full network to within ±5 cm a^{-1}. This indicates that the subset provides adequate areal coverage. Second, b_{map} generally agrees with the values we calculated using the balance vs. elevation curves to within one standard error (±8 cm a^{-1}), an encouraging result given the complex shape of the mass balance contours on these maps (e.g. Figure III.4). Third, with the exception of 1969, there is poor agreement between any of the recalculated values and those listed by Trabant and Benson (1986). This is somewhat puzzling, as we have used the same data. Because the specific methods used by these authors are not given, we cannot speculate as to why the differences exist, but they do imply that a reevaluation under our framework is needed to develop an internally consistent analysis of the mass balance record.

To facilitate this, we treated the 1970s data in exactly the same way as those of the 1990s. We first transformed the individual stake balances from the fixed date system into the stratigraphic system, subtracting the difference of the initial and final snow balances for the balance year. We then used the point balances for those poles in the 1995-96 subnetwork to construct balance contour maps for the years 1969 to 1972.

III.5.4 Results for the combined mass balance record 1970s and 1990s

The combined annual balance record for the periods 1969-72 and 1993-1996 is given in Table III.2. The first two data columns show the surface balance $b_{(s)}$ and its corresponding accumulation area ratio (AAR). The following columns show net balance b, net accumulation a, internal accumulation $a_{(i)}$, and the net balance AAR and ELA. For the 1990s, these quantities are given for minimum and maximum calculations of internal accumulation, which are discussed below. b_w and p_s are quantities needed for these calculations ; b_w denotes the maximum snow balance, taken to be the snow balance on the

date listed, and p_s is the summer precipitation measured at our precipitation gauge between the date listed and 10 August, the last day of significant melt. The ELA is an average elevation for the equilibrium line, which often spans 300 m in elevation.

The mean surface balance was -29±3 cm a^{-1} during the period 1969-1972 and -63±3 cm a^{-1} during the period 1993-1995, indicating a pronounced trend towards more negative surface balances from the 1970s to the 1990s. This trend is apparent despite the inclusion of the exceptionally cold year 1996, which had the most positive balance ever measured on McCall Glacier. The balance contour maps for the surface balances 1969-72 and 1993-95 are shown in Figure III.4 and III.5, respectively. In the 1970s, the lower (western) cirque was always an area of accumulation, and maximum ablation near the terminus was always less than 180 cm a^{-1}. In contrast, the years 1993-95 are characterized by considerable ablation of old firn and ice in the lower cirque and a maximum ablation of more than 200 cm a^{-1} near the terminus. In 1994, the year with the most negative surface balance, maximum ablation exceeded 350 cm a^{-1}. For these three years, firn accumulation was restricted to two small regions in the centers of the upper and middle cirques. In contrast, 1996 was more similar to the 1970s regarding the patterns of firn accumulation and ablation. Examination of the balance maps (Figures III.4 and III.5) confirms that there is no meaningful definition of an ELA on McCall Glacier.

From a climatological point of view, it is the surface balance of an arctic glacier, rather than its net balance, that corresponds to the usual mass balance of a temperate glacier: the simple difference of summer ablation and winter precipitation. On the other hand, the net balance of an arctic glacier includes the important contribution of internal accumulation. It therefore depends also on other factors, such as mean winter temperature, the permeability of the glacier surface to water, and rainfall on the cold snowpack. We require both surface and annual net balances to calibrate the mass balance model presented in a later section. This is because the model is tested against topographically measured values of net mass balance. Derivation of the annual net balances requires an accurate estimate of internal accumulation for the 1990s.

III.5.5 Scenarios of internal accumulation

Because internal accumulation is difficult to measure directly (Trabant and Mayo, 1986), we estimate it. We assumed that the capacity for internal accumulation was equal to its mean value in the 1970s (Trabant and Benson, 1986). We then propose two possible scenarios for the extent of the glacier surface where internal accumulation may occur (the 'permeable zone'): (1) an area equal to the region of positive firn balance in a given year, and (2) an area equal to the permeable zone in the 1970s. Scenario #1 provides a minimum of internal accumulation, while #2 provides a maximum. We begin with a discussion of these different assumptions.

The capacity for internal accumulation in old firn and ice is reset each winter by cooling. An increase in internal accumulation leads to higher firn temperature in autumn, which in turn increases the temperature gradient and the heat flux during winter. This negative feedback causes the capacity to depend mainly on the mean winter temperature and less so on the history of surface water input. While there is an increase in available surface water between the 1970s and the 1990s (more melt), there is no indication of a large (several K) change in mean winter temperature. Therefore, our assumption regarding a constant capacity seems justified.

In the 1970s, the area assumed permeable to surface water was approximately equal to the area of firn accumulation (i.e. where the local surface balance was positive). In contrast, for the years 1993-95, surface accumulation of new firn was negligible, with AARs as small as 0.02. Under these conditions, scenario #1 leads to very small amounts of internal accumulation (Table III.2, column 6). This scenario is not supported by observational evidence during 1993-95.

The maximum scenario (#2) involves considerable internal accumulation outside the area of new firn accumulation. In this so-called transition zone (Trabant and Benson, 1986), there will be an unknown partition of the available surface water into *permanent* internal accumulation and runoff. Water may freeze in the old firn early in the melt season, only to be ablated and, possibly, lost as runoff later in the melt season. The net amount

lost will depend on the evolving permeability and drainage patterns of the surface, which can be quite complex. Summers with high ablation may produce extensive ice layers in the firn that "seal" the surface to further percolation. On the other hand, internal accumulation need not be restricted to areas of the surface that are porous in a microscopic sense. For example, Sater (1959) noticed that a large number of small crevasses (5-20 cm wide) opened in the upper ablation area during the cold winter months, but they were closed by refreezing of water in summer - thus acting as a sink for internal accumulation.

Within the transition zone of scenario #2 the entire spring snow cover is ablated, and eventually also a considerable amount of old firn. Therefore, we estimate internal accumulation as the sum of the spring snow balance and summer precipitation, while we assume that late summer ablation of old firn (density = 0.75 g cm^{-3}) is released as runoff. Results for this maximum scenario are also shown in Table III.2. We note that for years 1993-95, internal accumulation exceeds net accumulation under this scenario. This is a direct result of the large amount of old firn that is ablated in the late melt season. Some of the early-season internal accumulation is lost or compensated by this firn ablation. For 1996, maximum and minimum scenarios of internal accumulation are similar, with internal accumulation being about 25% of the net accumulation. This is similar to that observed in the 1970s mainly because the permeable zone actually had about the same extent.

III.5.6 Topographical mass balance measurements

Average net mass balances for the longer time intervals between the different field programs can be determined using data on the surface elevation of the glacier as obtained by photogrammetry or optical surveying. These long-term topographic balances can then be compared to the annual balances presented above to give a picture of mass balance trends over the last 40 years. The long-term balances also provide useful constraints on the mass balance modeling described in a later section.

A photogrammetric stereo comparison by Dorrer and Wendler (1976) suggested a value of -13 cm a^{-1} for the long-term average mass balance from 1958 to 1971. This average balance is somewhat less negative than the mean of the 1970s net balances (-19

cm a^{-1}), but not significantly. In a later study, Rabus and others (1995) compared the elevations at about 60 locations on the glacier surface, as optically surveyed in 1972 (D. Trabant, pers. comm.) with a 1:10,000 scale topographic map with 5 m contours derived from aerial photography of 1958 (Anonymous, 1958). Unreasonably large values (up to three times Dorrer and Wendler's) and irregular apparent elevation changes revealed large systematic errors in the 1958 topographic map and, thus, it was difficult to make a reliable estimate for the 1958-72 mass balance using this method. A photogrammetric reevaluation of the 1958 air photos (J. Mitchell, pers. comm.) shows that the mapping errors cannot be reduced significantly. Irregularities in the 1958 photogrammetry are responsible for these problems. Unfortunately, we cannot directly evaluate the errors in Dorrer's (1975) analysis, but we believe them to be smaller than those associated with the 1958 map. As an independent check, we have also compared the above mentioned 1972 vertical elevations with a 1:63,360 scale topographic map produced by the US Geological Survey (USGS) from 1956 aerial photography. Despite the larger error inherent in the coarser contour interval (100 ft, or about 30 m), this comparison gave an estimate of -17 ± 6 cm a^{-1} for the long-term average balance from 1956 to 1972. This value is close to that of Dorrer and Wendler (1976), and we thus take -15 ± 5 cm a^{-1} as an estimate for the 1958-1972 average annual balance.

By resurveying the 1993 surface elevation at the same 1972 positions mentioned above, Rabus and others (1995) determined the long-term average net mass balance over the period 1972 to 1993 as -33 ± 1 cm a^{-1}. This is significantly more negative than the 1958 to 1972 average balance, thus giving further support to a change in climate in this region.

In June 1995 the surface elevations at about 40 of these positions were again resurveyed. Combination of these data with snow depths at each site allowed us to make a topographic estimate of the average stratigraphic mass balance for 1993 and 1994. The resulting value was -65 ± 6 cm a^{-1} for these two years. A density of 0.90 g cm^{-3} was used to convert volume change to water equivalent. This may introduce a slight bias toward a

more negative balance as there was significant ablation of old firn during both years. This effect has been discussed in detail by Krimmel (1989).

We can compare this average 1993-94 balance with those presented in Table III.2 under the different scenarios of internal accumulation. Taking the mean of the 1993 and 1994 balances in this table, we find $\langle b_{(s)} \rangle$ = -87 ±8 cm a^{-1}, $\langle b_{(min)} \rangle$ = -84 ±8 cm a^{-1} and $\langle b_{(max)} \rangle$ = -63 ±6 cm a^{-1} for the glaciological two-year average balances. The close agreement between the latter value and the topographical value (-65 ± 7 cm a^{-1}) implies that the scenario which predicts maximum internal accumulation is probably the more realistic. Comparison of the glaciological surface balance and topographical balance yields a value of 22 cm a^{-1} for the mean annual internal accumulation over this two year period. These results suggest that the zone of permeability, where internal accumulation occurs, is much larger than the area of firn formation during warm summers. As discussed before, this may lend importance to alternative processes of internal accumulation, such as refreezing of water in crevasses.

In a similar study, Haakensen (1994) has found that long-term topographic balances and cumulative stratigraphic balance on an arctic glacier in Norway disagree by about 14 cm a^{-1}, while these two types of balance agree quite well for the more temperate glaciers he studied. Haakensen interprets these differences as internal accumulation of an amount equal to 14 cm a^{-1}, which is similar to our findings on McCall Glacier

III.5.7 Mass balance gradient

The gradient of surface balance with elevation reflects the climatic regime of a glacier. Unlike the mass balance itself, the balance gradient often shows little variation from year to year. A long-term change in the balance gradient may indicate a change in the climate towards one which is more continental or more maritime. To investigate this possibility, the surface balance as a function of elevation was calculated from the balance contour maps in Figure III.4 and III.5 using 100 m elevation bands. For each of the two time periods (1970s and 1990s) we used the concurrent surface elevation, thus taking into account the significant thinning since the 1970s (Rabus and others, 1995). The results are

shown in Figure III.6a for the 1970s and in Figure III.6b for the 1990s. Interesting changes since the 1970s are the reduction of a local ablation maximum at ca. 1600 m and an increased variability of the local mass balance in the 1990s. Linear regression of all the mass balance curves as a function of (concurrent) elevation for the 1970s and for the 1990s gives the heavy lines shown in these figures. The corresponding balance gradients are 172±4 cm a^{-1} km^{-1} for the 1970s and 201±6 cm a^{-1} km^{-1} for the 1990s. Without the exceptionally cold year in 1996 the balance gradient in the 1990s would be slightly higher (210 cm a^{-1} km^{-1}). We conclude that there has been a significant increase in the balance gradient on McCall Glacier from the 1970s to the 1990s. One possible interpretation is a trend towards a larger mass exchange in the 1990s. The mass balance modeling described in a later section lends further support to such a change. This balance gradient is similar to that measured on White Glacier in the Canadian Arctic (Cogley and others, 1996).

III.6. Regional representivity of the McCall Glacier mass balance

The mass balance record of McCall Glacier is the only long-term record in arctic Alaska. One may question how representative this record is in a regional context. To investigate whether the trends in McCall Glacier balance reflect a coherent regional signal, we measured changes in surface elevation along the centerlines of ten other glaciers in the northeastern Brooks Range (Figure III.1). Our surveys were carried out once on each glacier during the period 1993-95, and the elevation changes with respect to 1956 or 1973 topographic maps were used to estimate long-term mass balances over the intervening time period.

The surveyed glaciers fall into three morphological groups (Figure III.2): Larger valley glaciers (McCall , Esetuk and the two Okpilak glaciers), smaller valley glaciers (Arey, Wolverine Crag, Gooseneck, Bravo, and the two Hubley glaciers,) and one cirque glacier (Hanging Glacier). The distance from McCall Glacier to Arey is about 5 km, and about 20 km to Esetuk and the Okpilak Glaciers. All the other glaciers are immediate neighbors of McCall Glacier, i.e. their drainage basins are within or have a common border with the McCall Glacier drainage basin.

The valley sections occupied by West Okpilak Glacier, the largest arctic glacier in Alaska, and East Okpilak and Esetuk Glaciers are somewhat wider and less shaded than the glacierized section of the McCall valley. This reflects the more erodable bedrock outside and near the tectonized margins of the granitic Okpilak Batholith (dotted outline in Figure III.1), in contrast to the more erosion resistant inner portions of the batholith, where McCall Glacier is situated. With the exception of Arey Glacier all other glaciers are also situated in the interior of the Batholith and occupy deeply incised valleys with steep, sometimes vertical, walls.

III.6.1 Topographic maps

Four adjacent USGS map sheets of scale 1:63,360 and a contour interval of 100 ft (about 30 m) were used in the study of these glaciers. The datum of the maps is NAD27, with elevation given above mean sea level. Mapping photography was acquired in two different years: 1956 and 1973. The maps, numbered from I to IV, and the dates of photography are listed in the first two columns of Table III.3. The map on which each glacier is located is listed in Table III.4.

Three significant error sources can be present in the elevation contours of these maps: (i) a random error on the order of ±15 m in elevation corresponding to half a contour interval, (ii) local systematic errors in regions where the air photos show poor stereoscopic quality, such as the accumulation areas of glaciers, and (iii) a systematic offset, spatially constant or not, between the map and the true elevation. The latter errors can be on the order of 20 m or so because geodetic control for the photogrammetry was extremely sparse in this part of North America.

The random error will cause fluctuations about a smooth curve of elevation change versus elevation on a glacier. Propagation of this random error into the calculation of the cumulative mass balance (as an area-weighted average of elevation change) leads to a division of the 15 m error in each contour by the square root of the number of contours along the glacier (Echelmeyer and others, 1996). Systematic offsets, on the other hand,

will not be reduced in their effect on the balance, and we therefore have made independent estimates of these latter errors for each map and glacier.

Potential systematic offsets were identified in two ways: Either we surveyed the true elevation of topographic highs that were labeled to ±3 m (10 ft) on the maps ("spot elevations") using static Global Positioning System (GPS) methods, or we made airborne laser/GPS profiles (Echelmeyer and others, 1996) over bedrock surfaces and evaluated the elevation difference between the profiled surface and the map contours. Both of these GPS elevation measurements were made with respect to the WGS84 ellipsoid; a geoid model (Alaska94) was used to relate these ellipsoid heights to mean sea level. Mean vertical deviations, $\langle \Delta z \rangle$, between our surveys and the map elevations are given in Table III.3 for both the spot elevations and the profile results. The corresponding standard deviation, σ, and the number of surveyed points, n, are also shown. The elevations determined by GPS have an accuracy of 0.5 m or better. Maximum horizontal deviations, determined for the spot elevations, were less than 25 m in all cases.

No significant vertical offset was found for the Demarcation Pt. B5 map. In the case of Mt. Michelson B1, both spot elevations and profile data show that the map is consistently 20±2 m higher than the measured elevations. The situation on the Mt. Michelson A1 map is somewhat more complex. A spot measurement made a few kilometers south of West Okpilak Glacier shows the map to be 17 m *higher* than the measured value, while profile measurements made about ten kilometers north of the glacier indicate that the map is 14 m *lower* than expected. In the immediate vicinity the glacier terminus we find that the map is 1.7±2.7 m lower than the profiled surface. The interpretation of this pattern as a ramp-like north/south offset clearly needs more survey data. In lieu of such data, we assume a zero constant offset ($\langle \Delta z \rangle \approx 0$ m) for this map in the vicinity of West Okpilak Glacier. The Demarcation Pt. A5 map was not field-checked, and we used $\langle \Delta z \rangle \approx 0$ m from the adjoining sheet Mt. Michelson A1. These choices assure similar and reasonably small elevation changes in the upper accumulation areas of

both West and East Okpilak Glaciers. The mean offsets for each map were used to correct map contour elevations.

Local systematic errors can be identified by unreasonable deviations in the elevation change curves of the different glaciers. Also, we have examined the actual mapping photos for areas of low stereoscopic contrast. In most cases these local errors appear to be relatively small. However, their effect on the cumulative balance depends crucially on the area distribution of the corresponding glacier, as errors in extensive accumulation areas can strongly influence the mass balance calculated from elevation changes.

III.6.2 Survey methods

Three different GPS-based methods were used to survey the centerline elevations and termini of the glaciers. In 1993, an airborne laser ranger system was used (Echelmeyer and others, 1996). A laser ranger and gyroscope, mounted in a small aircraft, are used to determine the distance of the sensor above the glacier surface, while the position of the airplane with respect to a benchmark with known coordinates is tracked using continuous kinematic GPS methods. The horizontal and vertical accuracies of this system are about ±0.3 m. In 1994 and 1995 we used two different ground-based methods to survey the smaller glaciers. The more accurate involved kinematic GPS profiling while walking or skiing down the glacier. The vertical accuracy of this method is similar to the airborne system, ±0.3 m. The second method utilized a lightweight GPS system which gave the coordinates of specific points along a centerline profile (about every 100 m). These latter data were then differentially corrected using data recorded at a second, stationary unit. The vertical accuracy of this method was ±3 to 8 m.

III.6.3 Elevation and volume change

The ground tracks of the profiles on each glacier are shown in Figure III.2 (solid dots connected by lines), superimposed on topographic maps. Profiles of Arey and Wolverine Crag glaciers consist of isolated survey points acquired with the less accurate ground-based method discussed above. On the other glaciers, the profiles are continuous, with

points spaced every 1 to 1.5 m along the profile. These were acquired with either the airborne or the high accuracy ground-based methods.

Horizontal coordinates of the profile were transformed from the WGS84 datum to the map datum (NAD27). Vertical height above the ellipsoid was transformed to elevation above mean sea level using the Alaskan geoid model. The geoid separation above the ellipsoid in our study area varies between +3 and +6 m.

Elevation change was obtained by determining the elevation at each point where the profile intersected a contour line on the map. Cubic spline interpolation was used between the data points on Wolverine Crag and Arey glaciers. The random error of elevation change is entirely dominated by the ±15 m random error for the map contours. Even in the case of the less accurate GPS method, the combined error is only slightly larger, ±17 m.

To determine the change in glacier volume between the mapped surface and a single longitudinal profile on each glacier, we assumed that the elevation change was constant across the width of the glacier at each contour. As the glacier thinned or thickened, its width, and therefore area, would also change. In most cases we did not measure this change in width; instead we estimated it by multiplying the elevation change along a specific contour line by the cotangent of the slope of the valley walls at that contour. The projected 1990s outline of the lower glacier, as determined using this algorithm, is shown in Figure III.2 as a dotted line for each glacier. The terminus outlines of McCall and West Okpilak glaciers were also surveyed to a horizontal accuracy of ±2 m using GPS methods. There was satisfactory agreement between these surveyed glacier outlines and those calculated by our algorithm.

Volume change was then calculated as the volume between the old and new (1990s') surfaces following the method of Finsterwalder (1954). The area-averaged thickness change was obtained by dividing the total change in volume by the area of the glacier, here taken to be the average of the mapped area and the 1990s' (estimated) area. The mean annual mass balance (water equivalent) was calculated assuming a density of 0.90 g cm^{-3}, thus taking the density distribution with depth to be constant.

A rigorous error estimate for the volume change calculation involving a single centerline profile is difficult to obtain. However, we carried out the following sensitivity test on the McCall Glacier data: Elevation changes along a centerline profile descending from the upper cirque, and another from the lower cirque, were determined using the optical survey data from 1972 and 1993 (surveyed points are shown as open symbols on the McCall Glacier map in Figure III.2). Following the algorithm described above, these elevation change data were then used to calculate the cumulative balance from 1972 to 1993. These results could then be compared to those from a two-dimensional interpolation of the entire set of surveyed positions (including all those off the centerline), as described by Rabus and others (1995). The centerline profiles down the upper and lower cirques yielded -7.9 and -7.3 m of water, respectively, which agree within 10% of the value -6.9 m, quoted by Rabus and others (1995). A similar error estimate was obtained by Sapiano (1997) on a different glacier. He used a variation of our procedure, but had the advantage of having two complete maps made about 30 years apart.

A second unknown in estimating the error in volume change is the contribution of local systematic errors. As described earlier, these errors may be enhanced by the often large surface area within the snow-covered regions of a glacier. In order to address this problem, we compared the volume change as calculated using a smoothed elevation change curve with that for the original, unsmoothed curve. In most cases, the smoothed curve did not lead to substantial differences in the calculated volume change. In only one case, West Okpilak Glacier, was the difference more than 10%. In that particular case we used the smooth version of the curve to calculate the volume change.

III.6.4 Results

Elevation changes on these different glaciers are shown as a function of 1990s elevation in Figure III.7 and Figure III.8 for the period 1956 to 1993 and 1973 to 1993, respectively. In both figures the plot in the upper left-hand corner shows the mean elevation change for all the glaciers in the time period considered (solid line), along with one standard deviation about this mean (light gray) and the envelope of all values of elevation change for the

glaciers (dark gray). This plot is useful in determining how meaningful the mean elevation change is. All glaciers show strong thinning at lower elevations, and a decrease in the magnitude of this thinning with increasing elevation. For 1956 to the 1990s, the mean elevation change was about -60 m at 1400 m and about -14 m at 2000 m; these values were about 15 meters smaller for 1972 - 1990s.

In the other plots of these two figures the elevation change on the individual glaciers is compared to the mean elevation change for all glaciers over the same time period. For the period 1956 to 1993 (Figure III.7), the elevation changes of Esetuk, Gooseneck, Bravo, and South Hubley Glaciers agree well with those on McCall Glacier. North Hubley and Wolverine Crag Glaciers show significantly larger elevation changes, on average, than those observed on McCall Glacier at corresponding elevations. The range of elevations on Hanging Glacier is too limited for a conclusive comparison. During the 1973 to 1993 period, elevation changes on West and East Okpilak and Arey Glaciers were similar to those on McCall Glacier. Table III.4 contains further results on the different glaciers. The first part of this table shows the dates of survey and the methods used, and geometric parameters of the glaciers, including mean glacier area A; glacier length L, elevation of the terminus, z_{min}, and of the head of the glacier, z_{max}, all at the time of mapping; and the mean aspect of the glacier. The second part of the table gives the results of the volume change calculations, ΔV, in cubic meters of ice, the area-averaged elevation change of the ice surface over the time period, $\Delta z_{<A>}$, the mean mass balance, b, and the change in terminus position, ΔL, from the date of mapping to the 1990s. In order to assess the representivity of McCall Glacier, we have also calculated the ratio of the mass balance of the study glaciers to the McCall Glacier mass balance (second to last column of Table III.4). Values range from 0.04 to 1.9. However, the majority of glaciers had values of 1.0 ± 0.2, i.e. their average mass balances are within 20% of the McCall Glacier balance.

In general, the elevation change as a function of elevation and the average mass balance on each of the glaciers is similar to that measured on McCall Glacier. There are, however, some differences. While most mass balances range between -25 to -31 cm a^{-1} (6

glaciers), a smaller group of glaciers has more negative balances around -50 cm a^{-1} (4 glaciers). The only cirque glacier in the set was close to equilibrium. The observed differences may be related to several factors.

The volume change and mass balance calculations depend on the value assumed for the systematic offset of each map. This is somewhat subjective, especially in the case of the glaciers on maps Mt. Michelson A1 and Demarcation Pt. A5- West Okplilak, East Okpilak and Arey Glaciers - where the offset is apparently not constant over the map (Table III.3). As explained above, we have attempted to minimize the effects of these errors by a judicious choice for the correction factor we apply. In this case, East Okpilak is similar to McCall Glacier, while West Okpilak Glacier, for which the chosen offset should be particularly well constrained, shows an "anomalous" volume change.

Geographic location of the glaciers does not appear to determine their mass balance, as there is no clustering of "anomalous" glaciers within the region. In addition, no correlation between mass balance and valley width or the height of the valley walls was found. Perhaps the most likely explanation for the different mass balances lies in the differences in glacier geometry, size and aspect. That the geometry may play an important role is brought out by the observations of Tangborn (1990) which show that different area-altitude distributions for two neighboring glaciers - North and South Klawatti Glaciers in Washington - lead to a decrease in volume on one glacier, while the other is growing. In our case, the area-altitude distributions of the glaciers which we studied generally show much less variation between the glaciers, and it seems unlikely that these variations can cause significant differences in mass balance. The effects of glacier aspect are shown in Figure III.9a, in which the average mass balance is plotted against aspect. The first diagram (1956-1990s) suggests more negative balances for glaciers with eastern aspect, but the diagram for 1973 to the 1990s shows the opposite trend. Thus there seems to be no conclusive cause of the observed balance differences.

In summary, the data from the various glaciers indicate that the mass balance trends of McCall Glacier are, in general, similar to those found elsewhere in the northeastern

Brooks Range. Most of the glaciers studied show an overall thinning at the rate of 30 to 40 cm a^{-1} (ice). As expected, the thinning is the greatest at lower elevations, amounting to nearly 60 m over 20 to 40 years. At higher elevations most glaciers thinned, albeit at a reduced rate. There does not appear to be any simple relation between the observed small variations in mass balance and the location of the glacier, or its geometry, aspect and size.

Another example of an equally uniform pattern of regional mass balance was given by Pelto (1996) for eight glaciers in the North Cascades. The mean annual balance of these temperate glaciers was -39 cm a^{-1} over a ten year period, 1984-94, with seven of the individual glaciers having balances between -20 and -53 cm a^{-1}. Correlation coefficients between the annual balance time series of the glaciers were all greater than 0.85. Both regional mean and variations of mass balance are of similar magnitude as found for our set of NE Brooks Range glaciers and we would consequently also expect equally high inter-glacier correlation coefficients of annual mass balance for our study area.

III.6.5 Mass balance and changes in terminus position

While the long-term mass balances of our different study glaciers are, for the most part, similar, the corresponding rates of terminus retreat are not. In Figure III.9b we show the fractional change in length of each glacier. There is no consistent picture, except that each glacier has retreated. For instance, compare McCall Glacier with Gooseneck and East Okpilak glaciers. The elevation change curves and the average mass balances over the respective time periods are nearly identical (Table III.4 and Figures III.7, III.8 and III.9a). Over the same time periods, McCall Glacier retreated substantially, while Gooseneck Glacier showed negligible retreat and East Okpilak Glacier showed nearly four to five times more retreat than McCall (Figure III.9b). This is probably due to the particular geometry of each glacier, especially that near the terminus. Inspection of the 1956 airphotos reveals that Gooseneck Glacier was a hanging glacier with a terminal ice face which was nearly vertical. Since then the terminal ice has thinned without much retreat, forming the gentle slope that exists today. Neither McCall nor East Okpilak Glacier showed a similar effect at the terminus. It is clear from the results of this section that

retreat of the termini of different glaciers is a complex function of glacier geometry and mass balance; a finding similar to that of Echelmeyer and other (1996) for different locations in Alaska. Lichenometric dates of late Holocene end moraines by Calkin and Evison (1996) confirm a complicated pattern of terminus changes since the end of the Little Ice age (about AD 1890) in this region of the Brooks Range.

While it is common to use the long-term fractional change in length, $\Delta L/L$, times the balance at the terminus, b_T, as a measure for the mass balance disturbance underlying the length change (Paterson, 1994), the results in Table III.4 and Figure III.9b clearly demonstrate that this cannot be applied indiscriminately. A more appropriate quantity to infer a mass balance disturbance from changes at the terminus would perhaps be $f = \Delta z_T/\Delta z_{<A>}$, the ratio of elevation change near the terminus and the average elevation change. Schwitter and Raymond (1993) postulate that after a step change in mass balance, f approaches a constant value of 0.2-0.3 for most glaciers after a time that is much shorter than their corresponding response times. However, for our set of NE Brooks Range glaciers, the high random uncertainty of ±15 m in *local* elevation change Δz_T makes it impossible to judge whether $f/\Delta z_T$ would indeed be a better measure of mass balance disturbance than $(b_T \Delta L)/L$.

III.7. Synoptic scale representivity of the McCall Glacier mass balance

In this section we investigate the correlation between the mass balance of McCall Glacier and climatological data from weather stations 100 to 650 km away from the glacier. These correlations are used to determine how representative the balance of McCall Glacier is on a synoptic scale. That is, how well does this mass balance record represent climatic variation in this part of the Arctic? We first describe correlations on a daily basis between meteorological variables measured on McCall Glacier in the 1990s with corresponding data from different arctic weather stations. Second, we develop an empirical degree day model for the mass balance of the glacier using annual mass balance data from the 1970s and 1990s and a combination of daily and monthly weather station data. Using this model

to fill in gaps of the mass balance record then allows us to speculate on the climatic causes of the increasing trend toward negative balances and thinning of the glacier.

The locations of the weather stations considered in this study are shown in Figure III.1 (inset), and relevant parameters are given in Table III.5. We focus on the summer temperatures at these stations, which are possibly related to ablation, and precipitation during the months in which accumulation is likely on the glacier.

III.7.1 Model description

Physical mass balance models use weather station data to predict the energy balance on the surface of a glacier, from which accumulation and ablation, and then mass balance, are calculated (e.g. Oerlemans 1992; Conway and others, 1995). These models require calibration of the basic energy balance parameters on the glacier, such as air temperature, windspeed, relative humidity, and albedo, as well as their effect on mass balance. Most models of this type have been applied to temperate glaciers, for which internal accumulation and superimposed ice are neglected. Because of this, and the scarcity of energy balance measurements on McCall Glacier, these models cannot be accurately applied.

A second type of mass balance model is empirical. These are essentially least-squares regressions of a measured mass balance series with one or more climatological parameters measured at nearby weather stations. Accumulation is often estimated using winter precipitation at some station. For modeling ablation, summer air temperature, or some function of it such as the sum of positive degree days, plays the most important role. Incoming radiation at the surface is often not as useful as air temperature in such models, a finding seemingly in contradiction with energy balance measurements on glaciers. These measurements suggest that radiative heat fluxes are far more important for ablation than the sensible heat flux, the latter of which depends primarily on air temperature. Braithwaite (1981) has shown that the radiative heat flux has a variance which is an order of magnitude smaller than that of the sensible heat flux, and it is this reduced variance that

causes the radiative flux to have minimal effect on a least-squares regression between climatological parameters and mass balance.

Herein we develop an empirical model of the McCall Glacier mass balance that has two main climatological inputs. The first is the sum of positive degree days, D, as calculated from twice-daily radiosonde soundings made in the atmosphere above one of the first order weather stations listed in Table III.5. D is calculated for the median elevation of the glacier, about 2000 m. The second input is accumulation, A, as calculated from precipitation measured at one of the stations. The balance model is then simply the linear combination

$$\Delta b = c_d \Delta D + c_a \Delta A \qquad (1)$$

where Δ marks per cent deviations of quantities from their corresponding means during the calibration period. (If, instead, b is modeled as a function of D and A, rather than of their deviations, Δ, then a third constant appears on the righthand side. This constant can be expressed as a function of the mean values of b, A, and D.) The constants c_d and c_a are determined by the least squares fit of Equation (1) to the set of eight measured mass balances given in Table III.2. Results for both the surface balances and the net balances with maximum internal accumulation (Table III.2) are presented.

The actual input parameters require some care in their specification. Surface temperature is often influenced by local effects, such as selective heating depending on the ground cover, fog and low stratus clouds, especially in arctic coastal locations. For this reason, we follow Samson (1965) and Conway and others (1995) in using the air temperature at the median elevation of McCall Glacier over the weather station. The median elevation of McCall Glacier generally falls between the 850 mbar and the 700 mbar pressure levels. In our investigations we have found that the mean layer temperature, $\overline{T}$ (in degrees C), as determined from the hypsometric equation (Anonymous, 1963)

$$\overline{T} = \frac{(z_{850} - z_{700})}{67.442 \times \log\left(\frac{850}{700}\right)} - 273.16 \qquad [^{\circ}C] \qquad (2)$$

shows a better correlation with measured temperatures on the glacier than does a simple interpolation of radiosonde temperatures. In this equation, z_{850}, z_{700} are the 850 mbar and 700 mbar pressure levels. Daily temperature at this median elevation, T_d , was calculated as the average of the two layer temperatures (Eqn. 2) available each day. This daily temperature can be compared to the air temperature measured at 2100 m on McCall Glacier (on the moraine) in the 1990s. An example of such a comparison for May to September 1994 is shown in Figure III.10a for the different weather stations listed in Table III.5. (Other years show similar correlations.) The daily temperature above Inuvik follows that on McCall Glacier most closely, with a correlation coefficient of $r^2 = 0.78$ for the entire period and $r^2 = 0.66$ if only positive temperatures are considered (Figure III.10b). These correlations are quite good, especially considering the distance between the stations. A high degree of correlation suggests further that the moraine location of the McCall weather station does not cause significant disturbance of the temperature record via local heating effects. Correlations with Barrow and Fairbanks are generally much worse (for the entire period $r^2 = 0.54$ and 0.51, respectively), as can be seen in Figure III.10a. Similar high correlation coefficients were found by Conway and others (1995) between Blue Glacier (Washington) temperatures and those at a nearby radiosonde station, although that station was much closer to the glacier (70 km).

The sum of positive degree days in a given year is obtained from these daily temperatures as

$$D = \sum_{BalYr} \max[T_d, 0°C] \qquad (3)$$

This sum was calculated for all years on record for each of the stations.

As a measure of precipitation on the glacier we tried the daily precipitation at Inuvik or Barrow. No acceptable correlation was found with the 1994 measurements on the glacier. Because of this, we chose to calculate the annual accumulation on the glacier, A, from the monthly precipitation, P_m, at Inuvik or Barrow. This was done in two ways in order to bracket the amount of internal accumulation. First, we summed the 'solid' precipitation over one year, beginning with month m_1 in autumn of the previous year. The

amount of solid precipitation was estimated using the fraction of days, $N_m(T_d < 0\ °C)/N_m$, during the month in which the daily temperature, T_d, on McCall Glacier was below freezing. Here N_m is the number of days in month m. Thus,

$$A = \sum_{m_1}^{m_1+1year} P_m \frac{N_m(T_d < 0°C)}{N_m} \qquad (4)$$

The remainder of the total precipitation is assumed to be lost as runoff. While this is reasonable for accumulation on temperate glaciers and for surface accumulation in general, net accumulation on arctic glaciers may be greater as a result of internal accumulation. To allow for this internal accumulation in the mass balance model we also used a second, alternate expression for A

$$A = \sum_{m_1}^{m_2} P_m \qquad (5)$$

In this case, all of the monthly precipitation falling between month m_1 in the previous autumn and month m_2 of the actual balance year is assumed to contribute to the net accumulation. Neither Equation (4) or (5) accounts for the part of internal accumulation that is due to refreezing of surface melt; this latter part depends however on summer temperature and is thus contained in Equation (3) to a certain extent.

The choices of the weather station(s) used to calculate the temperature and precipitation, and of the months when precipitation fell on the glacier (m_1 and m_2 in Eqns. 4 and 5), are part of calibrating the empirical model (Eqn. 1) in fitting it to the observed mass balances and the long term trends.

III.7.2 Results of the mass balance model

The mass balance model (Eqn. 1) was run using the degree days and accumulation calculated from the climatological variables of the different weather stations in an attempt to best fit the mass balances listed in Table III.2. As stated earlier, both the surface balances and the net balances in that table were used (independently) to calibrate the model. There were two main sets of criteria used to judge the quality of the fit, first the

single and multi correlation coefficients of measured mass balance with calculated degree days or accumulation (see e.g. Letréguilly, 1988), and second an examination of how well the long-term average net balances for the periods 1958-72 (-15 cm a^{-1}) and 1972-93 (-33 cm a^{-1}) were reproduced. The latter criterion applies mainly to the net balance evaluated from Equation (1), not the surface balance. Additional criteria were used to constrain the solutions, including the physically reasonable assumption that an increase in precipitation at a station should cause a more positive mass balance on the glacier - not more negative.

Many model runs were made to constrain the stations, the months of precipitation, and the relation between station precipitation and accumulation (Eqn. 4 or Eqn. 5). Here we present only the salient features of these runs, focusing on those which gave the best fits to the data. Parameters for two typical models of *surface* balance using data from Barrow are presented in Table III.6, and for Inuvik in Table III.7a. In Table III.7b we present similar results for the best models of *net* balance using Inuvik data. The first column lists the equation used to relate P_m and accumulation, the next four are the multi-parameter (C_{multi}), single parameter (C_D for D and C_A for accumulation), and cross (C_{DA}) correlation coefficients, the next two are the long-term balances calculated from the model (for Inuvik, the station record does not completely overlap the 1958-72 time period), and the last two columns are the coefficients c_d and c_a in the resulting model (Eqn. 1).

Surface mass balance predictions for the best fit model over the entire span of the station data are shown in Figure III.11a for Barrow, and in Figure III.12a for Inuvik. The models shown are those which use Equation (5) to define the D to A relationship with parameters given in the first row in Table III.6 and 7a. The shaded band in these figures is the error in the solution obtained by assuming variations of 15% in D and A, and an error of ±8 cm a^{-1} in the measured balances (shown as solid circles). In an approximate manner, this accounts for the limited number of measured balances used in the model calibration. A smoothed curve through the modeled balances is shown as a light line in each figure; this curve illuminates any trends. The input data for each model are shown in Figure III.11b

and III.12b, respectively. These include the yearly degree day sum and the estimated accumulation, along with a smooth curve of each. Figure III.12c shows the modeled *net* balance using the Inuvik data and Equation (5) (the first row in Table III.7b).

We describe results from each of the model runs in turn.

1) *Barrow:* At a first glance some of the multi-parameter correlations using the Barrow data seemed to be significant. However, the degree day correlation coefficients are small (C_D <0.28), implying that the balance is not strongly correlated with temperature. This is not to be expected for the climate of McCall Glacier. More importantly, there is a negative correlation between surface balance and accumulation - hardly a physical reality. In addition, the modeled long-term average net balances are -89 cm a^{-1} for 1958-72 and -57 cm a^{-1} for the 1972-93 period (the surface balances are even more strongly negative, Table III.6), which is in obvious contradiction to the measured values (-15 and -33 cm a^{-1}, respectively). The long-term trends and the estimated degree day sums are also in disagreement, as shown in Figure III.11a and III.11b, respectively. Thus, we conclude that there is no significant *and* realistic correlation between Barrow climatological data and the mass balance of McCall Glacier.

2) Inuvik: The correlations of Inuvik data with the balance on McCall Glacier are generally significant, especially when the most reasonable months are used as starting and ending dates in Equations (4) and (5). Based on the sonic ranger data shown in Figure III.3 and our observations in the field, accumulation for the balance year begins in mid August and ends in June. Thus we would expect that $m_1 = 8$ (to the nearest integer month) in Equation (4), and $m_1 = 8$ and $m_2 = 6$ in Equation (5) (i.e. accumulation from August of the previous year to 31 June). Models with these values of m_1 and m_2 give the best fits to the measured balances (Table III.7), although a variation of ±0.5 month in these parameters does not change the correlation a great deal. There is a strong negative correlation between balance and Inuvik degree days (C_D = -0.8), and a somewhat weaker, but positive (and, therefore, physically meaningful) correlation with Inuvik precipitation

(C_A = 0.3-0.4). The modeled long-term trends for surface and net mass balance are both towards more negative values, as observed. If the net balances in Table III.2 are used to calibrate the model, then the modeled long-term average net balances are -18±4 cm a^{-1} and -32±3 cm a^{-1} for 1961-72 and 1972-93, respectively. This is in excellent agreement with measured long-term net balances. The trends in balance and the estimated degree day sums agree well with the measured values, as shown in Figure III.12a-c. We conclude that the climatological variables at Inuvik are significantly correlated with the balance on McCall Glacier, and that they can be used to model this balance as a function of time. Equations (4) and (5) gave similar results for the model parameters and correlation coefficients, and, thus, they both appear to be useful in defining the precipitation-accumulation relationship.

The correlation coefficients between the McCall Glacier mass balance and meteorological parameters from Inuvik are similar to what Pelto (1996) found in his study of eight North Cascade (Washington) glaciers. Here correlation with ablation-season temperature ranged between 0.68 and 0.84, while correlation with accumulation-season temperature (a good measure of winter precipitation for these temperate glaciers) ranged between 0.35 and 0.59.

3) *Kaktovik:* The climatological record at Kaktovik, 100 km to the north, unfortunately ends in 1988, so we can only use four of the measured balances in Table III.2 to calibrate a model using this station data. In order to determine if such a limited calibration is meaningful, we first attempted it using the 1969-72 subset with the Inuvik data, which gave good results with the full balance set (Table III.7). The results showed a consistently good correlation using Equation (5) and similar values of m_1 and m_2 . The long term balances were also in good agreement with those listed in Table III.7a, implying that the reduced calibration set can produce meaningful results.

Applying this limited calibration method to the Kaktovik data, we obtain +15 cm

a^{-1} for the average surface balance from 1958 to 1972 and -35 cm a^{-1} for 1972-88 (Inuvik data yields -33 cm a^{-1}). These results for Kaktovik show the same qualitative trend towards more negative balances, but they are otherwise quite different from the corresponding measured values, and from the Inuvik model results. We also compared the annual balances from 1961 to 1988 predicted by the Inuvik model and that using Kaktovik data. The correlation coefficient was 0.59, which is rather low. We conclude that despite its closer proximity, Kaktovik is considerably less suitable than Inuvik for modeling the mass balance of McCall Glacier. Reasons for this are given below.

4) *Fairbanks:* Replacing the degree day sum in the Inuvik model with the sum for Fairbanks causes a general drop in multi-correlation and increases the misfit between measured and modeled long-term mass balances. However, the correlations and the modeled long-term values are superior to results from Barrow or Kaktovik. This implies that, while climate change in interior Alaska is clearly different from that at McCall Glacier, these differences are less pronounced than those between McCall Glacier/ Inuvik on the one hand and the two arctic coastal locations on the other.

III.7.3 Some further thoughts on internal accumulation

Long-term values of internal accumulation can be calculated as the difference between the modeled values of surface and net balance. Using Inuvik data, we obtain +12 and +13 cm a^{-1} for the periods 1961-71 and 1972-93, respectively. These mean values are somewhat lower than the annual estimates given in Table III.2, but they add additional support to the importance of internal accumulation.

III.7.4 Discussion

The excellent correlation of McCall Glacier mass balance with climatological parameters from Inuvik, 430 km to the east, suggests this glacier can provide a synoptic scale climatic index for this part of the Arctic. The trend over the last four decades towards increasingly negative balance is likely caused by a synoptic scale climate change.

On the other hand, mass balance records from other high northern latitude glaciers (summarized by Cogley and others, 1995 and 1996) do not confirm an arctic-wide trend in the climate. In fact, the 35 year-long mass balance record of White Glacier, the main focus of Cogley and others' (1995 and 1996) study, shows no significant trend. The White Glacier record, measured about 1500 km to the northeast of Inuvik, shows no correlation with climatological parameters from Inuvik, nor with the balance of McCall Glacier. The difference in trends between McCall and White glaciers is further illustrated by a comparison of their long-term balances, calculated for White Glacier from the data presented by Cogley and others (1995): From 1958 to 1972, the average balance on McCall Glacier was -15 cm a^{-1} , while on White Glacier (from 1960 to 1972) it was -12±4 cm a^{-1} . From 1972 to 1993 it was -33 cm a^{-1} on McCall, while on White Glacier it was -10 ± 3 cm a^{-1} from 1972 to 1991.

The poor correlation between the McCall Glacier mass balance and climatological parameters from Barrow and Kaktovik implies that climate change patterns have been different at these arctic locations. To reveal these different patterns, we compare the positive degree day sum and the accumulation calculated from Equation (4) ($m_1 = 8$) for the different stations in Figure III.13. The curves were smoothed by a gauss filter of width 2.5 years to reveal potential trends more clearly. The positive degree day sum (Figure III.13a) shows a regular pattern of maxima and minima, superimposed on a linear warming trend. The period of the oscillations is not well resolved because of the short record length, but we estimate it as about 18 to 20 years for Barrow and Kaktovik, and about 16 years for both Fairbanks and Inuvik. The most recent minimum (1983) is approximately in phase for all stations. Accumulation (Figure III.13b) overall shows a trend toward smaller values. A cyclic pattern is also present, but it is less well defined than that for *D*. Comparison with Figure III.13a suggests an anti-correlation between winter precipitation and summer temperature at Barrow and Kaktovik. Such an anti-correlation has also been observed between mean annual temperature and winter precipitation of these two stations (Zhang and Osterkamp, 1993). It is contrary to the generally accepted idea of

a coupled increase in temperature and precipitation in the Arctic (e.g. Houghton and others, 1992). Inuvik shows a somewhat different pattern in A, with smaller oscillations, and these are more in phase with those of the degree days. In particular, the pronounced recent increase of positive degree days at Inuvik is accompanied by a small increase in accumulation.

It is interesting that the McCall Glacier mass balance and the climatological variables at Kaktovik, only 100 km away, are poorly correlated, while conditions at locations that are several hundred km apart from another (such as McCall Glacier and Inuvik, and from Figure III.13, Barrow and Kaktovik) seem to be well correlated with one another. We propose that these correlations are related to the mean summer position of the Arctic front. The mean summer temperature of a region in the Arctic appears to be related to its position relative to the mean position of the front (Barry, 1967), and the term 'climatic summer' is defined to be the period when this front is north of a region for an extended time. Barry (1967) has compiled the statistics on the summer (July) position of the Arctic front over North America for a five year period. The front always lies to the south of White Glacier in the Canadian Arctic and, thus, this glacier never has a 'climatic summer' as defined. It is therefore truly arctic in regime. Barrow and Kaktovik were both north of the mean frontal positions for all five years. However, the front did move north of Barrow and Kaktovik for about 20% and 40% of the summer, respectively, during this 5 year period. On the other hand, the front was north of both Inuvik and McCall Glacier for about 65% of the time, and it was north of Fairbanks about 85% of the summer.

Changes in climate may be related to corresponding displacements in the mean summer position of the arctic front. This would synchronously affect regions located along the length of the front for possibly several hundred kilometers, and possibly cause similar climatic changes in a roughly east-west direction, parallel to the front (such as Inuvik and McCall Glacier or Barrow and Kaktovik), while locations separated in a north-south direction, normal to the front, may experience differing climate changes, even if they are relatively close together (McCall Glacier and Kaktovik). Further evidence for the

importance of the Arctic front is given by Scott (1992), who shows that mean summer temperatures at tree line in Canada are significantly correlated with the magnitude of the characteristic change in air temperature that marks the passage of the front in spring.

Unfortunately, we are not aware of studies on the mean summer position of the arctic front over North America that are more recent than Barry's. A long-term study on the time evolution of the mean summer position of the front from the 1960s to present would be essential to test our ideas in detail.

Other factors may also cause the climate of the coastal stations (Barrow and Kaktovik) to differ from those located some distance inland, namely McCall Glacier and Inuvik. For instance, changing mean sea ice conditions during summer may change boundary conditions which govern the atmosphere on a larger scale. However, one should keep in mind that the degree days shown in Figure III.13a are measured at an altitude of over 1000 m above ground. Local phenomena, such as frequent coastal fog, have an important influence on ground temperatures, but they cannot be directly linked to differences of these degree days.

III.8. Conclusions

We have determined an internally consistent annual mass balance record for McCall Glacier for the years 1969 to 1972 and 1993 to 1996. The 1970's data were reevaluated under the same framework as the 1990's data. Separate records of surface mass balance and net balance, which includes internal accumulation, were compiled. Average surface balance was -29±3 cm a^{-1} from 1969 to 1972, and -63±3 cm a^{-1} during the period 1993 to 1996. The corresponding net balances were about -19 and -43 cm a^{-1}, respectively. This pronounced trend towards negative mass balances is confirmed by long-term net balances, which were determined from topographical volume changes: -15 cm a^{-1} from 1958 to 1972, and -33 cm a^{-1} from 1972 to 1993. The gradient of the surface mass balance with elevation increased by 17% between the periods 1969-72 and 1993-96.

Surface mass balance is consistently about 25 to 30% more negative than the net balance on McCall Glacier. This is a result of internal accumulation in the cold firn and ice

of this polythermal glacier. In the years 1969 to 1972, about 50% of the net accumulation was internal, while during the period 1993 to 1996 almost all of it was internal. A direct comparison of the average surface balance from 1993 to 1994 with the corresponding net balance determined by repeat surveys of glacier surface elevation gave an average internal accumulation of $+22\pm13$ cm a^{-1} for this two-year period, which again was most of the net accumulation. Because of the large component of internal accumulation, estimates of water released by arctic glaciers and their contributions to sea level rise may need to be reevaluated if based solely on surface balance measurements. This has been discussed by Pfeffer and others (1990) in application to the Greenland ice sheet.

Long-term average net balances over the periods 1956 to 1993 and 1972 to 1993 for McCall Glacier and ten other glaciers in the northeast Brooks Range were determined by comparison of 1956 and 1973 photogrammetric maps with surface elevation profiles made in the 1990s. The glaciers revealed a broadly similar pattern of negative mass balances, most of which (including McCall) were about -0.3 m a^{-1} . A few of the glaciers showed somewhat more negative mass balances of about -0.5 m a^{-1}. The amount of thinning as a function of elevation on McCall Glacier was also roughly similar to that observed on the other glaciers. This implies that the mass balance of McCall Glacier is representative of the glaciers in this region.

Mean retreat rates and fractional length changes were also measured for these eleven glaciers. They show a more complicated regional pattern than the mass balances, with some glaciers showing a concomitant retreat with the ongoing thinning, and others showing little retreat under similar thinning. The differences in retreat rate and fractional length change are probably caused by differences in glacier geometry, especially near the termini. Similar complex patterns have been observed elsewhere (eg., Echelmeyer and others, 1996).

The measured mass balance record of McCall Glacier shows a significant correlation with climatological parameters from Inuvik, 430 km to the east. A mass balance model based on this correlation indicates that the trend toward more negative balances is due

primarily to an increase in summer temperatures, and secondarily to a simultaneous reduction in precipitation.

While there is a good correlation between McCall Glacier's mass balance and climate data from Inuvik, there is no reasonable correlation with climatological parameters from Barrow, 550 km to the northwest, Kaktovik, 100 km to the north, or from Fairbanks, 650 km to the south. We interpret the presence or absence of correlations between each of these stations and McCall Glacier, and between the stations themselves, as being determined by their locations relative to the mean summer position of the arctic front.

We conclude that the mass balance of McCall Glacier is representative on both a regional scale and a synoptic scale. As such, the McCall Glacier mass balance record is an important measure of ongoing climate change in the Arctic.

III.9. Acknowledgements:

This study was supported by grant NSF-OPP-9214954 as part of the LAII program. We wish to thank G. Adalgeirsdottir, U. Adolphs, J. DeMallie, S. Campbell, J. Sapiano, K. Swanson, D. Trabant and C. Trabant for help with the fieldwork, and to Tazlina D. for providing an especially entertaining field season in 1994. Special thanks are given to Dennis Trabant and Carl Benson for access to their data and for stimulating conversations, and to W. Harrison for many helpful comments. We are also grateful to the refuge manager and other personnel of the Arctic National Wildlife Refuge for providing valuable and non-bureaucratic assistance to this project.

III.10. References

Alley, R. 1995. Resolved: the Arctic controls global climate change. *Arctic Oceanography: marginal ice zones and continental shelves. Coastal and Estuarine Studies*, 49, 263-283

Anonymous. 1960. Nine glacier maps. *American Geographical Society, Special Publ.*, No. 34

Anonymous. 1963. Smithsonian meteorological tables. sixth edition prepared by R.J. List, published by the *Smithsonian Institution.*

Barry R.G. 1967. Seasonal location of the arctic front over North America. *Geographical Bulletin*, 9(2), 79-95.

Bowling, S.A. 1991. Problems with the use of climatological data to detect climatic change at high latitudes. *Proceedings, Intern. Conference on the Role of the Polar Regions in Global Change, 11-15 June 1990, Fairbanks, Alaska, G. Weller, C.L. Wilson, B.A Severin (Eds,), Geophysical Institute, University of Alaska, Fairbanks*, **1**, 206-209.

Braithwaite R.J. 1981. On glacier energy balance, ablation, and air temperature. *J. Glaciol.*, 27(97), 381-391.

Calkin P.E., and L.H. Evison. 1996. Holocene glaciation and twentieth century retreat, northeastern Brooks Range, Alaska. *The Holocene*, **6**(1), 17-24.

Cogley J.G., W.P. Adams, M.A. Ecclestone, F. Jung-Rothenhaeusler and C.S.L. Ommaney. 1995. Mass balance of Axel Heiberg Island glaciers 1960-91. *Science Report No.6, National Hydrology Research Institute, Saskatoon, Saskatchewan.*

Cogley J.G., W.P. Adams, M.A. Ecclestone, F. Jung-Rothenhaeusler and C.S.L. Ommaney. 1996. Mass balance of White Glacier, Axel Heiberg Island, N.W.T., Canada, 1960-91. *J. Glaciol.*,**42**(142), 548-563.

Conway H., L.A. Rasmussen and P. Hayes. 1995. On the use of radiosondes to model glacier ablation. *Ann. Glaciol.*, **21**, 245-250.

Dorrer, E. 1975. Contribution to a general stereoscopic block analytical aerotriangulation. In *Deutsche Geodätische Kommission.* 125-136. (Reihe B Nr.214.)

Dorrer, E. and G. Wendler. 1976. Climatological and photogrammetric speculations on mass-balance changes of McCall Glacier, Brooks Range, Alaska. *J. Glaciol.*, 17(77), 479-490.

Dowdeswell, J.A. 1995. Glaciers in the High Arctic and recent environmental change. *Phil. Trans. R. Soc. Lond.* **A 352**, 321-334.

Echelmeyer, K.A., W.D. Harrison, C.F. Larsen, J. Sapiano, J.E. Mitchell, J. DeMallie, B. Rabus, G. Adalgeirsdottir and L. Sombardier. 1996. Airborne surface profiling of glaciers: a case-study in Alaska. *J. Glaciol.*, **42**(142) 538-547

Finsterwalder. 1954. Photogrammetry and glacier research with special reference to glacier retreat in the Eastern Alps. J. Glaciol., **2**(15) 306-340.

Haakensen N. 1986. Glacier mapping to confirm results from mass-balance measurements. *Ann. Glaciol.*, 8, 73-77.

IPCC. 1992. Climate change 1992 - the supplementary report to the IPCC scientific assessment. WMO and UNEP. Cambridge University Press.

Jóhannesson, T., C. Raymond and E. Waddington. 1989. Time-scale for adjustment of glaciers to changes in mass balance. *J. Glaciol.*, **35**(121), 355-369.

Keeler, C.M. 1958. Ablation studies: Lower McCall Glacier, June 23 to September 1, 1957. In *IGY Glaciology Report Series* No.1. New York, IGY World Data Center, Glaciology, American Geographical Society, XII-11-XII-15.

Kelly, P.M., P.D. Jones, C.B. Sear, B.S.G. Cherry and R.K. Tavakol. 1982. Variations in surface air temperatures: Part 2. Arctic regions, 1881-1980. *Mon. Weather Rev.*, **110**(2), 71-83.

Krimmel, R.M.1989. Mass balance and volume of South Cascade Glacier, Washington 1958-85. In J. Oerlemans(ed.). *Glacier Fluctuations and Climate Change*, Kluwer Academ. Pub.,193-206.

Lachenbruch, A.1994. Permafrost, the active layer, and changing climate. *U.S.Geological Survey, Open file report*, 94-694. 43 pp.

Letréguilly, A. 1988. Relation between the mass balance of western Canadian mountain glaciers and meteorological data. *J. Glaciol.*, **34**(120), 11-18.

Lliboutry L. 1974. Multivariate statistical analysis of glacier annual balances. *J. Glaciol.*, **13**(69), 371-392.

Meier, M.F. 1962. Proposed definitions for glacier mass budget terms. *J. Glaciol.*, **4**(33), 252-261.

Oerlemans, J. 1992. Climate sensitivity of glaciers in southern Norway: application of an energy-balance model to Nigardsbreen, Hellstugubreen and Alfotbreen. *J. Glaciol.*, **38**(129), 223-232.

Orvig, S. and R.W. Mason. 1963. Ice temperatures and heat flux, McCall Glacier, Alaska. In *General Assembly of Berkeley*. International Association of Scientific Hydrology, I.U.G.G., 181-188. (IASH Publication No.61.)

Osterkamp, T.E. and V. E. Romanovsky, 1996. Characteristics of changing permafrost temperatures in the Alaskan Arctic, USA. *Arctic and Alpine Research*, 28 (3), 267-273.

Ostrem, G. and M. Brugman. 1991. Glacier mass balance measurements: a manual for field and office work. *Science Report No.4, National Hydrology Research Institute,*

Saskatoon, Saskatchewan, and Norwegian Water Resources and Electricity Board, Norway. 224p.

Paterson, W.S.B. 1994. The physics of glaciers. *Third edition*. Oxford, etc., Pergamon Press.

Pelto, M.S. 1996. Annual net balance of North Cascade glaciers, 1984-94. *J. Glaciol.*, **42**(140), 3-9.

Pfeffer, T.T.H. Illangasekare and M.F. Meier.1990. Analysis and modeling of melt-water refreezing in dry snow. *J. Glaciol.*, **36**(123), 238-246.

Rabus, B.T., K.A. Echelmeyer, D.T. Trabant and C.S. Benson. 1995. Recent Changes of McCall Glacier. *Ann. Glaciol.*, **21**, 231-239.

Samson C.A. 1965. Comparison of mountain slope and radiosonde observations. *Mon. Weather Rev.*, **95**, 327-330.

Sapiano, J.J. 1997. Elevation, volume, and terminus changes of nine glaciers in North America. *Masters thesis*, University of Alaska, Fairbanks

Sater, J.L. 1959. Glacier studies of the McCall Glacier, Alaska. *Arctic*, **12**(2), 82-86

Schwitter, M.P. and C.F. Raymond. 1993. Changes in the longitudinal profiles of glaciers during advance and retreat. *J. Glaciol.*, **39**(133), 582-590.

Scott, P.A. 1992. Annual development of climatic summer in northern North America: accurate prediction of summer heat availability. *Clim. Res.* **2**, 91-99.

Sturm, M., D.K. Hall, C.S. Benson and W.O. Field. 1991. Non-climatic control of glacier-terminus flucyuations in the Wrangell and Chugach Mountains, Alaska, U.S.A., *J. Glaciol.*, **37**(127), 348-356.

Tangborn, W.V. 1990. Effect of area distribution with altitude on glacier mass balance - a comparison of North and South Klawatti glaciers. *Ann. Glaciol.*, **14**, 278-282.

Trabant, D.C. and C.S. Benson. 1986. Internal accumulation and superimposed ice on McCall Glacier, Alaska: part of the IHD glacier mass balance program. *Materialy Glyatsiologicheskikh Issledovaniy*, **58**, 157-165.

Trabant, D.C. and L.R. Mayo. 1985. Estimation and effects of internal accumulation on five glaciers in Alaska. *Ann. Glaciol.*, **6**, 113-117.

Trabant, D.C., W.D. Harrison and C.S. Benson. 1975. Thermal regime of McCall Glacier, Brooks Range, northern Alaska. In Weller, G. and S. Bowling, eds. *Climate of the Arctic*. Fairbanks, Geophysical Institute, University of Alaska, 347-349. (Proceedings of the 24th Alaska Science Conference, 15-17 August 1973.)

Wakahama, G., D. Kuroiwa, T. Hasemi, and C. Benson. 1976. Field observations and experimental and theoretical studies on the superimposed ice of McCall Glacier, Alaska. *J. Glaciol.*, **16**(74), 135-149.

Wendler, G., C. Fahl and S. Corbin. 1972. Mass balance studies on the McCall Glacier, Brook Range, Alaska. *Arct. Alp. Res.*, **4**(3), 211-222.

Wendler, G., N. Ishikawa and N. Streten. 1974. The climate of McCall Glacier, Alaska in relation to its geographical setting. *Arct. Alp. Res.*, **6**(3), 307-318.

Wendler, G. and N. Ishikawa. 1974. The effect of slope, exposure and mountain screening on the solar radiation of McCall Glacier, Alaska: a contribution to the International Hydrological decade. *J. Glaciol.*, **13**(68), 213-226.

Zhang, T. and T.E. Osterkamp. 1993. Changing climate and permafrost temperatures in the Alaskan Arctic. In Cheng, G. (ed.), *Permafrost: Sixth International Conference Proceedings*. Vol. 1 Wushan, Guangzhou. S. China Univ. Technology Press, 783-788.

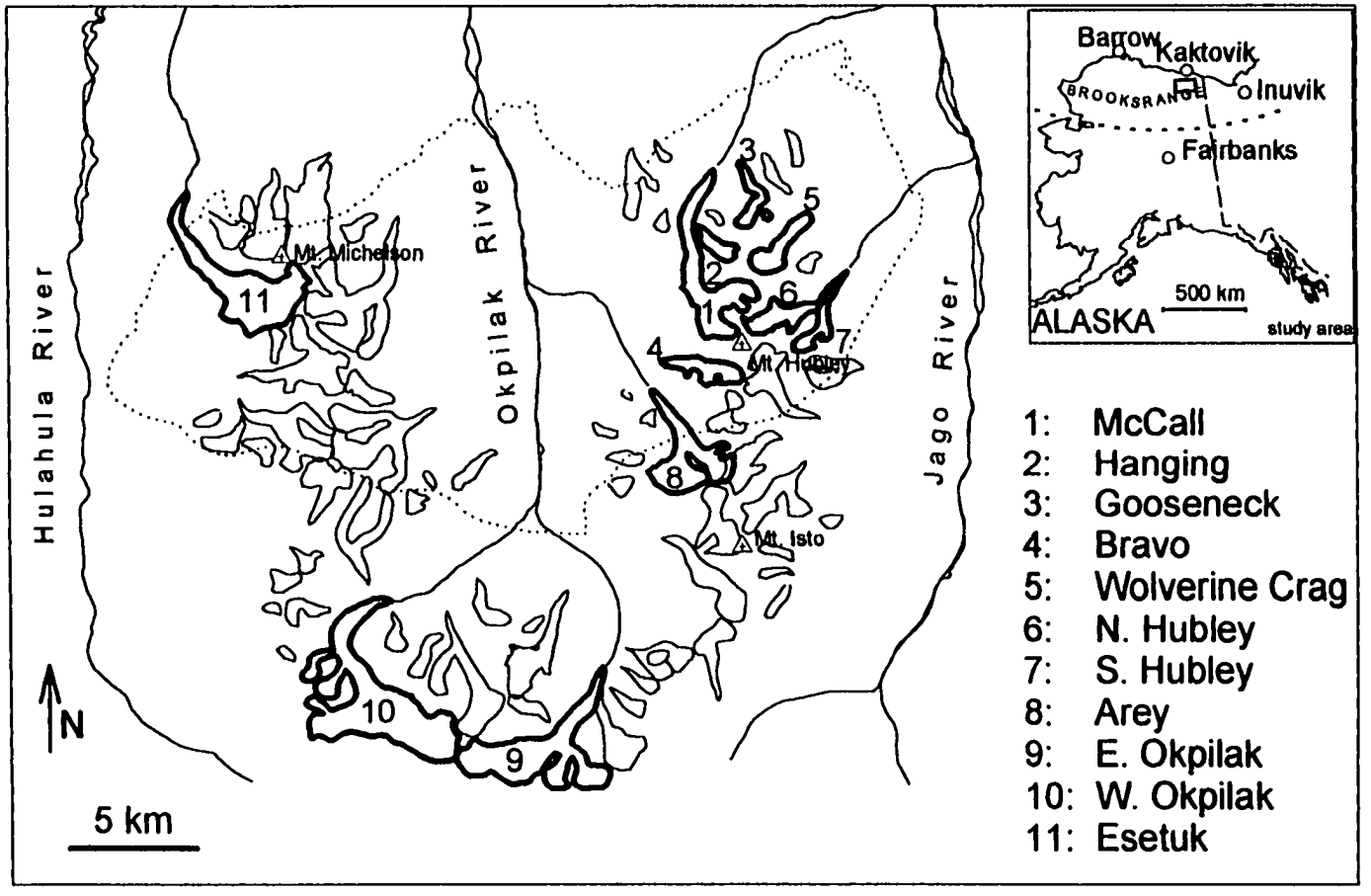

Figure III.1: Existing glaciers between the Hulahula and Jago Rivers, NE Brooks Range. Numbers indicate glaciers that were surveyed between 1993 and 1995. The outline of the Okpilak Batholith, a large granitic intrusion, is shown as a dotted line.

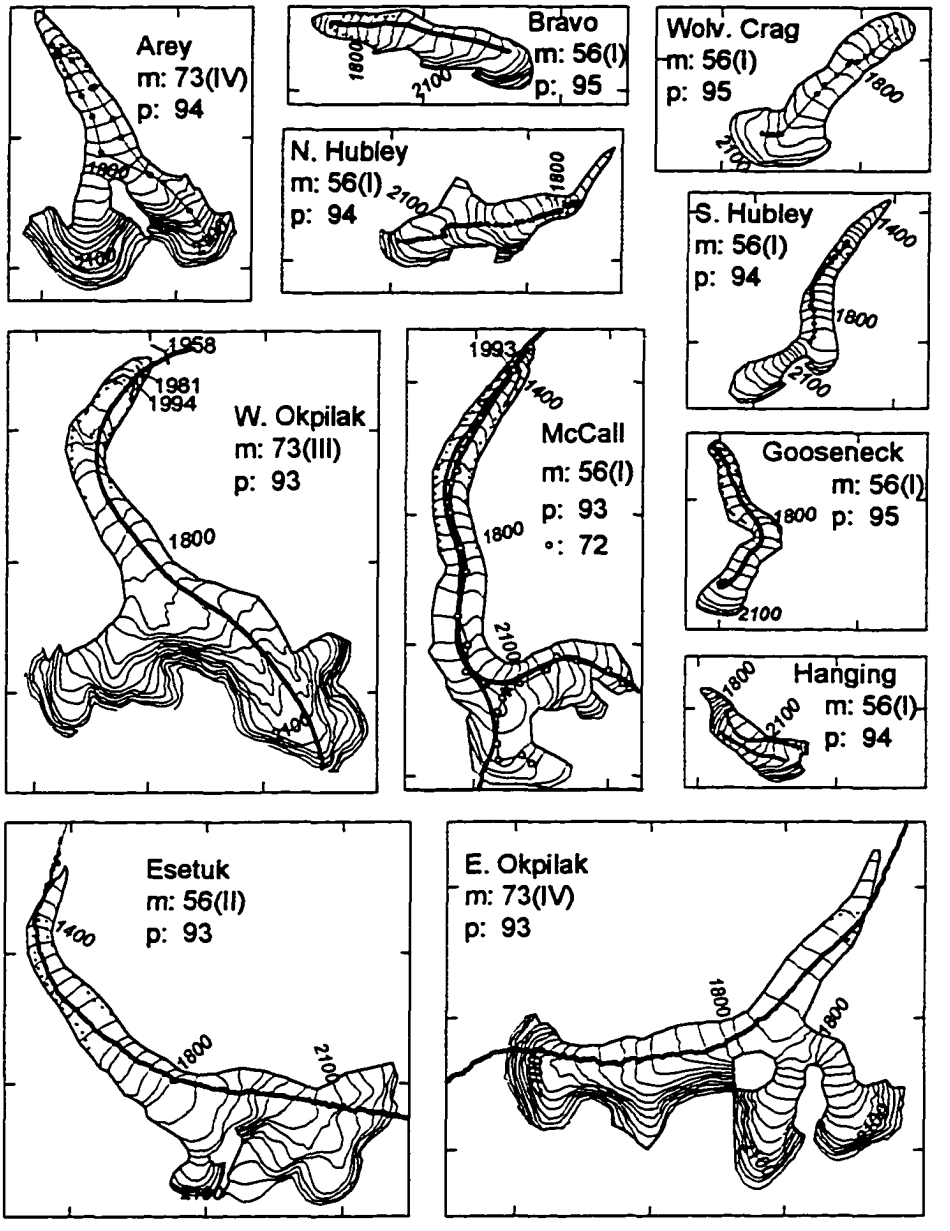

Figure III.2: Map views of surveyed glaciers. Contour interval is 100 ft (ca. 30.5 m). Elevation labels in meters are added where 100 ft contours coincide with 100 m contours (to better than ±5 m). Orientation is north up. Tick marks representing UTM Easting and Northing are shown every 2 km. GPS profiles are shown as solid lines, with small filled symbols corresponding to the individual point measurements; these appear as solid heavy lines for the continuous profiles. For McCall Glacier additional hollow symbols mark locations that were optically surveyed in 1972 and 1993. The acquisition dates for aerial map photography (m:) and GPS profiles (p:) are given for each glacier. (Roman numerals are map sheet numbers from Tab. III.3). Dotted curves are new terminus outlines calculated by our volume change algorithm. Surveyed terminus outlines for different years are shown for W Okpilak and McCall Glaciers.

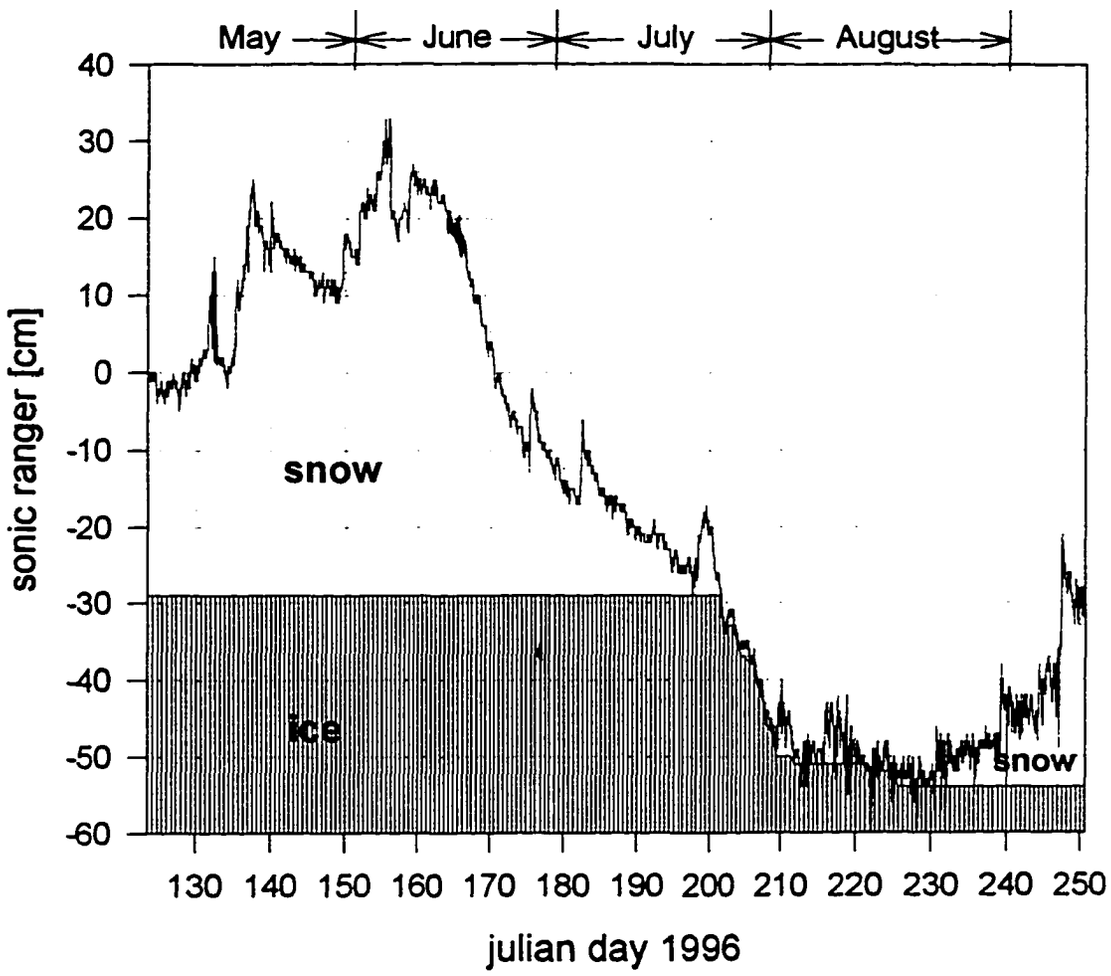

Figure III.3: Accumulation and ablation of snow and ice, measured from May through September 1996 by a sonic ranger located in the confluence area of the three cirques (star symbol in Fig. III.5). Units are in cm of snow or ice respectively; no conversion to water equivalent was performed.

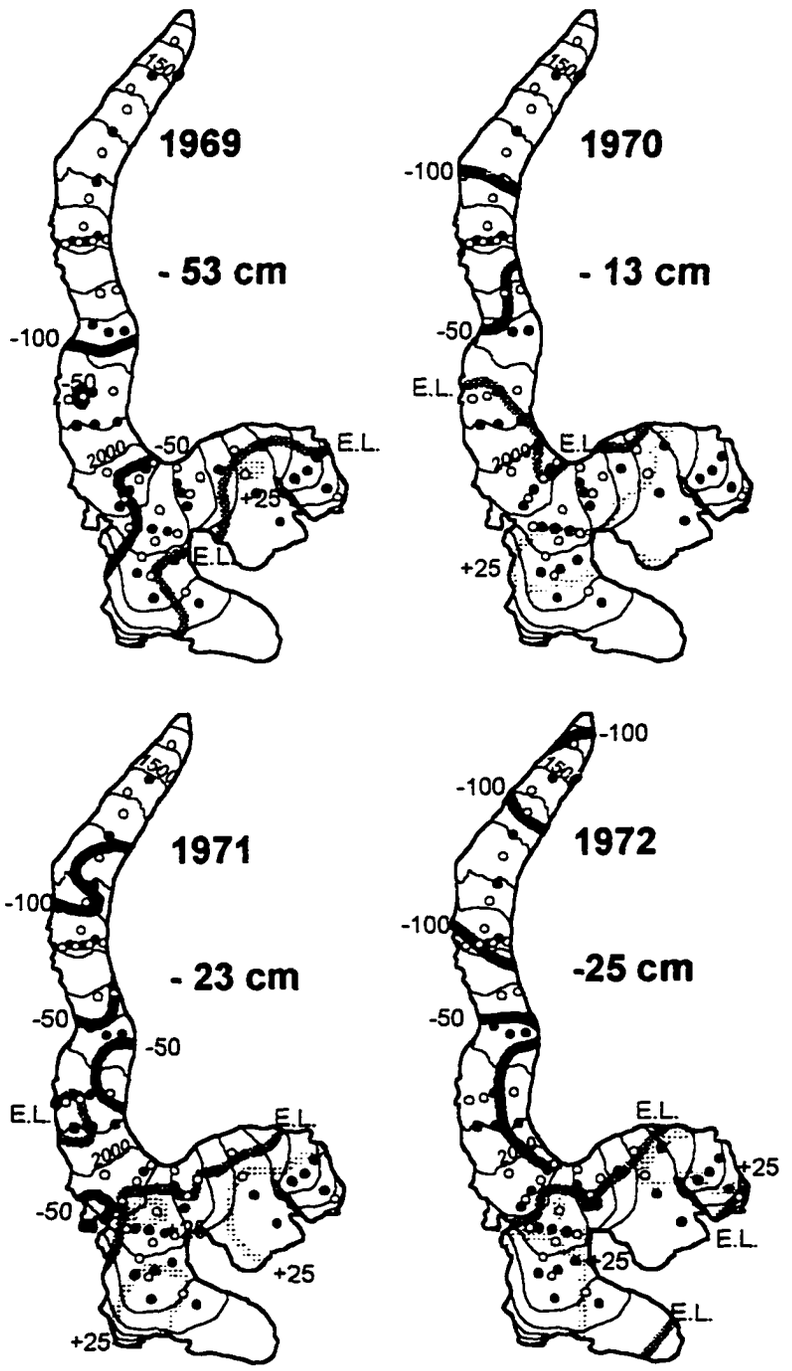

Figure III.4: Contour maps of the stratigraphic surface mass balance 1969 to 1972. Contours of equal mass balance are shown at -200, -100, -50, ±0, +25, +50 cm water equivalent. The ±0 cm contour is the equilibrium line and is marked as E.L.

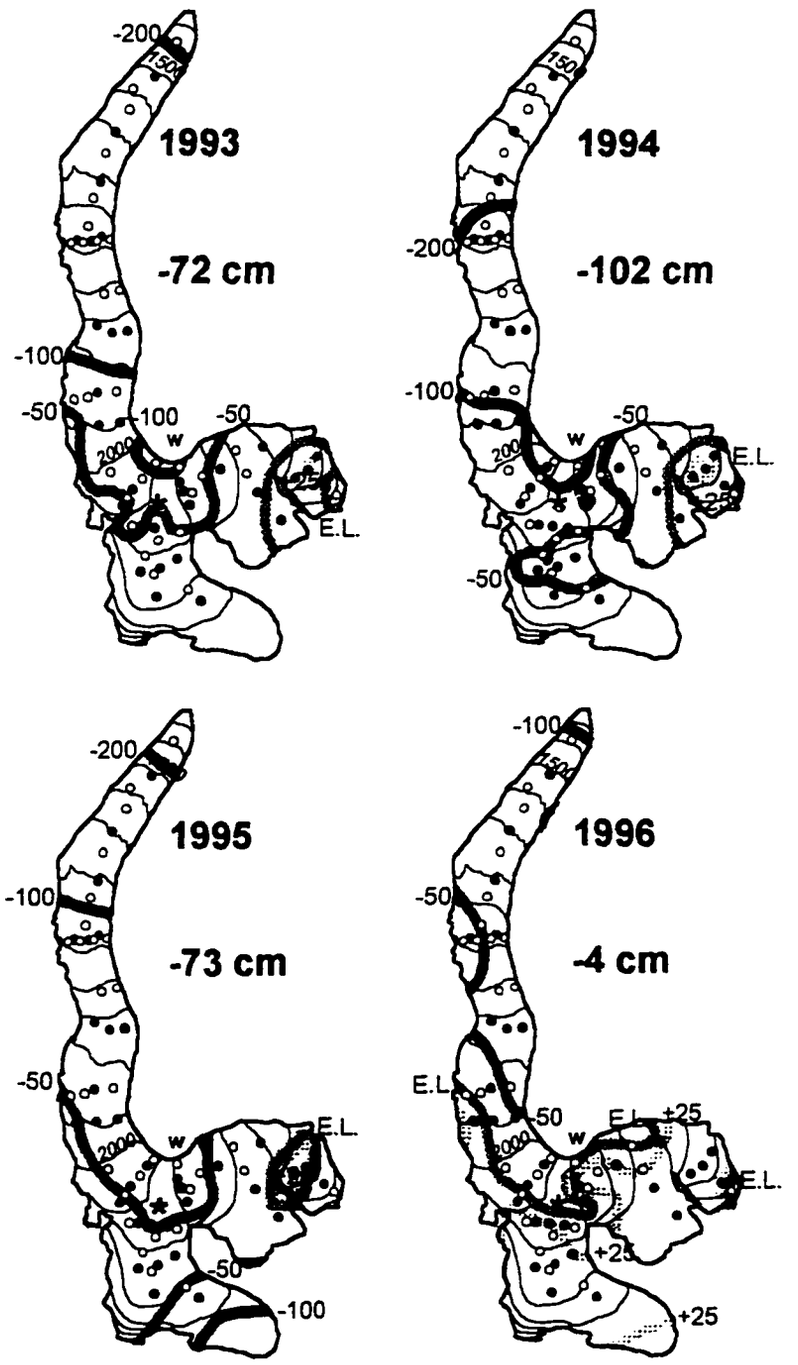

Figure III.5: Contour maps of the stratigraphic surface mass balance 1993 to 1996 (contour labels as in Fig. III.4). The symbols * and *w* mark the locations of the sonic ranger and the temperature/ precipitation gauge, respectively

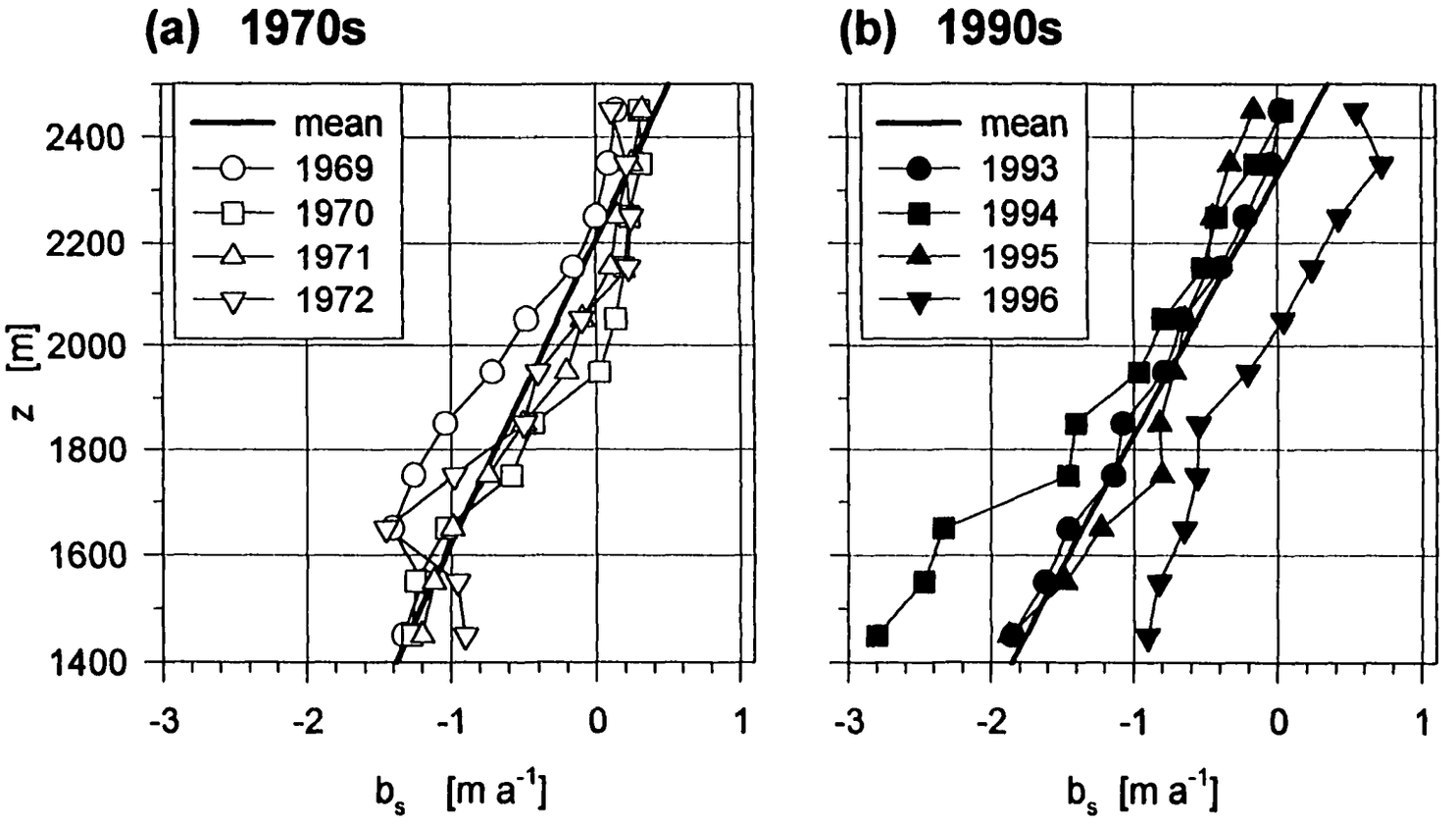

Figure III.6: Surface mass balance bs as a function of elevation *z*. (a) for the period 1969-72. (b) for the period 1993-96. For both periods, *z* is the actual surface elevation at that time. In each case, the heavy line represents a linear least squares fit of all four mass balance values $b_s(z)$.

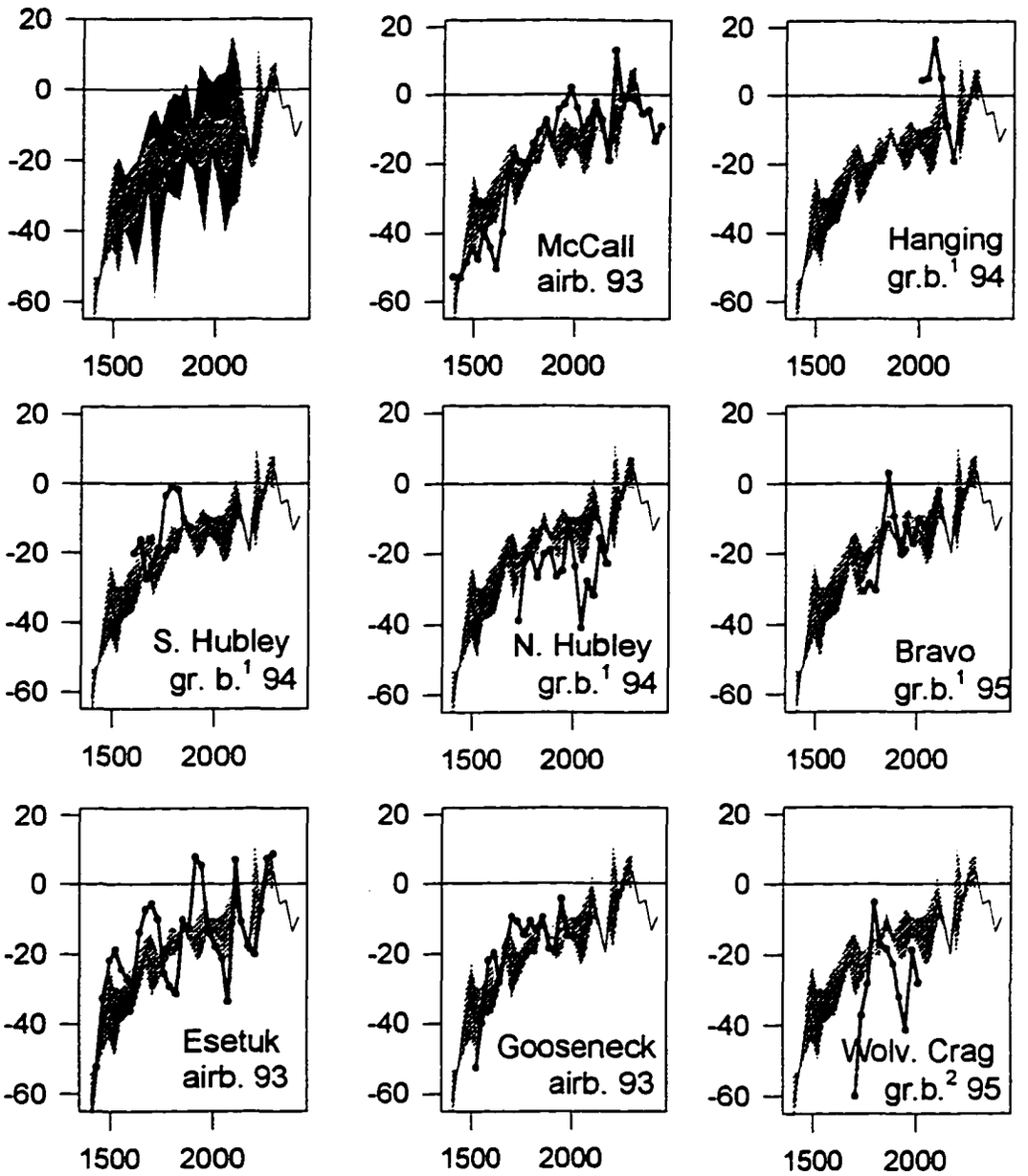

Figure III.7: Elevation change (in meters) between 1956 topographic maps and recently surveyed centerline profiles of McCall and 7 neighboring glaciers in the NE Brooks Range as a function of elevation (in meters). The upper left panel shows (i) the mean elevation change for all glaciers (solid line), (ii) one standard deviation (dark gray) and (iii) the maximum spread of elevation change (light gray) about this mean. The other panels compare the individual elevation changes (heavy solid curve and symbols) with the mean for all glaciers (thin solid line). The survey method and acquisition date of the individual centerline profiles is indicated. Abbreviations 'airb.', 'gr.b.$_1$', 'gr.b.$_2$' stand for airborne, high-accuracy ground based and low-accuracy ground based GPS methods, respectively.

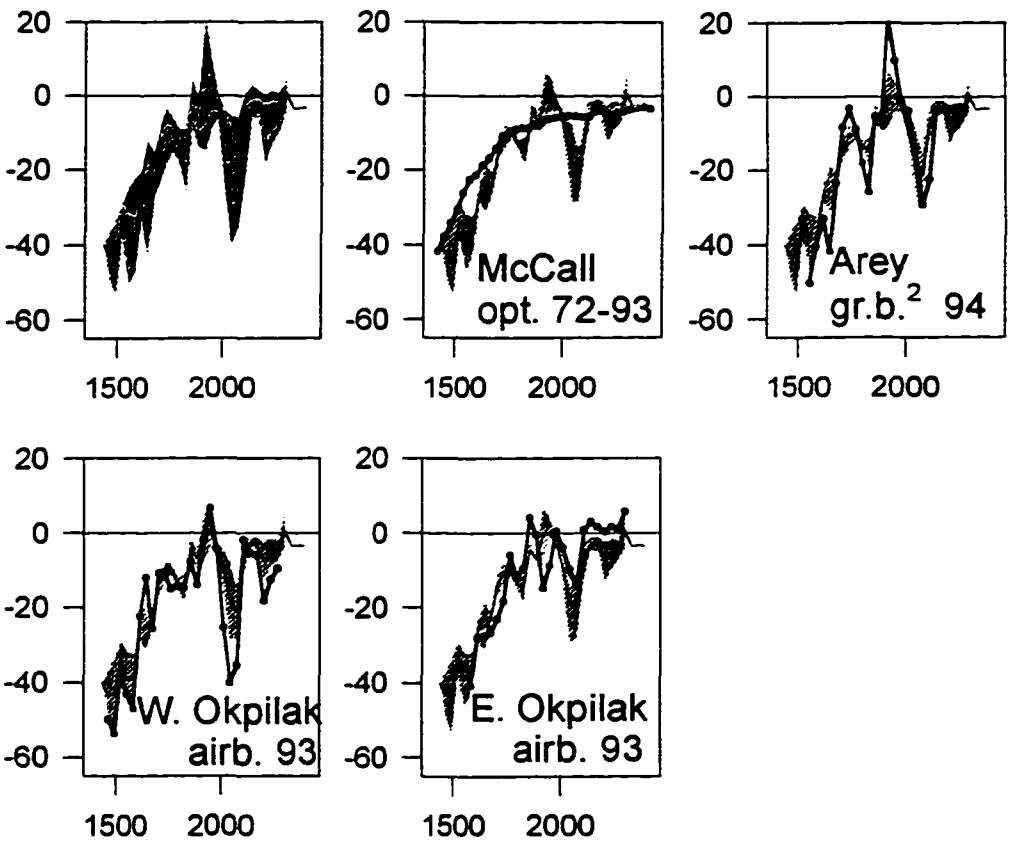

Figure III.8: Elevation change (in meters) between 1973 topographic maps and recently surveyed centerline profiles of McCall and 3 neighboring glaciers in the NE Brooks Range as a function of elevation (in meters). Explanations same as in Fig. III.7. The additional abbreviation 'opt.' stands for optical surveying, which was used in both 1972 and 1993 to calculate the corresponding elevation change of McCall Glacier.

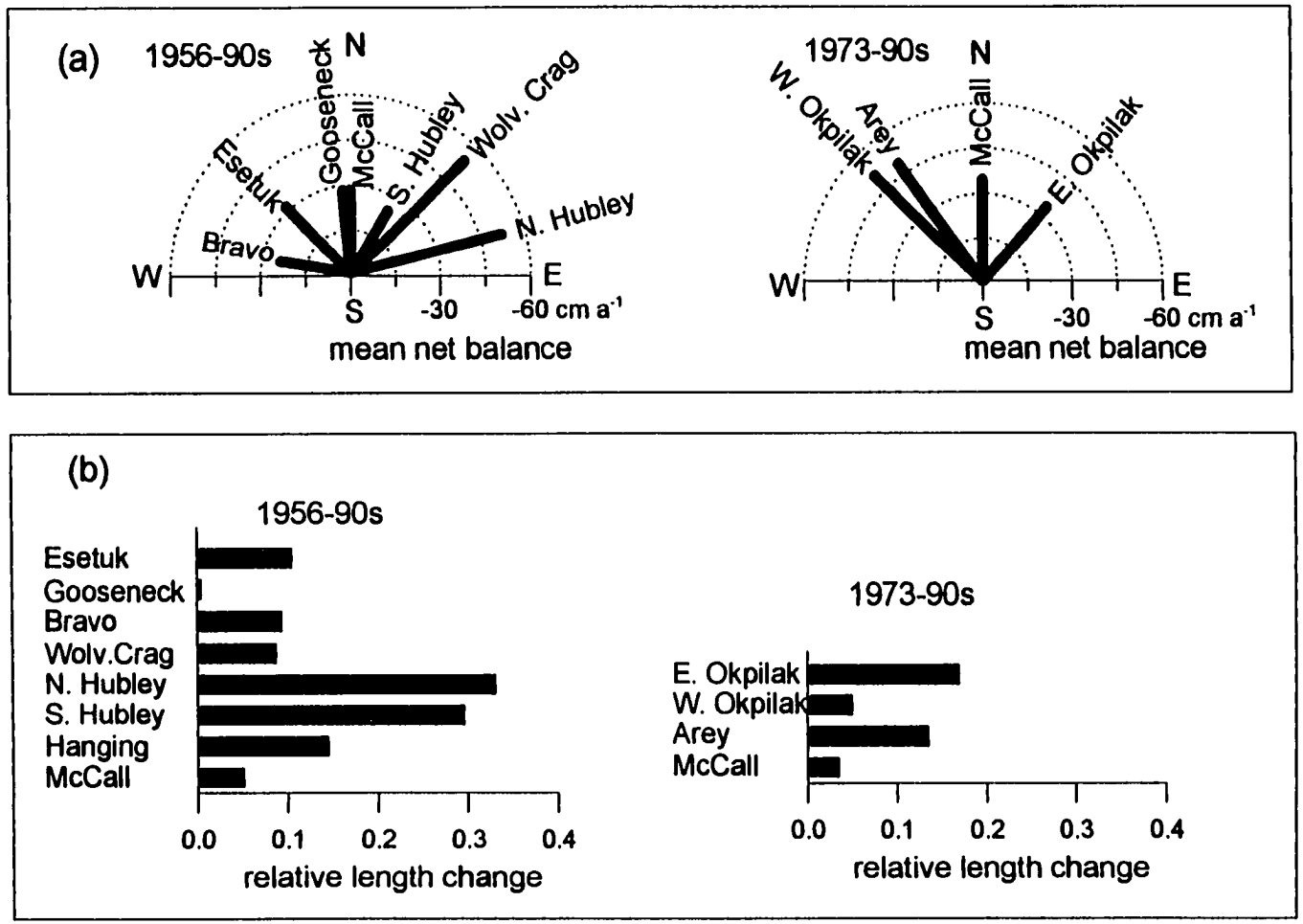

Figure III.9: Regional patterns of mean mass balance and changes in glacier length for the NE Brooks Range. (a) Mean mass balance 1956-90s and 1973-90s as a function of the aspect of the main glacier body. (b) Relative length changes for 1956-90s and 1973-90s.

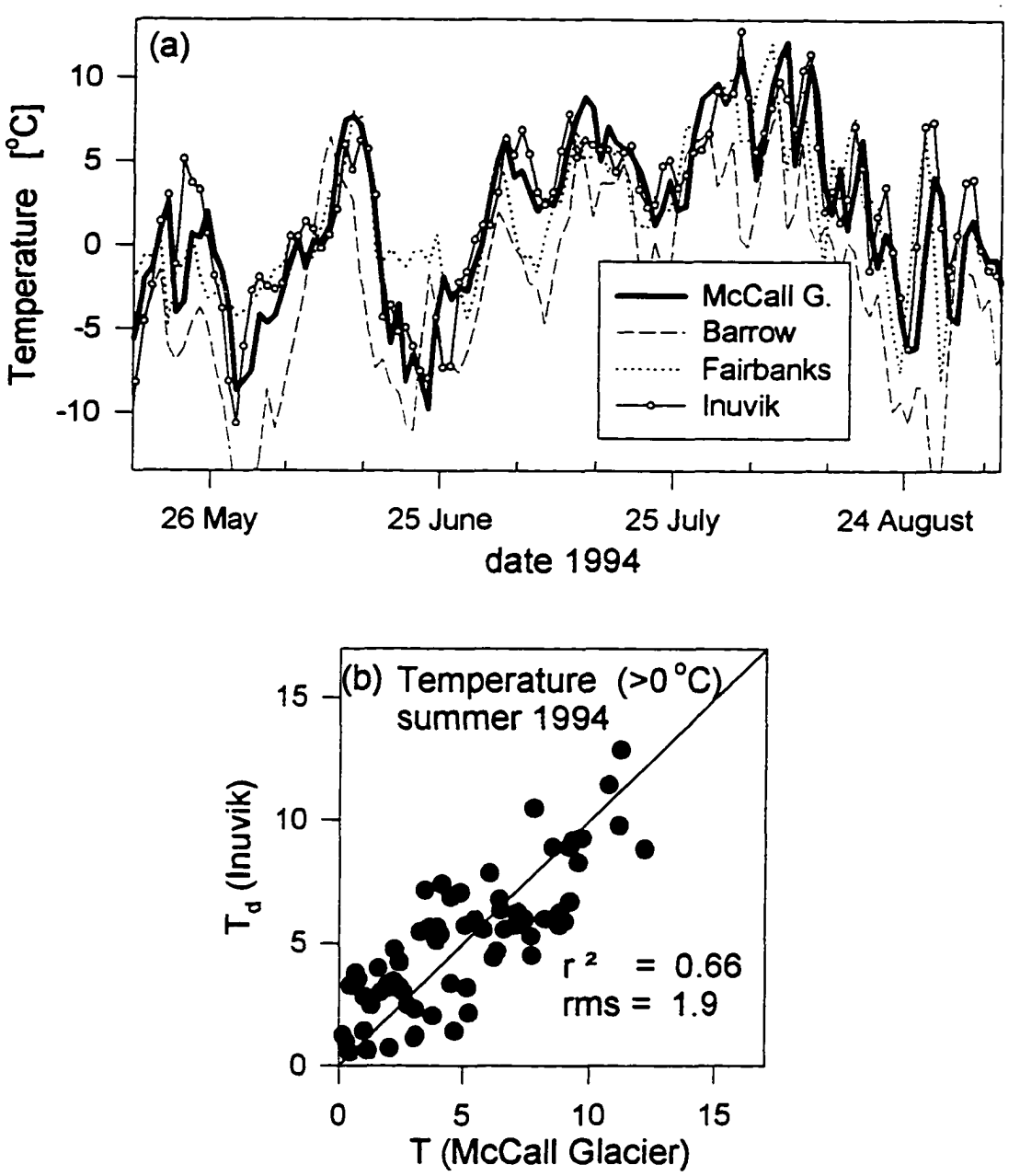

Figure III.10: (a) Mean daily temperatures measured on McCall Glacier at 2100 m during summer 1994 compared to the mean temperature of the 850-700 mbar layer over Inuvik, Barrow and Fairbanks. (b) Correlation diagram between the temperatures during summer 1994 on McCall Glacier and T_d from Inuvik soundings. Only positive temperatures, which enter the positive degree day sum, are shown.

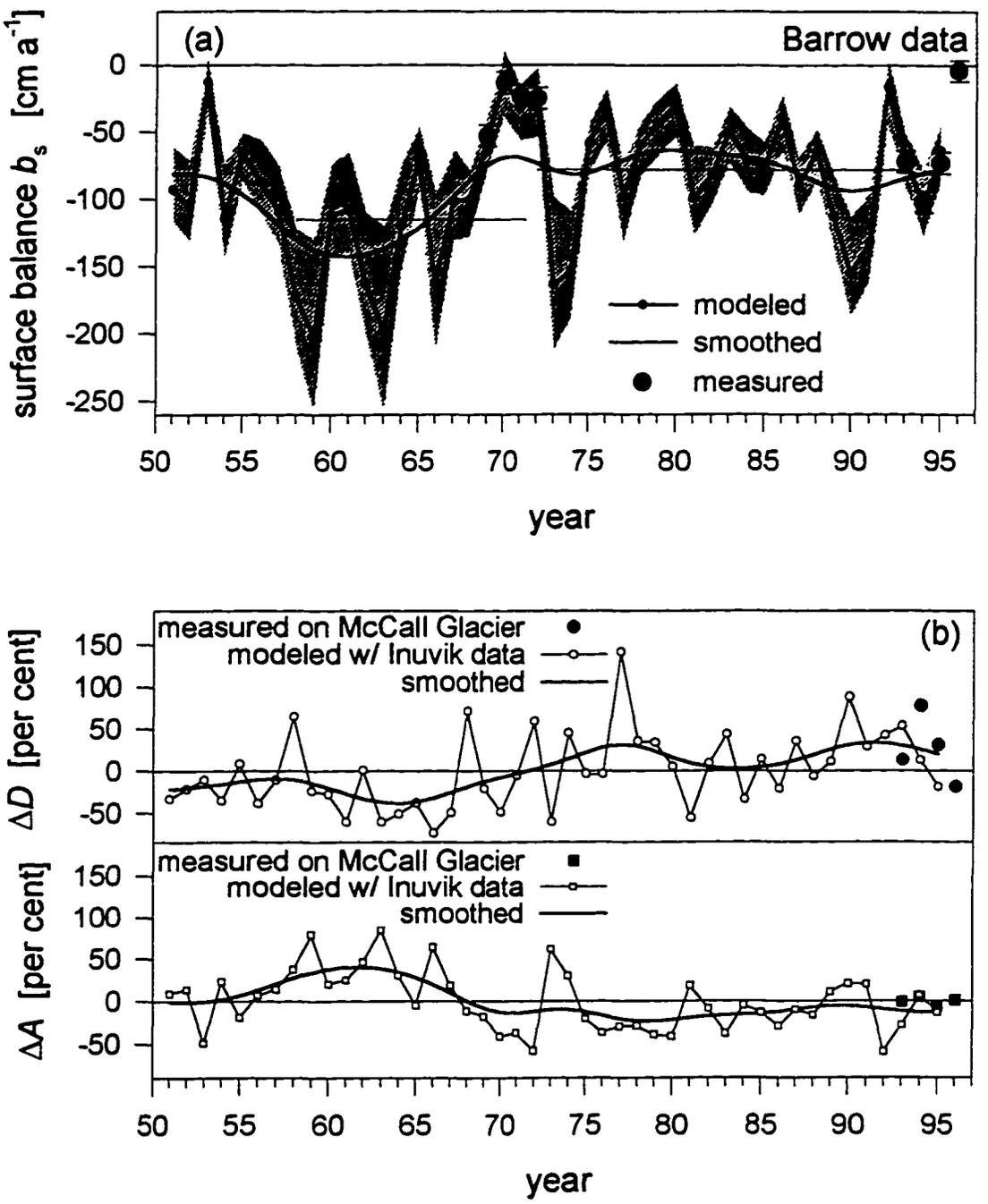

Figure III.11: Barrow data: (a) modeled, Equation (4) and m_1 = 8, and measured surface mass balance of McCall Glacier. (b) annual degree day sum (black curves and symbols) and precipitation in solid form (gray curves and symbols). Modeled values are represented by small symbols connected with solid lines, while those measured on McCall Glacier are represented by larger symbols.

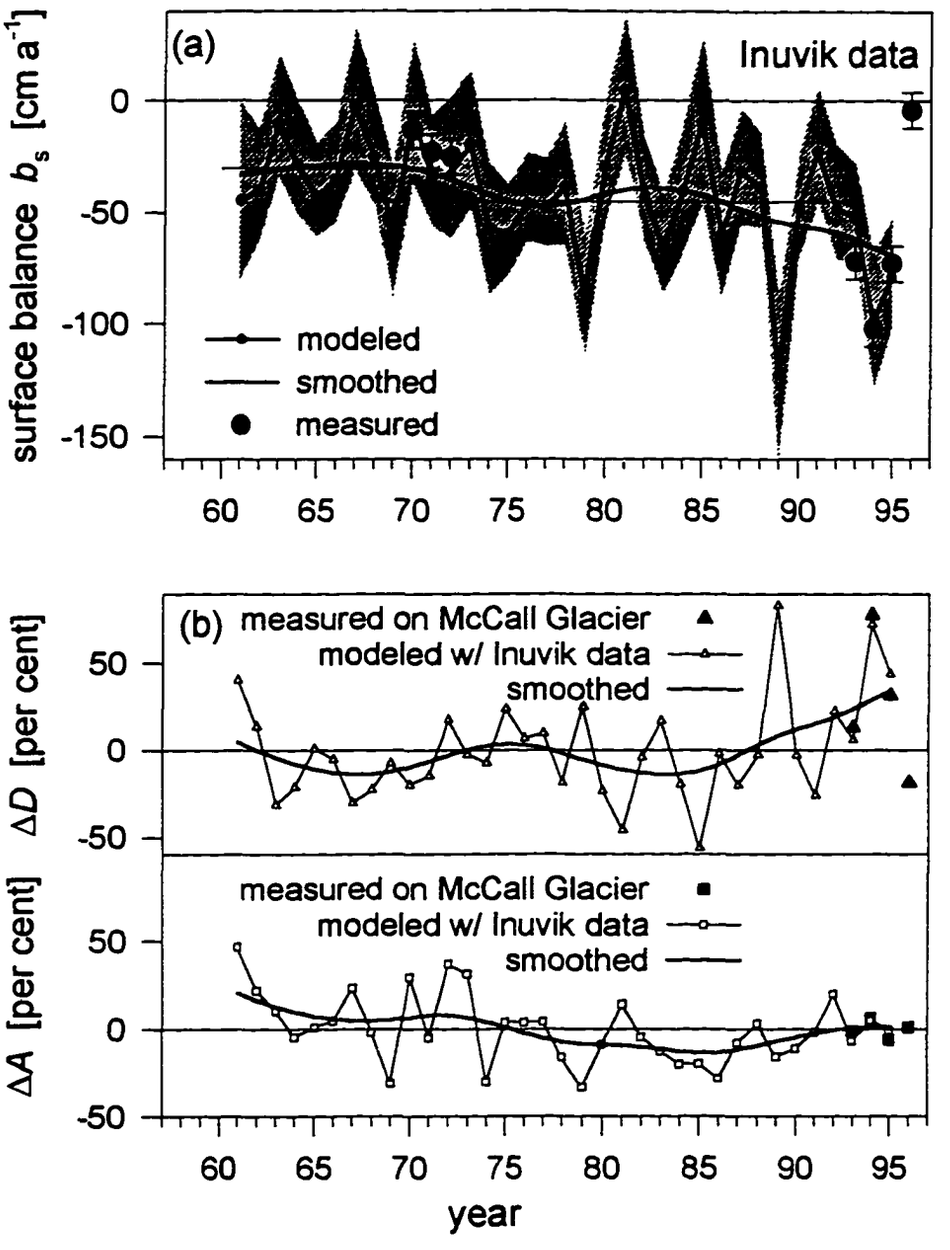

Figure III.12: Inuvik data: (a) modeled surface balance, using Eqn. (4) and $m_1 = 8$, and measured annual surface mass balances of McCall Glacier. (b) percent deviations from 1961-95 mean of annual degree day sum sum ΔD and precipitation in solid form ΔA (gray curves and symbols). Modeled values are shown as small symbols connected with solid lines. Measured values on McCall Glacier are represented by larger symbols.

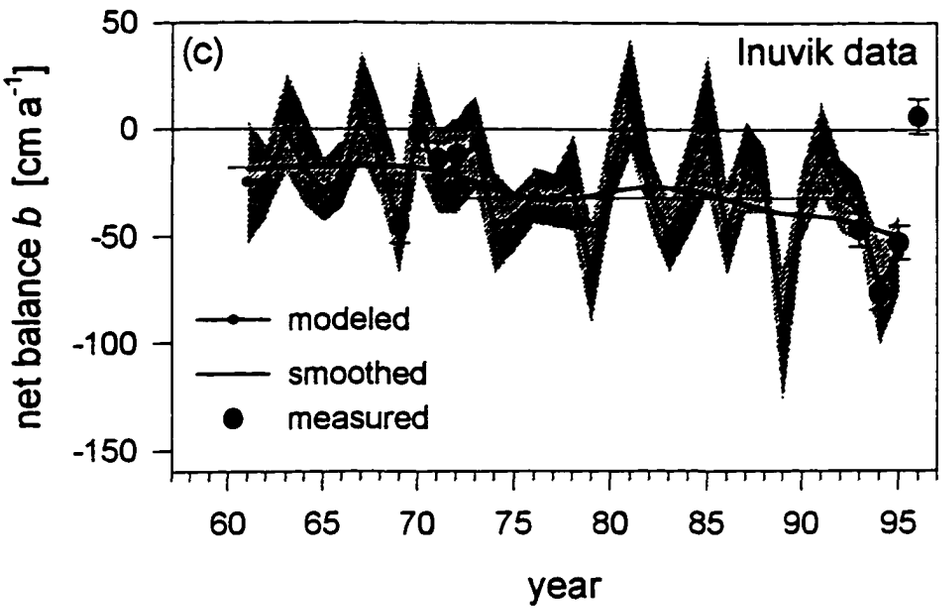

(c) modeled net balance, using Equation (4), $m_1 = 8$, and measured annual net mass balances of McCall Glacier.

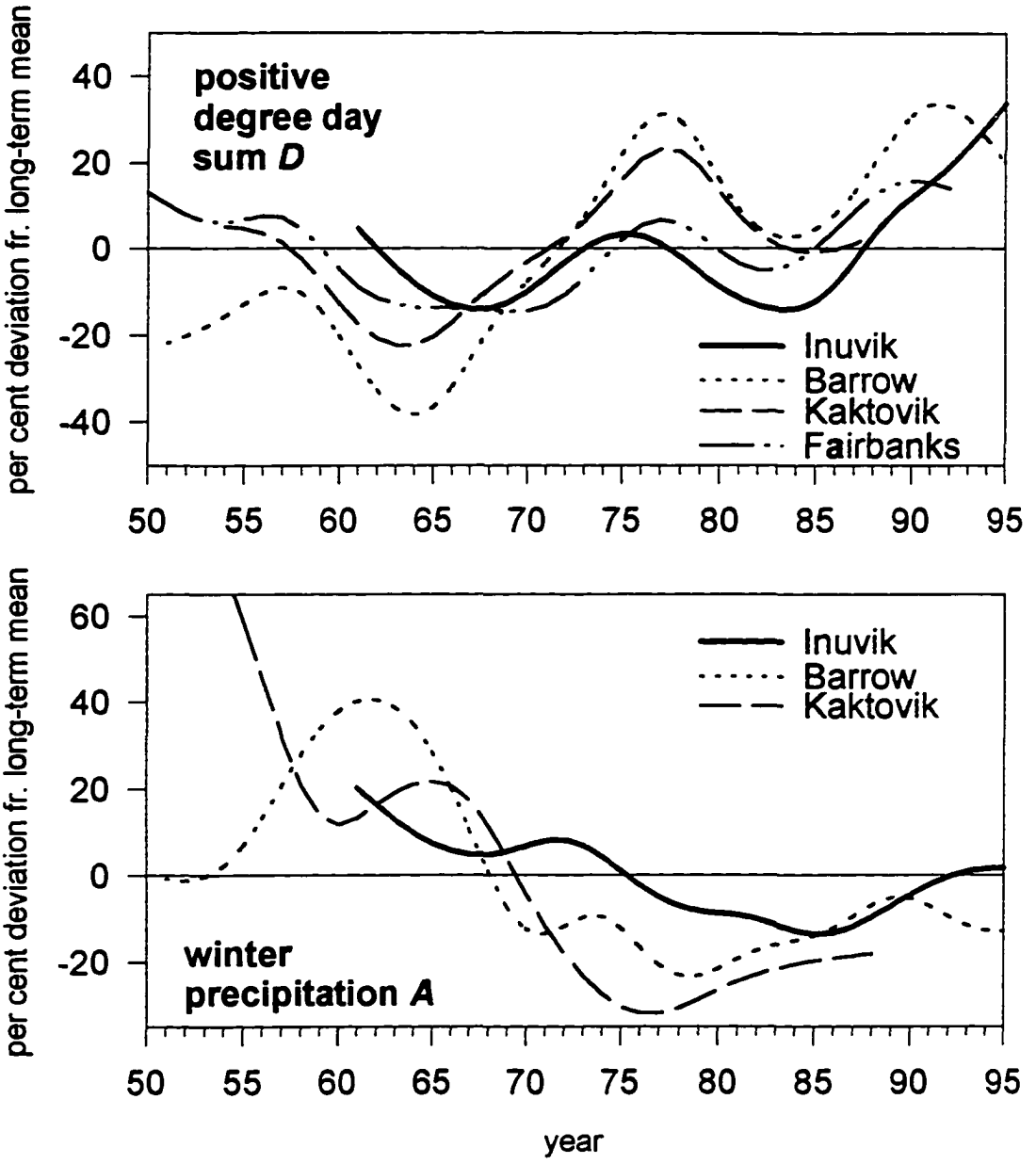

Figure III.13: Annual degree day sum and precipitation in solid form at 2100 m elevation as calculated from Inuvik, Barrow, Kaktovik and Fairbanks data and smoothed with a gauss filter of width 2.5 years. The Inuvik curves (heavy solid lines) are representative for the NE Brooks Range.

III.12. Tables

Table III.1: Reevaluation of 1970s mass balance data (fixed date system)

	1990s subset				full 1970s net				published			
year	b_{map}	a_{map}	b_{elev}	*AAR*	b_{map}	a_{map}	b_{elev}	*AAR*	*b*	*a*	$a_{(t)}$	*AAR*
69	-45	8	-41	0.34	-42	10	-43	0.38	-42	9.9	3.6	0.39
70	-3	23	-1	0.60	-1	28	-4	0.65	-8	19.0	5.4	0.68
71	-10	23	-5	0.49	-5	26	-8	0.55	-14	15.8	5.6	0.52
72	-18	19	-24	0.47	-12	22	-20	0.49	-19	14.1	5.7	0.48

all mass balances in cm, AAR dimensionless

Table III.2: Combined record of annual surface and net mass balances (stratigraphic system)

year	$b_{(s)}$	*AAR*	*b*	*a*	$a_{(t)}$	*AAR*	*ELA*
69	-53	0.27	-45	10	8	0.34	2150
70	-13	0.62	-4	23	9	0.62	1940
71	-23	0.47	-12	20	11	0.48	2070
72	-25	0.45	-14	23	11	0.47	2060

			minimum internal accu.					*maximum internal accu.*					date	b_w	p_s
93	-72	0.07	-69	4	3	0.07	2290	-50	9	22	0.30	2190	6-30	17	12.9
94	-102	0.08	-99	5	3	0.08	2340	-77	8	25	0.22	2260	6-30	26	12.8
95	-73	0.02	-72	1	1	0.02	2400	-55	5	18	0.18	2330	6-25	9	13.4
96	-4	0.52	1	25	5	0.53	1990	3	27	7	0.58	1970	5-6	20	11.5

all mass balances in cm, ELA in m, AAR dimensionless

Table III.3: Measured elevation offsets for the topographic map sheets of this study.

USGS 1:63,360 quadrangle: sheet:	#	year	<Δz> m	σ m	n	method
Demarcation Pt. B5	I	56	+1	3	5	spot
Mt. Michelson B1	II	56	+20	13	54	profile
			+22	-	1	spot
Mt. Michelson A1	III	73	+17	-	1	spot
			-2	6	5	profile
			-14	3	4	profile

Table III.4: Mean mass balance and terminus changes, 1956 or 1973 to present, of 11 Brooks Range glaciers

Glacier	map number and year	GPS method and year	A km^2	L km	z_{min} m	z_{max} m	aspect	ΔV $\times 10^7$ m^3	$\Delta z_{<A>}$ m	b cm a^{-1}	$\frac{b}{b_{McCall}}$	ΔL m
McCall	I 56	a 93	5.8	7.6	1350	2500	N	-7.0	-11.6	-28	1.00	390
Hanging	I 56	g_1 94	0.8	1.8	1800	2350	NW	-0.04	-0.5	- 1	0.04	260
S. Hubley	I 56	g_1 94	1.2	3.0	1540	2300	NNE	-1.3	-10.5	-25	0.89	890
N. Hubley	I 56	g_1 94	1.8	3.1	1690	2300	ENE	-4.2	-22.0	-52	1.86	1030
Wolv.Crag	I 56	g_2 95	1.9	3.0	1625	2100	NE	-4.6	-23.3	-54	1.93	265
Bravo	I 56	g_1 95	1.6	3.2	1690	2300	W	-1.8	-10.2	-24	0.86	300
Gooseneck	I 56	g_1 95	1.1	3.1	1470	2200	NNW	-1.4	-12.3	-28	1.01	16
Esetuk	II 56	a 93	7.1	7.7	1350	2500	NW	-9.2	-12.9	-31	1.11	814
McCall	op.72	op.93	5.8	7.6	1350	2500	N	-4.4	-7.7	-33	1.00	270
W.Okpilak	III 73	a 93	11.0	8.3	1410	2400	NW	-12.4	-11.3	-51	1.54	420
E. Okpilak	IV 73	a 93	8.8	6.0	1540	2400	NNE	-6.5	-7.3	-33	0.99	1020
Arey	IV* 73	g_2 94	4.6	4.2	1470	2300	NW	-5.3	-11.4	-49	1.48	570

* the immediate snout area of Arey Glacier is located on map: I 56

Table III.5: First order weather stations within 700 km radius of McCall Glacier.

weather station	record length	distance to McCall Glacier [km]	local climatic setting
Inuvik	1961-present	430	50 km inland, arctic slope
Barrow	1948-present	550	arctic coastal
Kaktovik	1948-1988	100	arctic coastal
Fairbanks	1948-present	650	continental, interior AK

Table III.6: Results of mass balance model with *Barrow* data.

using measured annual *surface* balances										
accumulation model	m_1	m_2	C_{multi}	C_A	C_D	C_{DA}	<*b*> 58-72 cm	<*b*> 72-93 cm	c_a	c_d
Equation (4)	8	-	0.98	-0.88	-0.23	-0.22	-115	-78	-1.53	-0.36
Equation (5)	8	6	0.99	-0.93	-0.23	-0.14	-96	-77	-1.30	-0.29

key: m_1, m_2 start/ending months in Equations (4) and (5)
C_A, C_D, C_{multi}, C_{DA} correlation coefficients: between mass balance and accumulation/ degree days/ both and between accumulation and degree days
<*b*> mean mass balance over period indicated
c_a, c_b fit parameters: for accumualation/ degree days

Table III.7: Results of mass balance model using annual *Inuvik* data.

a) using measured annual *surface* balances										
accumulation model	m_1	m_2	C_{multi}	C_A	C_D	C_{DA}	<*b*> 61-72 cm	<*b*> 72-93 cm	c_a	c_d
Equation (4)	8	-	0.95	0.42	-0.82	0.06	-29.6	-45.1	0.68	-0.82
Equation (5)	8	6	0.96	0.30	-0.82	0.22	-31.1	-45.8	0.68	-0.90
b) using measured annual *net* balances (maximum internal accumulation.)										
Equation (4)	8	-	0.96	0.49	-0.80	0.06	-18.1	-31.5	0.62	-0.66
Equation (5)	8	6	0.98	0.37	-0.80	0.22	-19.4	-32.1	0.62	-0.73

key: same as Table III.6

Appendices

Appendix A : Survey monuments from the 1970s that were reused in this study

Station	lat	lon	hae [m]	X [m]	Y [m]	Z [m]	state in 1990s
B'	69°17'44.9729"	143°49'39.3771"	2127.433	8572.0	9765.7	2122.8	stable
C	69°17'19.2524"	143°50'44.5993"	2199.072	7820.8	9002.9	2194.5	stable
E	69°19'33.6041"	143°51'47.5307"	1752.105	7325.9	13192.7	1747.5	stable
A	69°17'32.4839"	143°47'40.5004"	2365.947	9856.1	9319.4	2361.4	stable
B1	69°19'23.6607"	143°50'36.3244"	1636.516	8090.3	12848.6	1631.9	unstable
B27	69°20' 9.0093"	143°50'15.9927"	1460.680	8378.5	14241.7	1456.1	stable

key:
lat: latitude, lon: longitude, hae: height above ellipsoid (WGS84 datum)
X: easting minus 380,000 m, Y: northing minus 7,680,000 m (UTM, NAD27 datum), Z (height above sea level).

Brief description of monuments

Only stations **B'**, C, E and A (open triangles in Fig. I.2.) were used during surveys of surface markers in the 1990s. They are a subset of a former larger survey control network that was established in the 1970s. The actual survey monuments consist of 1 m long aluminum rods drilled or wedged in bedrock or large boulders.

Station B' is located on the eastern moraine where the confluence of the combined upper and middle cirques with the lower cirque causes a large bend in the glacier. The ascent to the monument through moraine boulders is easy (5 min from the glacier) and the monument provides the savest theodolite setup of all monuments.

Station C is located opposite B' on a rock band on the west side of the confluence in the lowermost flank of Mt.Mcall. Access through a steep slope of the glacier can be difficult when ice is exposed (15 min plus). Theodolite setup is somewhat dangerous.

Station E is located downglacier, high above the western moraine slightly south-east of the western end point of the 'upper profile' (Fig. I.2). Care is needed during access through large loose boulders (20 min plus). Setup is safer than at C, anchoring of theodolite is nevertheless essential.

Station A is located on a rock ridge between upper and middle cirques, just above the remains of the 1970s' weather station. Access is straightforward; theodolite setup is safer than at C or E.

Stations B1 and **B27** were exclusively used in surveys of the 'upper' and 'lower' transverse profiles (Fig. I.2.). Station B27 marks the west end of the 'lower profile'; the actual monument is an anchor in horizontal bedrock. (The east side of the 'lower profile' is marked by a square wooden pole on instable ice cored moraine). B1 marks the east end of the 'upper profile'; it is unstable (on ice cored moraine), however an anchor bolt in vertical bedrock on the other (east) side of the 'upper profile' provides a fixed reference bearing. (No theodolite setup is possible above this anchor bolt.)

Appendix B : Mean horizontal velocities 1993-1995

marker	X [m]	Y [m]	Vx [ma^{-1}]	Vy [ma^{-1}]	V [ma^{-1}]	marker	X [m]	Y [m]	Vx [ma^{-1}]	Vy [ma^{-1}]	V [ma^{-1}]
p26	10210	9407	-2.02	1.65	2.61	t10.4	8218	9521	-18.82	2.81	19.03
p26	10209	9409	-2.15	1.60	2.69	t10.8	7945	9194	-6.51	7.55	9.97
p24.5	10005	9593	-2.33	2.32	3.29	t10.7	8052	9314	-8.83	9.60	13.04
p34	9722	9056	-2.85	3.59	4.58	p10.5	8146	9414	-8.26	9.02	12.24
p34al	9724	9058	-2.84	3.56	4.55	p9.5	7840	9917	-3.12	13.35	13.71
p23.3	9525	9854	-5.11	-0.73	5.17	p9	7746	10407	2.02	12.94	13.10
p17	8867	8187	-4.56	1.85	4.92	p7.9	7884	11116	-0.53	15.45	15.46
p22	9071	9609	-7.31	-2.40	7.69	t2.6	7771	12082	-1.27	12.56	12.62
p20	8383	8236	-1.09	5.14	5.25	t2.5	7717	12060	-1.83	13.12	13.24
p20.1	8743	9193	-7.59	-2.08	7.87	t2.2	7502	12044	-1.73	12.28	12.40
p20.3	8680	9394	-8.79	-1.43	8.90	p2.4	7655	12044	-1.75	13.20	13.32
t20.2	8690	9325	-8.76	-1.95	8.98	t2.3	7567	12045	-1.77	13.38	13.50
t20.5	8619	9628	-4.23	-0.05	4.23	t2.8	7867	12058	0.75	5.02	5.08
t11.4	8631	8936	-1.94	4.25	4.67	p4	7757	12673	2.31	8.38	8.69
t11.3	8523	8955	-4.06	7.32	8.37	t3.4	7963	12931	1.98	3.62	4.12
p11.2	8363	8974	-4.98	8.88	10.18	t3.6	7699	13088	2.46	3.61	4.37
t11.1	8218	8994	-4.59	9.08	10.18	t3.5	7833	13008	2.04	4.54	4.98
t10.9	8108	9033	-6.39	21.94	22.86	p3	7919	13207	2.03	3.02	3.64
t10.3	8302	9608	-6.31	5.18	8.17	p2	8337	13800	1.12	1.60	1.95

key:
X: easting minus 380,000 m, Y: northing minus 7,680,000 m (UTM, NAD27 datum), Z: elevation above sea level (see app. A).
Vx, Vy, V: east-, and north component, and absolute value of the mean annual velocity 1993-95, respectively

Appendix C : Mass balance 1993, 1994, 1995 and 1996

stake	X [m]	Y [m]	Z (1993) [m]	mb (1993) [cm a^{-1}]	mb (1994) [cm a^{-1}]	mb (1995) [cm a^{-1}]	mb (1996) [cm a^{-1}]	stake	X [m]	Y [m]	Z (1993) [m]	mb (1993) [cm a^{-1}]	mb (1994) [cm a^{-1}]	mb (1995) [cm a^{-1}]	mb (1996) [cm a^{-1}]
p26	10210	9407	2362	-2.7	4.4	-19.9	18.9	mb11.1	8213	8997	2052	-58.2	-64.8	-44.7	20.7
mb24.3	9876	9508	2314	19.6	26.3	9.3	119.0	mb10.7	8014	9222	2027	-44.8	-57.2	-44.8	12.6
mb24.7	10104	9741	2312	6.9	8.7	0.0	119.0	mb10.3	8299	9612	2026	-104.4	-139.3	-94.7	-10.8
p24.5	10008	9592	2309	26.4	36.6	0.0	118.8	p10.5	8123	9392	2021	-82.8	-68.4	-82.4	-31.5
p34	9722	9056	2304	14.0	13.2	-4.8	115.2	mb9.7	7558	10075	1949	-54.8	-81.2	-55.3	13.5
p2.3	9522	9854	2248	-31.9	-34.2	-29.3	6.3	mb9.3	7990	10117	1943	-74.5	-91.5	-59.2	-50.4
mb31	9465	9359	2224	-9.0	-17.5	-12.9	50.0	mb9	7752	10087	1937	-99.0	-60.9	-88.3	-22.5
p17	8862	8189	2169	-31.5	-61.2	-74.0	36.9	tc9	7728	10435	1912	-89.7	-146.8	-83.0	-39.6
p22	9066	9607	2160	-32.0	-8.1	-37.3	17.1	mb7.10	7724	11154	1847	-108.6	-121.1	-79.1	-53.5
p20	8382	8240	2128	-28.8	-51.3	-31.1	32.4	mb7.9	7894	11074	1847	-110.9	-142.7	-83.4	-58.5
mb12.1	8208	8510	2115	-37.6	-47.4	-38.6	30.0	mb7.8	8061	11085	1842	-105.0	-132.9	-73.7	-54.9
p12.2	8419	8547	2111	-42.4	-48.0	-39.3	30.6	mb2.6	7770	12091	1714	-113.5	-148.7	-86.0	-81.9
mb20.2	8735	9223	2106	-71.6	-101.1	-74.9	12.6	p2.4	7657	12038	1714	-110.5	-147.3	-82.0	-57.6
mb12.3	8606	8644	2103	-15.0	-15.1	-10.4	22.5	mb2.2	7501	12047	1713	-115.7	-186.7	-81.5	-33.3
p20.3	8673	9368	2101	-62.0	-61.9	-70.4	72.0	p4	7758	12673	1622	-144.5	-239.6	-127.1	-68.4
tc20.4	8626	9462	2097	-89.1	-114.7	-81.8	10.8	p3	7918	13206	1557	-167.0	-255.9	-149.8	-70.0
mb11.3	8524	8958	2072	-58.2	-69.2	-52.0	10.8	tc2.2	8110	13571	1494	-145.7	-219.4	-134.6	-90.0
p11.2	8360	8979	2058	-28.6	-68.4	-63.0	15.0	p2	8339	13803	1459	-181.3	-274.4	-183.4	-86.4

key:

X: easting minus 380,000 m, Y: northing minus 7,680,000 m (UTM, NAD27 datum), Z: elevation above sea level (see app. A).

mb: annual surface mass balances (water equivalent) calculated within the stratigraphic system

Appendix D : Surface elevation change 1972-93 and 1993-95

spot elevation	X [m]	Y [m]	Z (1993) [m]	ΔZ (1972-93) [m]	ΔZ (1993-95) [m]	spot elevation	X [m]	Y [m]	Z (1993) [m]	ΔZ (1972-93) [m]	ΔZ (1993-95) [m]
p27	10320	9320	2395.7	-3.08	--	p10.8	7954	9185	2029.9	-4.66	--
p26	10211	9407	2362.6	-2.31	-0.18	p10.3	8311	9602	2029.5	-5.06	-0.94
p24.5	10005	9592	2309.2	-3.47	0.51	p10.7	8066	9300	2028.6	-4.36	-1.27
p34	9728	9049	2306.5	-0.25	0.52	p10.4	8228	9506	2023.3	-4.76	--
p23.3	9531	9748	2252.6	-3.89	-1.26	p10.5	8151	9411	2021.0	-4.26	-1.52
p31	9465	9412	2217.3	-4.04	-0.37	p10	7885	9580	2004.0	-4.53	-1.31
p22.7	9231	9811	2208.6	-4.83	--	p9.5	7915	9988	1955.7	-5.08	-1.61
p30	9349	9557	2189.0	-4.73	-0.66	p9.9	7468	10361	1929.5	-5.64	--
p17	8871	8186	2171.0	-3.03	-0.5	p9.7	7620	10387	1922.6	-6.88	-1.51
p22	9081	9612	2161.8	-2.73	-0.07	p9	7779	10432	1908.3	-6.08	-1.75
p16	8725	8310	2145.6	-3.62	-1.05	p7.9	7884	11112	1843.8	-8.08	-1.79
p20	8384	8231	2129.6	-4.25	-1.37	p7.7	7977	11523	1793.5	-7.96	-1.61
p12	8356	8479	2118.1	-3.26	-1.15	p2.1	7429	12014	1720.1	-10.24	--
p20.2	8703	9329	2105.7	-6.16	--	p2.6	7773	12068	1717.7	-9.56	-1.94
p20.4	8651	9523	2106.1	-4.56	--	p2.5	7720	12045	1717.4	-9.59	--
p20.1	8747	9195	2105.1	-4.36	-1.06	p2.2	7503	12022	1716.9	-8.56	-1.54
p20.3	8684	9396	2103.6	-5.06	-1.11	p2.4	7656	12038	1714.7	-9.69	-1.91
p20.5	8628	9626	2101.8	-4.26	-1.15	p2.8	7866	12056	1713.0	-11.26	--
p11.7	8261	8681	2102.0	-3.8	-1.71	p2.3	7569	12029	1713.5	-10.75	--
p11.4	8634	8931	2079.7	-4.26	-1.26	p6	7618	12198	1698.0	-10.89	--
p11.5	8398	8847	2078.7	-3.99	-1.45	p5.3	7676	12495	1661.5	-14.96	-2.56
p11.3	8529	8848	2079.8	-4.36	--	p4	7756	12669	1624.2	-16.49	-3.03
p11.2	8369	8963	2062.1	-3.96	-1.13	p3.5	7817	12977	1587.9	-19.79	-3.73
p10.9	8118	8999	2057.1	-4.76	-0.64	p3	7918	13206	1559.3	-21.09	-3.65
p11	8439	9181	2054.5	-5.57	-1.39	P2.5	8071	13444	1530.9	-21.89	-3.65
p11.1	8225	8981	2055.5	-3.76	--	p2	8108	13669	1502.2	-26.99	-3.52
p10.2	8376	9676	2033.8	-4.16	--	B2627m	8578	14264	1379.0	-42.00	--

key:
X: easting minus 380,000 m, Y: northing minus 7,680,000 m, (UTM, NAD27 datum),
Z: elevation above sea level (see app. A).
ΔZ: change in surface elevation (ice or firn) from about 5 July (1st year) to 5 July (2nd year). The true survey dates of individual markers are 5 July ±5 days.

Appendix E : Mass balance 1969, 1970, 1971 and 1972

stake	X [m]	Y [m]	Z (1972) [m]	mb (1969) [cm a^{-1}]	mb (1970) [cm a^{-1}]	mb (1971) [cm a^{-1}]	mb (1972) [cm a^{-1}]	stake	X [m]	Y [m]	Z (1972) [m]	mb (1969) [cm a^{-1}]	mb (1970) [cm a^{-1}]	mb (1971) [cm a^{-1}]	mb (1972) [cm a^{-1}]
p27	10320	9320	2399	15	38	52	27	p10.2	8376	9676	2038	--	--	--	-60
p26	10211	9407	2365	24	56	45	54	p10.8	7954	9185	2035	-85	17	-50	-27
p24.5	10005	9592	2313	21	58	44	43	p10.7	8066	9300	2033	-43	23	27	-11
p34	9728	9049	2307	35	59	66	49	p10.4	8228	9506	2028	--	--	--	-27
p23.3	9531	9748	2257	19	41	5	46	p10.5	8151	9411	2025	-43	3	-24	-5
p31	9465	9412	2221	33	57	61	55	p10	7885	9580	2009	-57	9	-21	-18
p22.7	9231	9811	2213	-27	3	-17	-20	p9.5	7915	9988	1961	-79	14	-10	-58
p30	9349	9557	2194	54	47	58	66	p9.9	7468	10361	1935	-58	13	6	0
p17	8871	8186	2174	28	51	50	62	p9.7	7620	10387	1930	-45	11	1	-9
p22	9081	9612	2165	-19	12	-4	-8	p9.3	7942	10446	1915	-82	-28	-68	-84
p16	8725	8310	2149	35	58	58	56	p9	7779	10432	1914	-93	-5	-46	-50
p21.5	8873	9528	2135	-12	20	2	-4	p7.9	7884	11112	1852	--	--	-46	-46
p20	8384	8231	2134	22	62	61	81	p7.7	7977	11523	1802	-116	-34	-46	-73
p12	8356	8479	2121	36	57	52	91	p7.3	7808	11483	1797	-103	-52	-81	-66
p21	8762	9353	2113	-33	17	-5	0	p2.1	7429	12014	1730	-117	-52	-74	-92
p20.4	8651	9523	2111	--	--	--	-23	p6	7618	12198	1709	-145	-69	-69	-125
p20.3	8684	9396	2109	--	--	--	-8	p5.3	7676	12495	1677	-141	-82	-115	-137
p20.5	8628	9626	2106	--	--	--	0	p4	7756	12669	1641	-134	-105	-83	-151
p11.7	8261	8681	2106	--	--	--	62	p3.5	7817	12977	1608	-139	-116	-96	-162
p11.5	8398	8847	2083	--	--	25	22	p3	7918	13206	1580	-135	-126	-104	-129
p11.2	8369	8963	2066	--	--	--	21	P2.5	8071	13444	1553	-104	-128	-100	-88
p10.9	8118	8999	2062	--	--	34	22	p2	8108	13669	1529	-121	-111	-123	-82
p11	8439	9181	2060	-34	24	40	40	p1.5	8577	14173	1430	-131	-123	-110	-93
p11.1	8225	8981	2059	--	--	--	3	p1	8827	14535	1335	-138	-159	-151	--

key:
X: easting minus 380,000 m, Y: northing minus 7,680,000 m (UTM, NAD27), Z: elevation above sea level (see app. A).
mb: annual surface mass balances (water equivalent) calculated within the stratigraphic system

Appendix F : Area - elevation distribution of 11 Brooks Range glaciers

glacier =>	Arey	Bravo	Esetuk	Goose-neck	Hang-ing	N. Hubley	S. Hubley	McCall	W. Okpilak	E. Okpilak	Wolv. Crag
map date	1973	1956	1956	1956	1956	1956	1956	1956	1973	1973	1956
ΔA [km^2]											
1250-1350m	--	--	0.05	--	--	--	--	0.01	--	--	--
1350-1450m	0.01	--	0.18	--	--	--	0.04	0.14	0.11	--	--
1450-1550m	0.12	--	0.29	0.03	--	--	0.04	0.28	0.47	0.10	--
1550-1650m	0.39	0.01	0.59	0.12	--	0.04	0.14	0.38	0.33	0.57	0.08
1650-1750m	0.53	0.11	0.51	0.18	0.01	0.06	0.14	0.39	0.77	1.08	0.26
1750-1850m	0.60	0.21	0.73	0.19	0.03	0.15	0.23	0.42	1.31	0.99	0.40
1850-1950m	0.66	0.36	0.98	0.23	0.07	0.41	0.25	0.79	1.86	1.51	0.46
1950-2050m	0.55	0.40	0.82	0.30	0.21	0.46	0.07	0.73	2.06	1.73	0.66
2050-2150m	0.84	0.37	1.42	0.13	0.23	0.57	0.15	1.27	2.48	1.73	0.12
2150-2250m	0.81	0.13	1.44	--	0.21	0.25	0.23	1.01	1.64	0.90	--
2250-2350m	0.10	0.05	0.20	--	0.08	0.04	0.02	0.46	0.52	0.29	--
2350-2450m	--	--	--	--	--	--	--	0.10	--	--	--
$\Sigma(\Delta A)$ [km^2]	4.6	1.6	7.2	1.2	0.8	2.0	1.3	6.0	11.5	8.9	2.0
δA [km^2]	0.10	0.15	0.19	0.13	0.04	0.15	0.19	0.20	0.37	0.17	0.19

key:

ΔA: mean glacier area in given elevation interval (based on USGS 63,360 map and 1990s' GPS surveys)

$\Sigma(\Delta A)$: mean total area = 0.5 x [total area (based on USGS 63,360 map) + total area (constructed fr. 1990s' GPS surveys)]

δA: total area change: map date to 1990s (1993-95)